

ISTANBUL TECHNICAL UNIVERSITY ★ GRADUATE SCHOOL OF SCIENCE
ENGINEERING AND TECHNOLOGY

**UTILIZATION OF TITANIUM-SILICALITE-1 (TS-1) AS INORGANIC
FILLER IN MIXED MATRIX MEMBRANE FORMATION FOR CO₂
SEPARATION**

M.Sc. THESIS

Özlem Haval DEMIREL

Department of Chemical Engineering

Chemical Engineering Programme

Thesis Advisor: Prof. Dr. Ş. Birgül TANTEKİN-ERSOLMAZ

JANUARY 2015

ISTANBUL TECHNICAL UNIVERSITY ★ GRADUATE SCHOOL OF SCIENCE
ENGINEERING AND TECHNOLOGY

**UTILIZATION OF TITANIUM-SILICALITE-1 (TS-1) AS INORGANIC
FILLER IN MIXED MATRIX MEMBRANE FORMATION FOR CO₂
SEPARATION**

M.Sc. THESIS

**Özlem Haval DEMİREL
(506111033)**

Department of Chemical Engineering

Chemical Engineering Programme

Thesis Advisor: Prof. Dr. Ş. Birgül TANTEKİN-ERSOLMAZ

JANUARY 2015

İSTANBUL TEKNİK ÜNİVERSİTESİ ★ FEN BİLİMLERİ ENSTİTÜSÜ

**CO₂ AYIRIMI İÇİN KARIŞIK MATRİSLİ MEMBRANLARDA (KMM)
İNORGANİK KATKI MADDESİ OLARAK TİTANYUM-SİLİKALİT-1 (TS-1)
KULLANIMI**

YÜKSEK LİSANS TEZİ

**Özlem Haval DEMİREL
(506111033)**

Kimya Mühendisliği Anabilim Dalı

Kimya Mühendisliği Programı

Tez Danışmanı: Prof. Dr. Ş. Birgül TANTEKİN-ERSOLMAZ

OCAK 2015

Özlem Haval Demirel a **M.Sc.** student of ITU **Graduate School of Science and Engineering** student ID **506111033**, successfully defended the **thesis/dissertation** entitled “**Utilization of Titanium-Silicalite-1 (TS-1) as Inorganic Filler in Mixed Matrix Membrane Formation for CO₂ Separation**” which she prepared after fulfilling the requirements specified in the associated legislations, before the jury whose signatures are below.

Thesis Advisor : **Prof. Dr. Ş. Birgül Tantekin-Ersolmaz**
Istanbul Technical University

Jury Members : **Prof. Dr. Ahmet Sirkecioğlu**
Istanbul Technical University

Ass. Prof. Dr. Sennur Deniz
Yildiz Technical University

Date of Submission : 15 December 2014
Date of Defense : 23 January 2015

To my mother and brother,

FOREWORD

First of all, I wish to express my deepest gratitude to my supervisor Prof. Dr. Ş. Birgöl Tantekin-Ersolmaz for her guidance, criticism and supervision throughout my thesis study. I would also like to thank to Dr. Ing. Vlastimil Fila and Ing. Violeta Martin for their guidance, support and interest throughout all stages of my study during my stay at Institute of Chemical Technology, Prague. I would like to express my special thanks to my colleagues Ayşe Kılıç, Ahmet Halil Avcı and Dr. Sadiye Halitoğlu-Velioğlu for their helps, suggestions and valuable contributions to all field of my study. I am also very thankful to Dr. Çiğdem Atalay Oral for her encouragement and making every conditions at laboratory easier for us. I would also like to express my gratitude to Prof. Dr. Ahmet Sirkecioğlu for his precious suggestions. I want to record my thanks to Prof. Dr. Hale Gürbüz, Prof. Dr. Seniha Güner and Prof. Dr. Ömer Işık Ece for their contributions to my measurements. Thanks to all MeMaSep members for their contributions to all field of my study during the group meetings.

My deepest gratitude to my colleagues Didem Aycan, Pelin Uzun, Ezgi Bilgiç, Marcel Balçık, Gülizar Balcı and Cansu Ülker for their support, encouragement and understanding. I would like to express my very special thanks to Sule Zeynep Ozer for her unwavering support and encouragement from the very beginning of my study in Prague. Foremost, I owe special thanks to my mother Fatma Özyılmaz and my brother Umut Demirel for their unconditional love and unlimited patience from the very beginning.

December 2014

Özlem Haval DEMİREL
(Chemical Eng.)

TABLE OF CONTENTS

	<u>Page</u>
FOREWORD	ix
TABLE OF CONTENTS	xi
ABBREVIATIONS	xiii
LIST OF FIGURES	xvii
SUMMARY	xix
ÖZET	xxi
1. INTRODUCTION	1
2. THEORY AND BACKGROUND	5
2.1 Titanium-Silicalite-1	5
2.2 Mixed Matrix Membranes (MMMs).....	8
2.3 Problems Occurred in Fabrication of MMMs.....	10
2.4 Prediction of MMM Performance.....	17
3. METHODS AND METHODOLOGY	19
3.1 Material Selection	19
3.1.1 Titanium-Silicalite-1 as an Inorganic Filler	19
3.1.2 Polymer Selection	20
3.2 Titanium Silicalite-1 (TS-1) Synthesis.....	22
3.3 Modification of TS-1 Fillers	22
3.4 Membrane Formation.....	24
3.4.1 Formation of Pure Polymer Films.....	25
3.4.2 Formation of Mixed Matrix Membranes (MMMs).....	25
3.5 Characterization of TS-1 Fillers.....	26
3.5.1 Powder X-Ray Diffraction	26
3.5.2 Fourier Transform Infrared Spectroscopy.....	27
3.5.3 Scanning Electron Microscopy	27
3.5.4 Dynamic Light Scattering	28
3.5.5 Volumetric and Gravimetric Sorption.....	28
3.6 Membrane Characterization.....	29
3.6.1 Thermal Characterization.....	30
3.6.1.1 Thermogravimetric Analysis.....	30
3.6.1.2 Differential Scanning Calorimetry Analysis.....	30
3.6.2 Gas Permeation Measurement.....	32
3.6.2.1 Leak Measurements	33
3.6.2.2 Masking of Membranes.....	33
3.6.2.3 Single Gas Measurement.....	33
3.6.2.4 Mixed Gas Measurement	34
4. RESULTS AND DISCUSSION	37
4.1 TS-1 Synthesis and Characterization	37
4.1.1 TS-1 Samples As a Candidate Filler for MMM Formation.....	48

4.2	Effect of Modification on TS-1 Properties.....	50
4.3	Effect of Modification on Membrane Formation.....	54
4.4	Gas Separation Properties of MMMs.....	58
5.	CONCLUSIONS AND RECOMMENDATIONS.....	65
	REFERENCES.....	67
	APPENDICES.....	73
	APPENDIX A.....	75
	APPENDIX B.....	79
	APPENDIX C.....	83
	CURRICULUM VITAE.....	85

ABBREVIATIONS

6FDA	: 4,4'-(Hexafluoroisopropylidene)diphthalic anhydride
APTES	: 3-aminopropyltriethoxysilane
ASAP	: Accelerated Surface Area Porosimetry Analyser
DAM	: 2,4,6-trimethyl-m-phenylene diamine
DLS	: Dynamic Light Scattering
DMAc	: N,N'-dimethylacetamide
DMF	: N,N'-dimethyl formamide
DSC	: Differential Scanning Calorimetry
FTIR	: Fourier Transformed Infrared Spectroscopy
GC	: Gas Chromatography
IGA	: Intelligent Gravimetric Analyser
IPA	: Isopropanol
MMM	: Mixed matrix membrane
NMP	: N-methylpyrrolidone
SEM	: Scanning Electron Microscope
TGA	: Thermal Gravimetric Analyser
THF	: Tetrahydrofuran
TOL	: Toluene
TPAOH	: Tetrapropylammonium hydroxide
TS-1	: Titanium-silicalite-1
XRD	: X-Ray Diffraction
T_c	: Crystallization temperature
T_{aging}	: Aging temperature
t_{aging}	: Aging duration

LIST OF TABLES

	<u>Page</u>
Table 1.1 : Typical natural gas compositions [2]	3
Table 2.1 : Ideal selectivity of TS-1 membranes for different gases [24].	7
Table 2.2 : Gas transport properties of pure 6FDA-ODA and Matrimid [®] 5218, 25% grafted zeolites-6FDA-ODA and Matrimid [®] 5218 and cross-linked MMMs at 35°C and 150 psi [41].	16
Table 2.3 : Single gas properties of Silicalite-1 and Titanium-Silicalite-1 zeolites on a porous α -Al ₂ O ₃ tubular support.	17
Table 3.1 : Properties of solvent used in membrane preparation [53].	21
Table 3.2 : Chemical structure and T _g values of polymers used in this work [51,52].	21
Table 3.3 : The properties of synthesized TS-1 crystals.	23
Table 3.4 : Properties of the solvents used in modification of TS-1 powders.	24
Table 3.5 : Heating sequence for DSC measurements.	31
Table 4.1 : Particle size of the TS-1 samples synthesized in different conditions.	44
Table 4.2 : The maximum amount of adsorbed CO ₂ at 30°C for the TS-1 samples calculated with Langmuir Equation.	47
Table 4.3 : The effect of crystallization temperature on surface area characteristics of TS-1 samples.	48
Table 4.4 : Surface characterization of bare and modified TS-1 samples.	54
Table 4.5 : Cumulative weight loss (%) of the membranes obtained from TGA.	57
Table 4.6 : T _g values of MMM measured by DSC.	58
Table 4.7 : Gas separation properties of the MMMs.	59

LIST OF FIGURES

	<u>Page</u>
Figure 1.1 : Atmospheric concentrations of carbon dioxide (CO ₂) from Mauna Loa	2
Figure 2.1 : The channel system of MFI-type zeolite [16].....	5
Figure 2.2 : Isolated, tetrahedrally coordinated Ti(IV) site [11, 19].	6
Figure 2.3 : Upper bound correlation for CO ₂ /CH ₄ and CO ₂ /N ₂ separation [27].	9
Figure 2.4 : Schematic of a mixed matrix membrane [8].....	10
Figure 2.5 : Schematic of transport mechanism in mixed matrix membranes [31].....	10
Figure 2.6 : Non-idealities of mixed matrix membranes [31].	11
Figure 2.7 : Summary of the relationship between mixed matrix membrane morphologies and transport properties. Circles represent calculated values; squares represent experimental in Ultem® data. Solid markers are 35 vol% zeolite 4A; open markers are 15 vol% 4A [32].....	12
Figure 2.8 : Structure and abbreviations of aminopropylsilanes [39].	14
Figure 2.9 : (a) Chemical structure of APTES; (b) chemical modification on zeolite surface [40]. ...	15
Figure 2.10 : SEM picture of asymmetric mixed matrix hollow fiber PES membrane prepared with : (a) unmodified zeolite 4A, (b) modified zeolite 4A [40].	15
Figure 2.11 : SEM micrographs of (a) non-grafted FAU/EMT-Matrimid®(b) APTES-IPA FAU/EMT-Matrimid® MMMs [41].	16
Figure 3.1 : Preparation procedure of MMMs containing TS-1 fillers.....	26
Figure 3.2 : In-house constant-volume-variable-pressure system.	32
Figure 4.1 : XRD Patterns of TS-1 zeolites; literature [68] and synthesized in this study (T _c =160°C, Si/Ti=100 and T _{aging} =40°C, t _{aging} =3 days).....	38
Figure 4.2 : SEM pictures of TS-1 samples prepared under different Si/Ti molar ratios (a) 25, (b) 50, (c) 200, (d) 100. The crystallization temperature 160°C, aging at room temperature for 3 days.	39
Figure 4.3 : SEM images of TS-1 samples prepared under different crystallization temperatures, (a) 140°C, (b) 160°C, (c) 180°C. Aging at room temperature for 7 days.	39
Figure 4.4 : SEM pictures of TS-1 samples prepared under different aging time, (a) no aging, (b) 1 day, (c) 2 days, (d) 3 days, (e) 7 days. The crystallization temperature 140°C and aging at room temperature.	40
Figure 4.5 : SEM pictures of TS-1 samples prepared under different aging time (a) no aging, (b) 1 day, (c) 2 days, (d) 3 days, (e) 7 days. The crystallization temperature 160°C and aging at room temperature.	41
Figure 4.6 : SEM pictures of TS-1 samples prepared under different aging time, (a) no aging, (b) 1 day, (c) 2 days, (d) 3 days, (e) 7 days. The crystallization temperature 180°C and aging at room temperature.	42
Figure 4.7 : SEM pictures of TS-1 samples prepared under different aging time (a) 1 day, (b) 2 days, (c) 3 days, (d) 7 days. The crystallization temperature 140°C and aging at 40°C.	43
Figure 4.8 : SEM pictures of TS-1 samples prepared under different aging time (a) 1 day, (b) 2 days, (c) 3 days, (d) 7 days. The crystallization temperature 140°C and aging at 80°C.	43
Figure 4.9 : Effect of crystallization temperature on CO ₂ adsorption at 30°C, Si/Ti=100, aging time 3 days aging at room temperature.	45
Figure 4.10 : Effect of aging temperature on CO ₂ adsorption at 30°C, Si/Ti=100, crystallization temperature 140°C, 3 days aging time.	45
Figure 4.11 : Effect of molar ratios on CO ₂ adsorption at 30°C, crystallization temperature 160°C, 3 days aging at room temperature.	46
Figure 4.12 : Effect of aging time on CO ₂ adsorption at 30°C, crystallization temperature 160°C aging at room temperature.	46

Figure 4.13 : FTIR spectrum of TS-1 sample.	49
Figure 4.14 : Size distribution of TS-1 samples by number.	49
Figure 4.15 : SEM image of TS-1 sample.	49
Figure 4.16 : FTIR spectrum of (a) TS-1, (b) TS1-APTES-TOL, (c) TS1-APTES-THF, (d) TS1-APTES-IPA samples between 400 and 1300 cm^{-1}	51
Figure 4.17 : FTIR spectrum of (a) TS-1, (b) TS1-APTES-TOL, (c) TS1-APTES-THF, (d) TS1-APTES-IPA samples between 3000 and 3600 cm^{-1}	51
Figure 4.18 : XRD pattern of unmodified and modified TS-1 samples.	52
Figure 4.19 : Volumetric sorption isotherms of non-modified and modified TS-1 samples.	52
Figure 4.20 : Gravimetric sorption isotherms of bare TS-1, TS1-APTES-TOL and TS1-APTES-IPA.	53
Figure 4.21 : SEM images of Matrimid [®] MMMs prepared using a) TS-1 b) TS1-APTES-TOL c-d) TS1-APTES-THF.	55
Figure 4.22 : SEM images of 6FDA-DAM MMMs prepared using a) TS-1 b) TS1-APTES-TOL c) TS1-APTES-IPA.	56
Figure 4.23 : TGA thermograms for Matrimid [®] based membranes.	56
Figure 4.24 : TGA thermograms for 6FDA-DAM based membranes.	57
Figure 4.25 : Ideal and real gas separation properties of TS1-APTES-TOL / Matrimid [®] for CO_2/CH_4 separation: (a) CO_2 permeability (b) CH_4 permeability (c) CO_2/CH_4 selectivity.	60
Figure 4.26 : Ideal and real gas separation properties of TS1-APTES-IPA / 6FDA-DAM for CO_2/CH_4 and CO_2/N_2 separation: (a) CO_2 permeabilities, (b) CH_4 permeability (c) N_2 permeability (d) CO_2/CH_4 selectivity, (e) CO_2/N_2 selectivity.	61
Figure 4.27 : CO_2/CH_4 gas separation performances of MMMs on Robeson diagram with pure polymer and maxwell prediction results (a) Matrimid [®] (b) 6FDA-DAM as a continuous phase. Circles (●) for single gas measurements, diamonds (◆) for maxwell predictions and triangles (▲) for mixed gas measurements.	62
Figure 4.28 : CO_2/N_2 gas separation performances of MMMs on Robeson diagram with pure polymer and maxwell prediction results (a) Matrimid [®] (b) 6FDA-DAM as a continuous phase. Circles (●) for single gas measurements, diamonds (◆) for maxwell predictions and triangles (▲) for mixed gas measurements.	63

UTILIZATION OF TITANIUM-SILICALITE-1 (TS-1) AS INORGANIC FILLER IN MIXED MATRIX MEMBRANE FORMATION FOR CO₂ SEPARATION

SUMMARY

Mixed matrix membranes (MMMs) play an important role in the field of gas separation as synergistic effects of polymers and inorganic fillers is expected to overcome the limitations of polymeric membranes. These composite membranes have been prepared by dispersing the inorganic fillers into the polymer matrix. Material selection for both polymer and filler is a key aspect in the development of successful MMMs.

Titanium-Silicalite-1 (TS-1) is a crystalline zeotype material in which tetrahedral [TiO₄] and [SiO₄] units are arranged in a MFI structure. Owing to this structure TS-1 shows a three-dimensional system of channels having molecular dimension of 5.1-5.6 Å. TS-1 is widely known for its unique catalytic selectivity for industrial oxidation reactions due to the specific features of its Ti active sites; however the selective adsorption properties of TS-1 and its potential as inorganic filler in MMMs have not been investigated. Its shape selectivity, hydrophobic nature, and high thermal stability make TS-1 an attractive candidate for MMM applications. The objective of this work is to explore its potential for CO₂/CH₄ and CO₂/N₂ separation applications.

This work focuses on the synthesis of MMMs based on TS-1 dispersed in two different polyimides. Commercially available Matrimid[®] 5218 and in-house synthesized 6FDA-DAM polyimides are chosen as polymer matrix due to their CO₂ separation properties which also depend on MMM synthesis scheme and casting conditions. Matrimid[®] has relatively lower (3-8 Barrer) CO₂ permeability whereas 6FDA-DAM exhibit much higher (25-840 Barrer) CO₂ permeability. TS-1 samples with an average crystal size of 200-300 nm were synthesized by hydrothermal method and characterized by X-Ray Diffraction (XRD), Dynamic Light Scattering (DLS), Scanning Electron Microscopy (SEM), Accelerated Surface Area Porosimetry Analyser (ASAP) and Intelligent Gravimetric Analyzer (IGA). IGA results showed that CO₂ adsorption on TS-1 was approximately four times more than that of N₂ and two times more than that of CH₄.

The transport properties of MMMs are strongly dependent on the nanoscale morphology at the interfacial region between the polymer matrix and the filler surface. One type of morphology obtained at the interface is the formation of interfacial voids which hinder the success of MMMs. The method used to improve the interface morphology and the membrane fabrication protocol change depending on the filler/polymer combination. In this work, an amino silane coupling agent ((3-aminopropyl)triethoxysilane-APTES) as integral chain linker was used to overcome

the compatibility problem between the polymer and TS-1. Modification with APTES was performed in three different solvents; toluene (TOL), tetrahydrofuran (THF), isopropanol (IPA). Different polarities and kinetic diameters of the solvents in the modification reaction performances were also investigated. The results show that using IPA as a modification reaction solvent lead to less reduction in gas sorption due to pore blockage. MMMs were prepared using the APTES-modified TS-1 particles using various preparation conditions. TS1-APTES-TOL / Matrimid[®] and TS1-APTES-IPA / 6FDA-DAM exhibited good compatibility with the polymer phase without any observable void in the SEM analysis. The separation properties of the MMMs were characterized by pure and mixed gas permeability measurements. Single gas measurements supporting with Maxwell model predictions demonstrated that incorporating TS-1 zeolites into the polymer matrix only concluded as increase in permeability and slight change in the selectivity due to lack of molecular sieving properties of the MFI zeolites for the gas pairs of CO₂/CH₄ and CO₂/N₂. On the other hand, interesting results were obtained from mixed gas experiments compared the single gas measurements. Deterioration of permeability and enhancement in the selectivity that transfer the related MMMs beyond the upper bounds for specifically CO₂/CH₄ separation. This change may be attributed to difference sorption capacity of the TS-1 zeolites for different gases, thus competitive adsorption inside the pore of the TS-1 crystals.

CO₂ AYIRIMI İÇİN KARIŞIK MATRİSLİ MEMBRANLARDA (KMM) İNORGANİK KATKI MADDESİ OLARAK TİTANYUM-SİLİKALİT-1 (TS-1) KULLANIMI

ÖZET

Son yıllarda gaz ayırma alanında membran teknolojileri önem kazanmaya başlamıştır. Düşük çevresel etki, operasyon ve kurma kolaylığı, kurulum alanını gereksiniminin diğer teknolojilere kıyasla daha az olması gibi özellikler membran teknolojisinin avantajlarındandır. Ancak bir membran prosesinin endüstriyel alanda kullanımının ön şartı yüksek seçicilik ve geçirgenlik özelliklerine sahip bir membran malzemesi üretebilmektir. Polimerler kolay işlenebilirlik ve ekonomik avantajlarından dolayı membran malzemesi olarak yoğun olarak kullanılmasına karşın, ticari anlamda kullanımında bazı problemlerle karşılaşmaktadır. Polimerler gaz ayırma alanında seçiciliği arttırıldığında geçirgenlikte düşüş, yüksek geçirgenlik değeri elde edildiğinde ise seçicilik değerinde düşüş görülmektedir. Bu ikilem polimerlerin gaz ayırma membranlarında kullanımını kısıtlamaktadır. Diğer taraftan, inorganik malzemeler yüksek seçicilik ve geçirgenlik değerlerine sahip olması nedeniyle membran alanında ümit vadeci olmasına rağmen, kırılma yapıları, işlenmesindeki zorluklar ve ekonomik sebeplerden ötürü ticari anlamda kullanılamamaktadır. Ayrıca genellikle destek malzemeleri üzerinde hazırlanan inorganik membranlar gerçek gaz ayırma performanslarını gösterememektedir. Bu problemlerin aşılması için, polimer malzemelerin kolay işlenebilirlik özellikleri ile inorganik malzemelerin ise üstün gaz ayırma özelliklerinin bir araya getirilme fikri öne sürülmüştür. Bu iki malzemenin sinerjik etki sonucu istenilen yüksek seçicilik ve geçirgenlik değerlerine ulaşılması ve aynı zamanda kolay işlenebilen ticari membranların üretilmesi amaçlanmıştır. Bu şekilde inorganik katkı malzemelerinin polimer matrisi içinde dağıtılarak hazırlanan membranlara karışık matrisli membran (KMM) adı verilmiştir. Hem polimer hem de katkı maddesi seçimi yüksek performanslı KMM geliştirilmesinde önemli bir yer teşkil etmektedir.

Bu çalışmada, CO₂/CH₄ ve CO₂/N₂ ayırmada kullanılmak üzere karışık matrisli membranlarda (KMM) inorganik katkı maddesi olarak zeolit tipi kristalin bir malzeme olan titanyum-silikalit-1'in (TS-1) performansı incelenmiştir. KMM'lerin hazırlanmasında sürekli faz olarak ticari Matrimid® 5218 ve çalışma grubumuz tarafından sentezlenen 6FDA-DAM poliimidleri kullanılmıştır. Zeolit-polimer ara yüzeyindeki yapışma sorununun giderilmesi için amino-silan bağlayıcı ajanı, ((3-aminopropil) trietoksisilan-APTES), integral zincir bağlayıcısı olarak kullanılmıştır. APTES ile yapılan modifikasyon reaksiyonunda farklı polarite ve etkin çapa sahip toluen (TOL), tetrahidrofloran (THF) ve izopropanol (IPA) solvent olarak kullanılmıştır. Yapılan deneylerde APTES ile modifiye edilmiş TS-1 kullanılan

KMM'lerin, saf matrimide kıyasla tek gaz geçirgenliklerinin 2 kat daha fazla olduğu, ideal seçiciliklerinde ise küçük bir artış olduğu gözlenmiştir. Bu sonuçlar titanyum-silikalit-1 malzemesinin inorganik katkı maddesi olarak gaz ayırma alanında umut vadeci bir malzeme olduğunu göstermektedir.

Titanyum-silikalit-1, tetrahedral [TiO₄] ve [SiO₄] birimlerinin MFI yapıda düzenlendiği zeolit tipi kristalin bir malzemedir. MFI yapıya sahip TS-1'in üç boyutlu moleküler kanalları 5.1-5.6 Å'dur. TS-1, Ti aktif bölgelerinin eşsiz katalitik özellikleriyle endüstriyel oksidasyon reaksiyonlarında yaygın olarak kullanılan bir katalizör olmasına karşın, seçici adsorpsiyon özellikleri ve KMM'lerde inorganik katkı maddesi olarak kullanımı daha önce hiç araştırılmamıştır. TS-1, şekil seçicilik özelliği, hidrofobik yapısı ve yüksek ısı dayanımı ile KMM uygulamaları için ilgi çekici bir aday olmaktadır. Bu çalışmanın amacı CO₂/CH₄ ve CO₂/N₂ ayırımında TS-1'in KMM'lerdeki potansiyelinin araştırılmasıdır.

TS-1 numuneleri hidrotermal yöntemle sentezlenmiş ve XRD, DLS, SEM, ASAP ve IGA ile karakterize edilmiştir. Sürekli faz olarak Matrimid® 5218 ve kendi sentezlediğimiz 6FDA-DAM poliimidleri, zeolit olarak TS-1, silan bağlayıcı ajan olarak APTES ve çözücü olarak DMF kullanılarak karışık matrisli membranlar döküm-eyaporasyon yöntemi ile hazırlanmıştır. Membranlar çözücüsünü uzaklaştırmak üzere 130°C'de kurutulmuş ve 3-4 gün ısıtılma tabii tutulmuştur. Hazırlanan filmlerin ısı ve yapısal özellikleri DSC, TGA ve SEM ile karakterize edilmiştir. Geçirgenlik ölçümleri 35°C'de ve 4 bar basınçta sabit hacim-değişken basınç yöntemi ile ölçülmüştür.

Çalışmanın ilk kısmında Si/Ti bileşimi, kristalizasyon sıcaklığı ve yaşlandırma parametrelerinin TS-1 kristallerinin parçacık boyutuna ve parçacık boyutu dağılımına etkisi amaçlanmıştır. Tekdüze ve yaklaşık küçük parçacık boyutuna sahip olan TS-1 numuneleri Si/Ti oranının 100, kristalizasyon sıcaklığının 140°C, yaşlandırma sıcaklığının 40°C ve yaşlandırma süresinin 7 gün olduğu şartlarda sentezlenmiştir. IGA sonuçları, hidrotermal sentezle hazırlanan ortalama 200-300 nm kristal boyutuna sahip TS-1 örneklerinin CO₂ adsorpsiyonunun N₂'den 4 kat, CH₄'den 2 kat daha fazla olduğunu göstermektedir. APTES ile modifiye edilmiş TS-1 örneklerinin sorpsiyon sonucu deneylerinde bir miktar düşüş olduğu saptanmıştır. Bu düşüşün sebebi gözeneklerin APTES ile ya da çözücü ile tıkanmasından kaynaklandığı düşünülmektedir. Üç farklı çözücü ile modifiye edilen TS-1 kristalleri içinde göreceli olarak IPA çözücüsünde modifiye edilmiş olan örneklerin orjinal zeolite daha yakın sonuçlar verdiği görülmüştür. Bu durum IPA çözücüsünün yüksek polaritesine ve düşük etkin çapı ile ilişkilendirilebilir. THF ile hazırlanan kristallerin BET alanı, FTIR ve sorpsiyon analizleri APTES ile modifikasyonun başarılı bir şekilde gerçekleşmediğini göstermektedir. Gaz sorpsiyon sonuçlarına bakılarak, TS1-APTES-TOL örneklerinin sorpsiyon kapasitelerinin ciddi şekilde düştüğü görülmektedir. Bu durum hem düşük polariteye sahip toluenin aminopropilsilan moleküllerinin hareketini kısıtlayarak homojen bir dağılımın engellenmesi ile hem de zeolitin gözenek büyüklüğünden daha büyük kinetik çapa sahip olması sebebiyle çözücünün uzaklaşması sırasında zeolit yapısına zarar vermesi ile açıklanabilir.

Karışık matrisli membranların termal gravimetrik analiz sonuçları, membran hazırlama aşamasında kullanılan DMF çözücüsünün yeterince uzaklaştığını göstermektedir. Polimer-katkı maddesi ara yüzeyinde yapışma sorunlarının

incelenmesi için yapılan DSC analizlerinde TS1-APTES-THF katkı maddesi ile hazırlanan karışık matrisli membranların camsı geçiş sıcaklıklarında saf polimer membrana kıyasla düşüş olduğu, diğer örneklerde ise artış olduğu tespit edilmiştir. Bu durumund THF ile modifiye edilmiş olan örneklerin membran hazırlanırken aglomere olmasından kaynaklandığı düşünülmektedir. Camsı geçiş sıcaklığındaki artış ise polimer-katkı maddesi ara yüzeyinin varlığına işaret etmektedir. TS1-APTES-TOL/Matrimid® ve TS1-APTES-IPA/6FDA-DAM KMM'lerinin SEM görüntülerinde polimer/katkı maddesi ara yüzeyinde görülebilir bir boşluk tespit edilmemiştir, zeolit ile polimerin etkileşiminin iyi olduğu görülmüştür. Matrimid® ve 6FDA-DAM polimerlerine TS-1 eklenmesi ile geçirgenlik katsayısında iyileşme görülürken, seçiciliklerde çok az bir düşüş ya da hiç bir değişim olmadığı görülmüştür.

Bu durum Maxwell Modeli ile de doğrulanmaktadır. TS-1 zeolitinin gözenek büyüklüğünün CO₂/CH₄ ve CO₂/N₂ ayırması için moleküler elek özelliği göstermemesi bunun başlıca sebebidir. Ancak, 50/50 gaz karışımı ile yapılan deneylerde geçirgenlik değerlerinde düşüş gözlenirken, seçicilikler arttığı tespit edilmiştir. Bu değişim KMM'lerin CO₂/CH₄ ayırma uygulamaları için tanımlanan üst sınır doğrusunu aşmasını sağlamıştır. Bu durumun moleküler elek özelliği göstermeyen ancak farklı gaz sorpsiyon kapasitesine sahip TS-1 kristallerinin CO₂, CH₄, N₂ gazlarının adsorplanmasında rekabet oluşumundan kaynaklandığı düşünülmektedir.

1. INTRODUCTION

Carbon dioxide (CO₂) is responsible 60% of the effect of greenhouse gases on global climate change [1]. Natural gas streams, flue gas from fossil fuel combustion, product of coal gasification and biogas from anaerobic digestion contain CO₂ and give rise to CO₂ emissions to the atmosphere. As it is clearly seen from in Figure 1.1, atmospheric concentrations of CO₂ has been exponentially raised with respect to world population increment and energy demands. Greenhouse gas emissions and climate change have been directly effected by the CO₂ concentration in the atmosphere. Action plan for mitigation of greenhouse gases is based on two components: use of cleaner energy and energy efficient products and services [2]. Natural gas becomes prominent with respect to these concern. However, as the cleanest, safest and most efficient energy source, natural gas contains various amount of gases including CO₂ as it is given in Table 1.1. The presence of CO₂ and other acid gases deteriorate the calorific value of the natural gas and make the gas streams become more acidic and corrosive. CO₂ concentrations must be below 2% based on pipeline specifications [3]. CO₂ removal will improve the energy efficiency of natural gas, decrease the volume of gas to be transported, inhibiting atmospheric pollution and preventing pipeline corrosion [2]. Traditional methods such as absorption, adsorption, cryogenic distillation for removing CO₂ are suffering from high energy requirement, corrosion and flow problems caused by change in viscosity [2]. On the other hand, membrane based separation is a convenient alternative method to traditional separation processes for CO₂ removal. Advantages of membrane based separation can be listed as follows [4]:

- Low capital investment
- Ease of operation, process can be operated unattended
- Good weight and space efficiency
- Ease of scale up.
- Minimal associated hardware
- No moving parts

- Ease of installation
- Flexibility
- Minimal utility requirements
- Low environmental impact
- Reliability
- Ease of incorporation of new membrane developments.

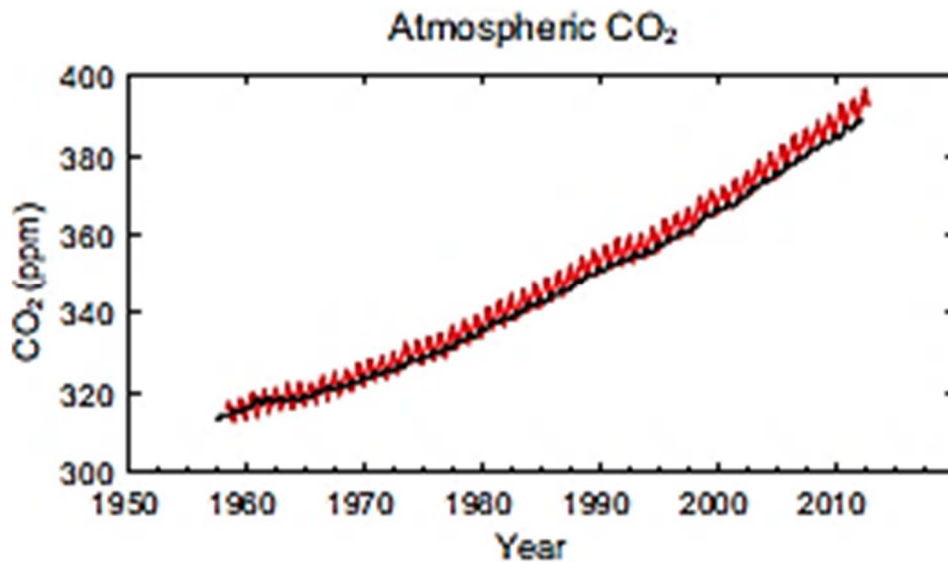


Figure 1.1 : Atmospheric concentrations of carbon dioxide (CO₂) from Mauna Loa (red) and South Pole (black) since 1958 [5].

Membrane history starts in middle of eighteenth century, Abbe Noblet used the word “osmosis” for the first time to describe permeation water through a diaphragm, thus the studies of membrane phenomena have been commenced. Through the nineteenth and early twentieth centuries, application area of membranes was limited only as a laboratory tools to develop physical/chemical theories. At the end of World War II, utilization of membranes was submitted in the testing of drinking water. Loeb-Sourirajan process for making defect free, high flux, anisotropic reverse osmosis membranes were attributed as a seminal discovery. These membranes provides mechanical strength due to thicker and more permeable microporous material as support to ultrathin, selective layer. This development accelerated the transformation of membranes from a laboratory scale to an industrial process [6]. Principal development in the 1980s was the emergence of industrial membrane gas separation processes. The first major development was the Monsanto Prism membrane for hydrogen separation, introduced in 1980 [6].

Table 1.1 : Typical natural gas compositions [2].

Component	Composition range (mol%)
Helium	0.0-1.8
Nitrogen	0.21-26.10
Carbon dioxide	0.06-42.66
Hydrogen sulfide	0.0-3.3
Methane	29.98-90.12
Ethane	0.55-14.22
Propane	0.23-12.54
Butanes	0.14-8.12
Pentanes and heavier	0.037-3.0

Membrane-based technology plays an important role in gas separation applications in order to reduce the environmental impact and cost of industrial processes [7]. Polymeric membranes are the most used materials in gas separation processes such as natural gas sweetening, landfill gas recovery, hydrogen recovery and purification, flue gas separation and air separation, etc. [8]. However, polymeric membranes are suffering from insufficient gas permeability and thermal stability for high temperature applications. It is very necessary to enhance these properties of polymeric membranes by addition of the inorganic particles with their inherent superior separation characteristics. Therefore, mixed matrix membranes (MMMs) were investigated for gas separation in 1970s with the discovery of a delayed diffusion time lag effect for CO₂ and CH₄ when adding 5A zeolite into rubbery polymer polydimethyl siloxane (PDMS) [9].

MMMs are based on solid–solid system comprised of inorganic dispersed phase inserted in a polymer matrix. These kinds of membranes have the potential to achieve higher selectivity, permeability, or both, high thermal stability, relative to the existing polymeric membranes, resulting from the addition of the inorganic particles with their inherent superior separation characteristics [8].

Zeolites and carbon molecular sieves are the most commonly used inorganic fillers for mixed matrix membranes (MMMs). Most works have focused on the synthesis and characterization of MFI-type zeolites due to their suitable channel opening size and thermal stability which make them potentially useful for gas separation applications. TS-1 zeolite is well known to be an efficient catalyst for several oxidation reactions. With the incorporated titanium into zeolite framework, TS-1 zeolites are expected to exhibit interesting properties for the permeation. TS-1 zeolites are in a quite new branch of MFI-type zeolites as inorganic fillers. Up to date, there is no study focused on the usage of TS-1 in MMMs in the field of gas separation applications.

In this study, potential of TS-1 fillers as a inorganic filler in MMMs for gas separation applications are desired to be investigated. To achieve this purpose, the following steps are applied:

- Synthesizing TS-1 crystals with hydrothermal method and obtaining small crystal with narrow size distribution.
- Characterization of morphological, structural and sorption properties of synthesized TS-1 crystals.
- Modified the TS-1 zeolite surface with silane coupling agent, 3-aminopropyltriethoxysilane (APTES) in order to provide compatibility with polymer phase.
- Characterization of structural and sorption characteristic of modified samples in order to approved the success of modification reaction and investigating the effect of modification into zeolite characteristic.
- Preparation of mixed matrix membrane with modified TS-1 particles.
- Preparing neat polymeric membranes and MMMs consist of bare TS-1 particles for comparison.
- Investigating the gas transport properties of MMMs through single and mixed gas measurements in order to identify the role of TS-1 as an inorganic filler.

The thesis is organised with respect to aforementioned objectives. Chapter 2 gives the background about the TS-1 zeolite and current situation of MMMs. Chapter 3 gives detailed informations about the materials, experimental methods and characterization techniques. Chapter 4 clarifies the results and the discussion. Finally, conclusions of the discussions and suggestions for further studies are given in Chapter 5.

2. THEORY AND BACKGROUND

2.1 Titanium-Silicalite-1

Titanium-Silicalite-1 (TS-1) is first reported by Taramasso et al. in 1983 as a porous crystalline catalyst in the form of parallelepipeds with rounded edges [10]. TS-1 is a Ti-substituted zeolite in which $[\text{TiO}_4]$ and $[\text{SiO}_4]$ units arranged in a MFI structure [11]. As it is depicted in Figure 2.1, three dimensional channel system of MFI type zeolites consist of straight channels with a pore opening 0.56×0.54 nm along its b axis, sinusoidal channels with a pore opening of 0.51×0.55 nm along its a axis and tortuous pathway in the c direction in which b-channels and c-channels are interconnected [12]. TS-1 is a well known selective-oxidation catalyst for conversions of alkenes to epoxides, alcohols to aldehydes, alkanes to secondary alcohols and ketones, phenol to hydroquinone and pyrocatechol, and amines to hydroxylamines with hydrogen peroxide as a oxidant [13]. Incorporation of isolated, tetrahedrally Ti^{IV} sites into the MFI structure (Figure 2.2) is responsible of its unique catalytic activity and caused an increase in the unit cell dimensions [14]. Introduction of one formal negative charge per Ti atom is also caused by the introduction of Ti^{IV} sites [15].

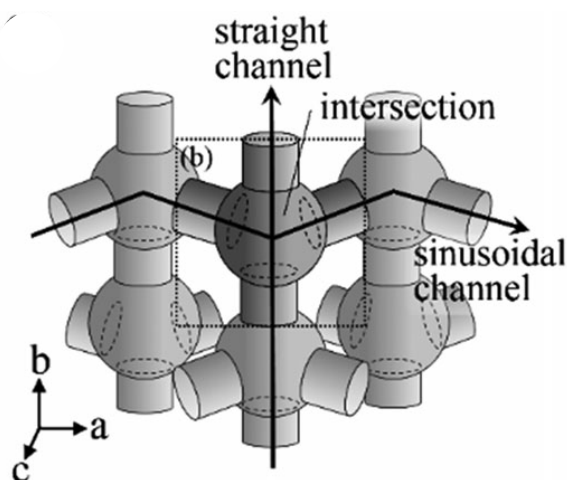


Figure 2.1 : The channel system of MFI-type zeolite [16].

Schoeman et al. synthesized colloidal TS-1 crystals by hydrolysis of a mixture of tetraethoxysilane and tetraethoxy titanate with tetrapropylammonium hydroxide (TPAOH) followed by hydrothermal treatment at 100°C [17]. While Ti content varied between $x=0.14-17$, average crystal size of the samples varied in the range of 80-110 nm. The high surface area of TS-1 was calculated as 450-500 m²/g based on BET equation, which also indicated well crystallized samples. Han et al. reported the thermal stability of TS-1 crystals as up to 1073 K [18].

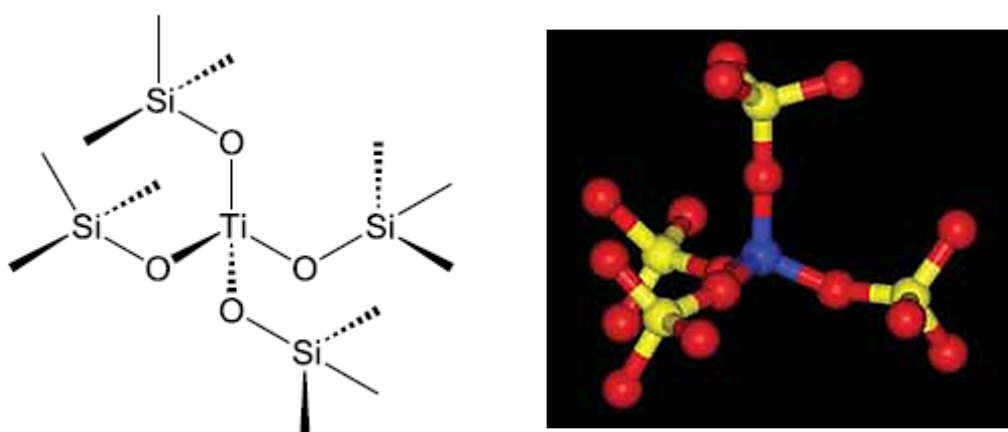


Figure 2.2 : Isolated, tetrahedrally coordinated Ti(IV) site [11,19].

As it is known presence of Al in the zeolite network provide hydrophilic character to the zeolite such as ZSM-5. On the other hand, TS-1 with Si/Al ratio infinite exhibits hydrophobic character like silicalite-1. This hydrophobic character of TS-1 leads its use in hydrocarbon adsorption processes under the presence of water. Serrano et al. investigated the potential of MFI zeolites: silicalite-1, titanium-silicalite-1 and ZSM-5 (aluminasilicate) as a volatile organic compounds (VOCs) adsorbents [20]. Their study showed that TS-1 could be used as an adsorbent for the removal of toluene and isopentane in water containing systems with respect to its Ti sites with high hydrophobic nature adsorbing considerable amounts of these hydrocarbons.

Avoiding of forming anatase (TiO₂) phase during the synthesis of TS-1 is required because it is resulted as decreasing the hydrophobicity and the performance of the samples [21]. On the other hand, TiO₂ phase does not dissolve into Ti^{IV} sites and decreased the catalytic activity [22]. Sebastian et al. stated that large TS-1 crystals

with extra-framework titanium in the form of anatase were obtained by the long crystallization time [21].

TS-1 ceramic membranes are studied in the field of pervaporation due its hydrophobic characteristics. Sebastian et al. prepared TS-1 ceramic membranes on α -Al₂O₃ support with MW-assisted hydrothermal heating method [21]. The samples exhibited high flux and intermediate selectivity for ethanol/water separation. Investigation of synthesis parameter pointed out that Ti/Si ratio, synthesis temperature and duration were effected the performance of TS-1 samples. Chen et al. reported TS-1 membranes which were synthesized onto mullite porous tubes by in situ crystallization showed high ethanol selectivity in pervaporation of a ethanol/water mixture [22].

Gas permeation properties of TS-1 membranes was studied by Au et al. in 2001 for gases H₂, N₂, Ar, SF₆, CH₄, i-C₄H₁₀, n-C₄H₁₀ [23]. However, the difficulties of preparing ceramic membranes hindered the actual performance of the TS-1 membranes. Cracks were formed after air-calcination to remove the organic templates in spite of the fact that TS-1 membrane was successfully intergrown. Ideal selectivity results are given in Table 2.1. In this study, the effect of Ti atoms in the framework was stated as altering the separation performance of the membranes. Comparison with silicalite-1 and vanadium-silicalite membranes was pointed out that these metal ions (Ti and V) change the physical and chemical properties of the pores. Physically restriction of the access within the pore was ensued, meanwhile different interaction with the diffusing molecules was imposed through their chemistry.

Table 2.1 : Ideal selectivity of TS-1 membranes for different gases [23].

Gas	Kinetic Diameter (nm)	H ₂ /gas ratio
N ₂	0.364	2.5
Ar	0.340	3.2
SF ₆	0.550	4.0
CH ₄	0.380	2.2
i-C ₄ H ₁₀	0.500	2.6
n-C ₄ H ₁₀	0.430	2.5

Motuzas et al. prepared TS-1 membranes by a microwave-assisted secondary growth method for the first time in 2010 [24]. Synthesis temperature (150-200°C), duration (90-150 min) and Si/Ti ratio were investigated parameters. The gas permeances reported for the gases (He, CO₂, O₂, N₂, n-C₄H₁₀, i-C₄H₁₀ and SF₆) indicated that most selective TS-1 membranes possessed an ideal selectivity of 40 for n/i- C₄H₁₀ and 105 for CO₂/SF₆ at 25°C.

Up to now, no literature research focused on titanium-silicalite-1 as an inorganic filler in the formation of mixed matrix membrane applications has been published. Besides its unique catalytic properties and utilization as a ceramic membranes by using supports for pervaporation applications, its performance as a filler in the MMM for gas separation could be promising due to its hydrophobic properties and possible preferential interaction with diffusing molecules.

2.2 Mixed Matrix Membranes (MMMs)

Polymeric membranes have been dominantly used in the field of membrane separation applications. Polymeric materials are very attractive for preparing membranes with respect to economical concerns. Their inexpensive processability, physical properties and being highly reproducible are the key factors that makes them attractive candidate as a membrane material. Glassy polymers especially play major role in gas separation applications due to their good mechanical properties and better size separation properties compared to rubbery polymers. Various types of polymer families have been developed for gas separation like polycarbonate, polyester, polysulfone, polyethersulfone, polyetherimide, or polyimide, among others. However, polymeric membranes do not meet the requirements for the current advanced membrane technology due to their lower separation performance [25].

The performance of a membrane is defined as permeability of a specific component of gas mixture and the selectivity. However, these parameters have been found as a trade-off parameters. Trade-off behaviour can be explained by selectivity decrease with increasing permeability and vice versa [26]. In 1991, and updated in 2008 as it is depicted in Figure 2.3, Robeson plotted the selectivity versus permeability graphs by using data of many polymers for membrane separation of gas pairs and obtained the

upper bound trade-off line, which current polymer membrane materials can not overcome [27].

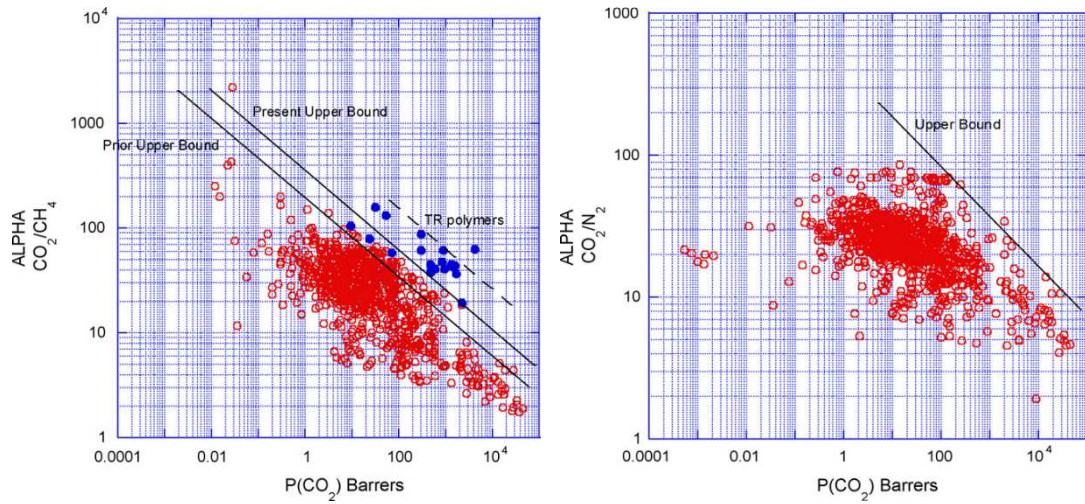
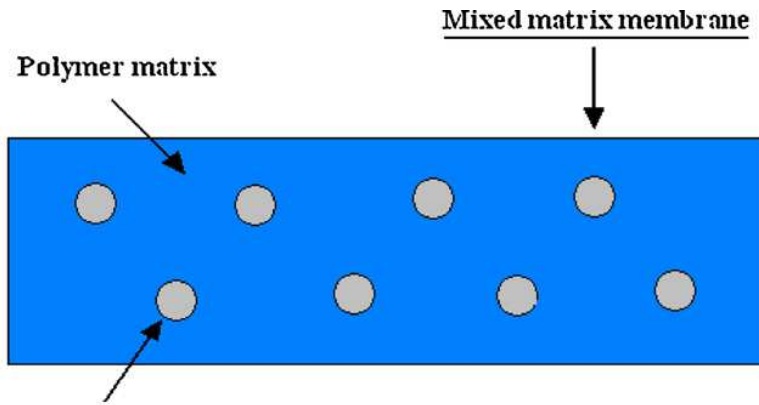


Figure 2.3 : Upper bound correlation for CO₂/CH₄ and CO₂/N₂ separation [26].

On the other hand, inorganic membranes such as prepared from zeolitic materials are also promising in the membrane technology. Inorganic materials such as zeolites or zeotypes possess very high and adjustable adsorption capacity, catalytic sites of different strengths which can be generated in the frameworks, channels and cavities in the range of many molecules of interest and ion exchange capabilities. High thermal, mechanical and chemical stability are also advantages of zeolitic materials. Separation properties of zeolitic materials are determined by the crystallographic structure (pore size) and chemical composition (affinity) [25]. Their superior permeability and/or selectivity at high temperatures and pressure overried polymeric membranes. Nevertheless, higher cost due to high temperature requirements for synthesis and difficulty to scale up the membrane area without defects are the main drawbacks of these membranes [28].

The idea of hybrid system in mixed matrix membrane (MMM) is arised from synergistically combining the processability of polymers with the highly selective characteristic of inorganic materials [29]. As it is depicted in Figure 2.4, MMMs are prepared by dispersing inorganic materials into the polymer matrix. Paul and Kemp prepared for the first time MMM by dispersing zeolite 5A into a rubbery polymer of polydimethylsiloxane (PDMS) [9]. Invesitgation of delayed diffusion time lag effect on CO₂/CH₄ separation showed improvement in the diffusion lag.



Zeolite particles dispersed in the polymer matrix

Figure 2.4 : Schematic of a mixed matrix membrane [8].

Figure 2.5 exhibits the typical transport mechanism when fillers ideally contacts with polymer matrix. Combination of the solution-diffusion and Knudsen diffusion is dominant in MMMs [6, 31]. Proper selection of MMM material is able to significantly enhance the transport properties of the individual materials.

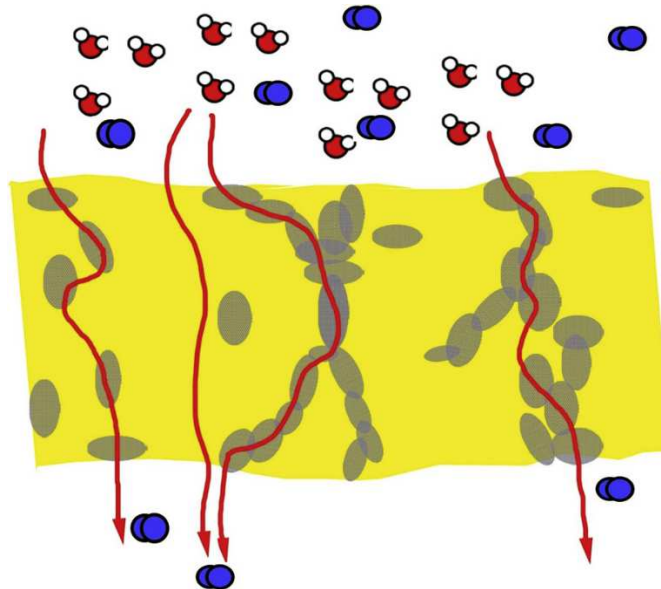


Figure 2.5 : Schematic of transport mechanism in mixed matrix membranes [30].

2.3 Problems Occurred in Fabrication of MMMs

The main problem associated with mixed matrix membranes is forming undesirable morphologies at the polymer-filler interface which hinders the idea of synergistic performance of two components. In Figure 2.6, there are four types of undesirable morphologies can be occurred at the interface: i) sieve-in-a-cage, ii) leaky interface,

iii) matrix rigidification, iv) plugged sieves [30]. Accomplishing the mixed matrix membrane performance is only possible when these non-idealities overcome.

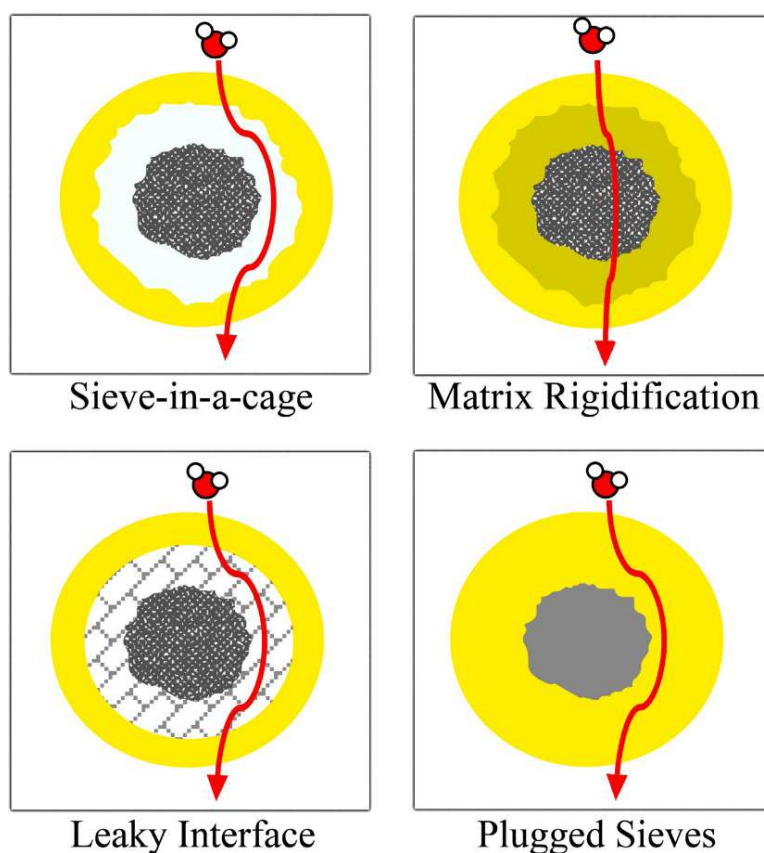


Figure 2.6 : Non-idealities of mixed matrix membranes [30].

“Sieve-in-a-cage” morphology occurs when poor interfacial adhesion encounters between polymer and filler. Gas molecules prefer to pass through the least resistance path which is formed due to voids at the interface. Therefore, much higher permeability compared to that of poor polymeric membrane is obtained. The selectivity is effected by “sieve-in-a-cage morphology” depending on void size. When the void size is larger than the permanent gas molecule, significantly enhancement in permeability is observed with decreament of selectivity. This phenomena is known as “leaky interface” which is subtype of “sieve-in-a-cage” morphology. “Matrix rigidification” is formed at the filler/polymer interface as a result of rigidified polymer layer around the filler. Polymer chains at the interface are immobilised due to rigidified polymer which decrease the permeability. In some cases, zeolite pores can be sealed by the solvent or by the rigidified polymer which is denominated as “plugged sieves”. This phenomena causes low permeability without any change in selectivity [30].

Koros and Moore studied the Maxwell model by expanding it based on the morphologies depicted in Figure 2.7 and also supported with experimental data for 15 and 35 vol.% loading in commercially available polymer, Ultem[®]. Figure 2.7 shows the close relationship between morphology and transport properties. Each type of non-ideal behaviour has different impact on the permeability and selectivity of the mixed matrix membrane. By the help of this signature of the morphology on transport properties, the membrane preparation conditions can be enhanced [31].

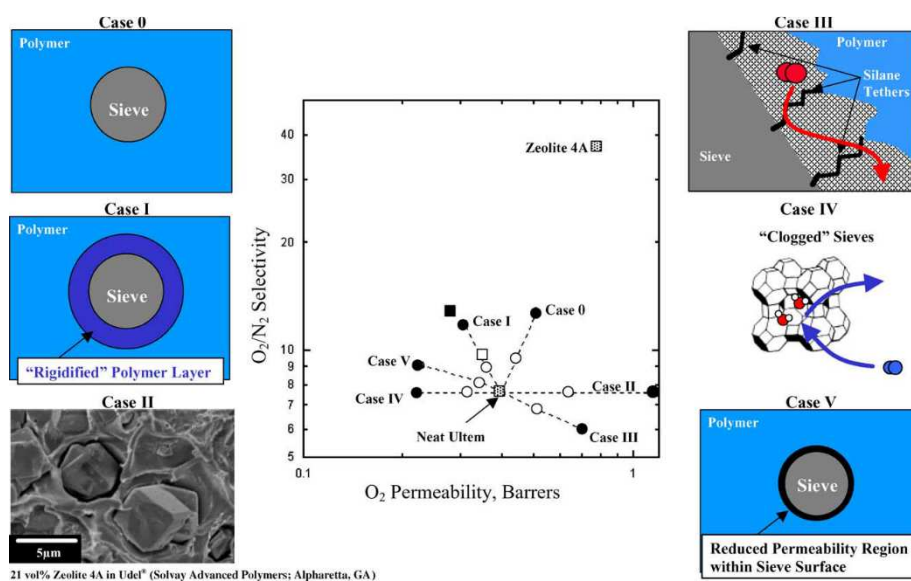


Figure 2.7 : Summary of the relationship between mixed matrix membrane morphologies and transport properties. Circles represent calculated values; squares represent experimental in Ultem[®] data. Solid markers are 35 vol% zeolite 4A; open markers are 15 vol% 4A [31].

As it is aforementioned, undesired morphology at the polymer/filler interface effects the membrane performance in the mean of permeability and selectivity. The behavior of the interface is able to be determined via overall transport properties which is strongly effected by morphology. The ideal case in which there is no non-ideal effect is observed can be obtained with Maxwell prediction which is explained in detail below.

Problems occurred during the preparation of MMMs like poor contact between the filler and the polymer phase must be overcome in order to achieve high performance defects-free MMMs. For this purpose, many modification techniques has been proposed. Some classes of this techniques have been focused on maintaining polymer chain flexibility during membrane preparation and maximize the stress relaxation by casting or annealing the membrane at temperature above the glass transition

temperature of the polymer, introducing plasticizer into polymer solution and melt processing. Incorporation a low molecular-weight additive as a third component into the MMM matrix which links the polymer chain to the inorganic filler; selecting both inorganic fillers and polymer matrix with hydrophobic characteristic; using copolymers which possess rubbery sections which is able to contact with zeolites without void formation; reducing the stress at the polymer-filler interphase by primarily coating the surface of the inorganic filler with dilute polymer dope are all commonly used methods to enhance filler-polymer interphase and dispersing inorganic particles homogenously into the polymer matrix [32].

Apart from these methods, silane coupling agents are used as an effective method to eliminate the non-idealities at the polymer-filler interface by creating a chemical bridging between the zeolite phase and polymer matrix in a widespread manner [33]. The structures of some of mainly used silane coupling agents are depicted in Figure 2.8. Silane coupling agents consist of two reactive groups; the alkoxy groups that react with the zeolite hydroxyl groups and amino groups can react with some functional groups in polymers. The typical formula of silane coupling agents is $R-(CH_2)_n-Si-X_3$ in which X represents a hydrolyzable group like ethoxy, methoxy, whereas R is an organo functional group like amino, epoxy, methacryloxy [34]. During grafting hydrolyzable alkoxy groups react with the zeolite hydroxyl group, while functional groups react with the some functional group in the polymer, thereby silane coupling agents become a integral chain linker between two phases [35].

Pechar et al. studied modification of ZSM-2 zeolites with 3-aminopropyltrimethoxysilane (APTMS) before dispersing them into polyimide membranes [36]. In spite of elimination of interfacial voids, CO₂ selectivity and permeability displayed poor performance which indicates to pore blockage on zeolites [37]. In their further study, as a coupling agents 3-aminopropyltriethoxysilane (APTES) has been used. Gas transport properties of prepared MMMs with modified zeolite L has dropped compared to pure polymeric membrane. This reduction of CO₂ permeability and selectivity showed that the zeolite pores were also partially blocked by APTES [34].

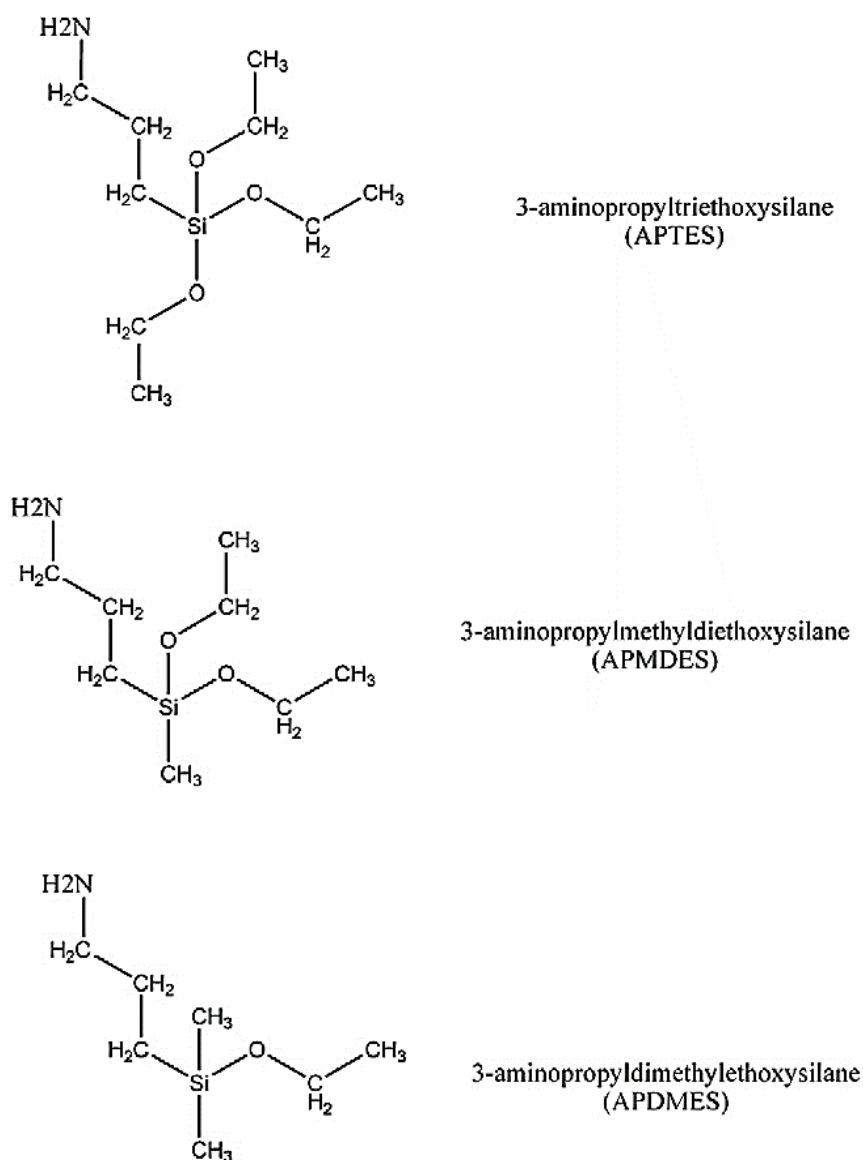


Figure 2.8 : Structure and abbreviations of aminopropylsilanes [38].

Ismail, A.F. et al. have prepared mixed matrix hollow fibers with dispersing zeolite-4A into polyethersulfone (PES) matrix [39]. The effect of chemical modification with 3-aminopropyltriethoxysilane (Dynasylan Ameo[®]) in ethanol on zeolite surface towards gas separation performances has been investigated and the related mechanism is given in Figure 2.9. They have reported that mixed matrix hollow fibers prepared with unmodified zeolite indicated “sieve-in-a-cage” morphology, whilst the membranes prepared with modified fillers has shown good compatibility with polymer phase which can be seen from Figure 2.10. The selectivity of CO₂/CH₄ has been reported as 2.86 and 28.75 for PES mixed matrix hollow fiber membranes with loading of 20 wt. % unmodified and modified zeolite 4A fillers, respectively. Enhancement in the morphology has also yielded gas transport properties.

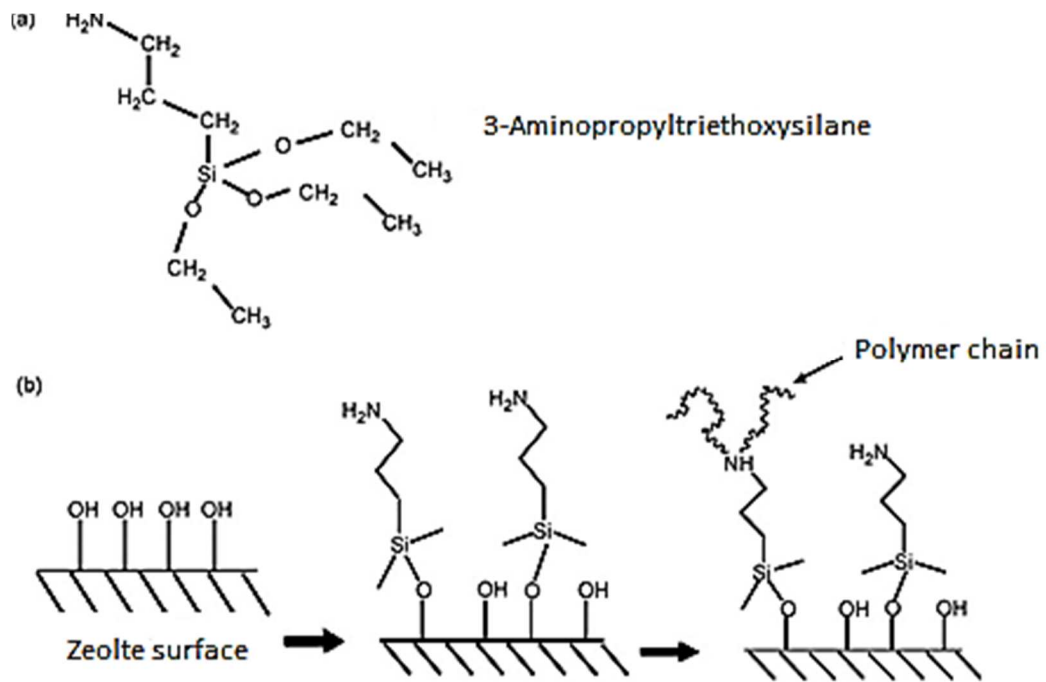


Figure 2.9 : (a) Chemical structure of APTES; (b) chemical modification on zeolite surface [39].

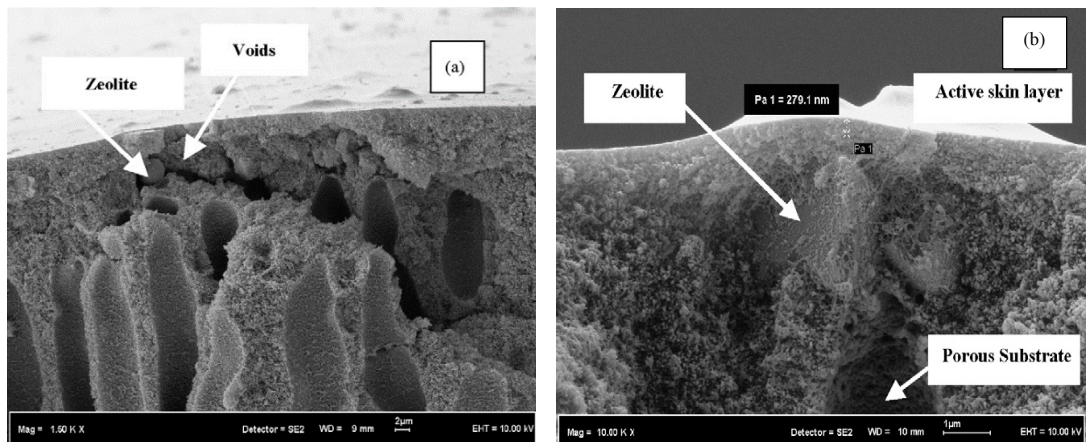


Figure 2.10 : SEM picture of asymmetric mixed matrix hollow fiber PES membrane prepared with : (a) unmodified zeolite 4A, (b) modified zeolite 4A [39].

Nik, O.G. et al. reported the grafting reaction of FAU/EMT zeolites with 3-aminopropyltriethoxysilane (APTES), 3-aminopropylmethyldiethoxysilane (APMDES), and 3-aminopropyl dimethylethoxysilane (APDMES) in solvents with different polarities [38]. Their systematic study showed that the grafting aminosilanes on zeolites by using polar solvents have positive impacts on amount of grafted amine groups, the surface area, micropore volume and CO₂ adsorptive properties. In their further study, mixed matrix membranes with grafted FAU/EMT zeolites have been

dispersed into 6FDA/ODA and Matrimid[®]5218 polymer matrixes [40]. As it can be seen from Figure 2.11, heterogeneously dispersion, sedimentation, agglomeration of non-modified FAU/EMT zeolites and some voids have been able to be eliminated by using grafted zeolites. Moreover, gas transport properties of the MMMs has been altered with introducing grafting zeolites into the polymer matrix. As it can be derived from Table 2.2, MMMs with zeolites grafted with isopropanol (IPA) exhibits better results compared to those grafted in toluene (TOL), which indicates that solvents with high polarity leads to increase the mobility of aminopropylsilane molecules, thus more uniform distribution of grafting sites can be obtained.

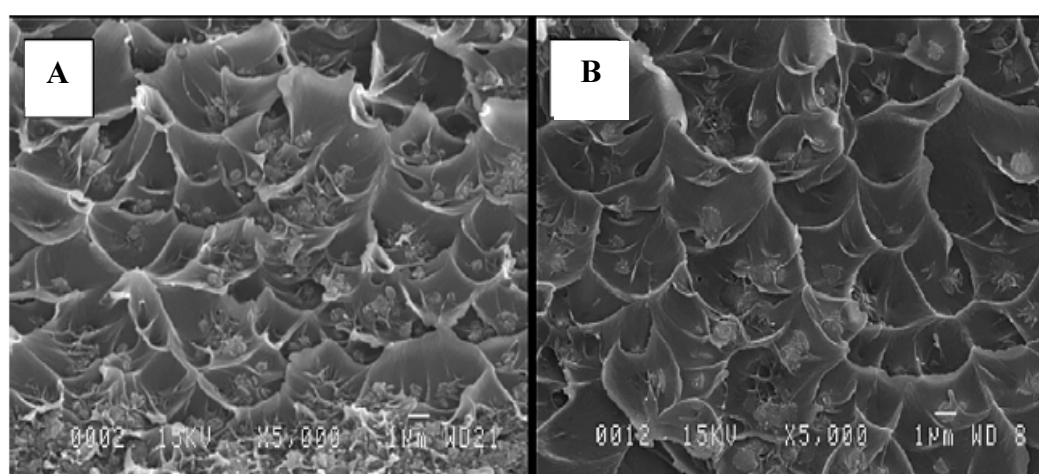


Figure 2.11 : SEM micrographs of (a) non-grafted FAU/EMT-Matrimid[®], (b) APTES-IPA FAU/EMT-Matrimid[®] MMMs [40].

Table 2.2 : Gas transport properties of pure 6FDA-ODA and Matrimid[®]5218, 25% grafted zeolites-6FDA-ODA and Matrimid[®]5218 and cross-linked MMMs at 35°C and 150 psi [40].

Membrane Samples	P _{CO2} (Barrer)	P _{CH4} (Barrer)	Ideal Selectivity	Real Selectivity (50/50%)
6FDA-ODA	16.4	0.33	49.7	42.3
6FO-ZO	16.2	0.58	27.9	37.0
6FO-APTES-TOL	16.9	0.53	31.9	29.5
6FO-APTES-IPA	40.9	0.51	80.2	40.1
Matrimid [®]	6.2	0.20	31.0	28.0
M-ZO	9.4	0.39	24.1	26.8
M-APTES-TOL	8.2	0.31	26.5	21.6
M-APTES-IPA	8.9	0.27	33.0	31.7

2.4 Prediction of MMM Performance

There are various models proposed in order to predict the gas permeability in mixed matrix membrane. Three-phase-Maxwell model, Higuchi model effective media theory and Bruggeman model have been proposed up to present [42, 43, 44]. Although the goal of these models is predicting the mixed matrix membrane performance accurately, they are not able to provide noteworthy improvement over classic Maxwell model which is presented below [44]:

$$P_{eff} = P_c \left[\frac{P_D + 2 P_C - 2\phi_D(P_C - P_D)}{P_D + 2 P_C + \phi_D(P_C - P_D)} \right] \quad (2.1)$$

where P_{eff} is the effective permeability in mixed matrix membrane, ϕ_D is the volume fraction and subscripts D and C refer to the dispersed and continuous phase, respectively [28]. The Maxwell predictions assume an ideal case between continuous and the dispersed phases without any defect and change in the properties of individual phases [45]. In spite of the fact that, this prediction is very useful in order to clarify the interface when it is compared with the experimental results.

Table 2.3 : Single gas properties of Silicalite-1 and Titanium-Silicalite-1 zeolites on a porous α -Al₂O₃ tubular support.

	Permeance (mol.m ⁻² .s ⁻¹ Pa ⁻¹)			Thickness (μ m)	Referance
	CO ₂	CH ₄	N ₂		
Silicalite-1	4.3 x10 ⁻⁶	6.4 x10 ⁻⁶	4.6 x10 ⁻⁶	2	[46]
Titanium-Silicalite-1	5.5x10 ⁻⁶	-	6.8x10 ⁻⁶	0.8	[21]

In the calculation of Maxwell model for predicting ideal mixed matrix membrane performance, the datas given in Table 2.3 were used as a single gas permeability of dispersed gas. By using the given thickness values, permeance datas are able to convert to permeability with the unit of Barrer.

3. METHODS AND METHODOLOGY

In this section, criteria considered during material selection and properties of selected materials are covered. Following with experimental procedure and characterization methods are presented.

3.1 Material Selection

The focus of this thesis is investigating the gas separation potential of titanium-silicalite-1 (TS-1), which has been mostly known as a heterogeneous catalysis for industrial oxidation reactions, in order to use as an inorganic filler in mixed matrix membranes (MMMs) application. In this respect, selection of polymer plays an important role in determining the performance of TS-1, because the minimum performance of the MMMs are highly dependent on polymer matrix.

3.1.1 Titanium-Silicalite-1 as an Inorganic Filler

Zeolites and carbon molecular sieves are the most commonly used inorganic fillers for mixed matrix membranes (MMMs). Most works have focused on the synthesis and characterization of MFI-type zeolites due to their suitable channel opening size and thermal stability which make them potentially useful for gas separation applications. MFI type zeolites also possess hydrophobic behaviour due to their Si/Al ratio of 20- ∞ . Titanium-silicalite-1 (TS-1) is the alumina-free form of MFI as silicalite-1 [47]. It is well known efficient catalyst for several oxidation reactions. With the incorporated titanium into zeolite framework, TS-1 zeolites are expected to exhibit interesting properties for the permeation and better interaction within the polymer matrix. TS-1 zeolites are in a quite new branch of MFI-type zeolites as inorganic fillers. Up to date, there is no article focused on the usage of TS-1 in MMMs.

3.1.2 Polymer Selection

Proper selections of inorganic filler and polymeric matrix are the most important key factor for creating synergistic combination in MMMs [48]. The minimum performance of the MMMs in which no defects are existed is fixed by the polymer properties [8]. Rubbery polymers such as poly(dimethyl siloxane), ethylene oxide / propylene oxide-amide copolymers are expected to show better interaction with inorganic fillers [48]. On the other hand, these polymers exhibit high permeability and low selectivities. Thus, their separation performances are at below the upper bound trade off curve [8]. Cellulose acetate, polycarbonates, polyimides, polysulfone, etc. belong to family of glassy polymers. This type of polymers are very attractive for gas separation applications due to their high gas selectivities. Although glassy polymers usually exhibit relatively lower permeability than rubbery polymers, their mechanical properties and selectivities are much higher than rubbery polymers. Therefore, glassy polymers are used in almost all industrial membrane gas separation process applications [48].

Among the glassy polymers, polyimides are good candidates for gas separation membranes with good permselective performance and good chemical, thermal and mechanical stability [28]. Matrimid[®]5218 is commercially available polyimides that is widely used in MMMs application. In the literature, introducing zeolite, carbon molecular sieve, fullerenes, mesoporous material, carbon aerogel, metal oxide nanoparticles and metal organic frameworks into Matrimid[®] network have been studied [49]. Moreover, 6FDA (4,4'-(Hexafluoroisopropylidene)diphthalic anhydride) based polyimides membranes offer excellent gas permeability and selectivity due to presence of bulky $-C(CF_3)_2-$ group which impedes the intrasegmental mobility, hamper interchain packing and stiffens backbone [28]. 6FDA based polyimides show higher permeability compared to Matrimid[®].

In this study, commercially available Matrimid[®] 5218, which consists of 3,3',4,4'-benzophenone tetracarboxylic dianhydride and diaminophenylindane monomers, was selected as one of the polymer material for preparing membranes and was purchased from Huntsman Advanced Materials Americas Inc. It is soluble in many common organic solvents such as N-methylpyrrolidone (NMP), N,N'-dimethyl formamide (DMF), N,N',dimethylacetamide (DMAc) and chloroform [50]. As the other polymer

material, 6FDA-DAM was chosen and it synthesized by our study group with molecular weight 200000 and polydispersity constant of 3.7. It is also soluble in N-methylpyrrolidone (NMP) and N,N'-dimethyl formamide (DMF) [51]. As a solvent, DMF which is able to solve both polymers used in this study was selected. The properties of DMF is given in Table 3.1. The chemical structure and glass transition temperatures of the polymers are given in Table 3.2. The performance of TS-1 particles in low and high permeable polymeric materials was desired to be investigated by selecting Matrimid[®] and 6FDA-DAM.

Table 3.1: Properties of solvent used in membrane preparation [52].

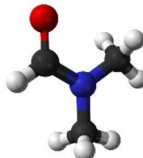
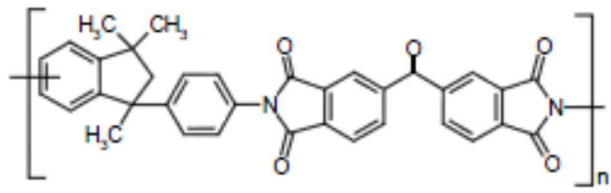
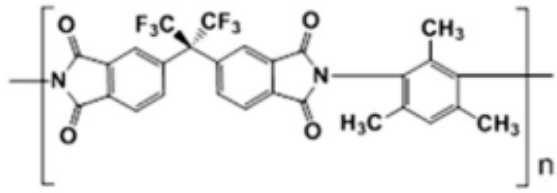
<i>N,N- Dimethyl- formamide</i> (DMF)	C_3H_7NO	
Molecular Weight (g mol⁻¹)	73.09	
Density (g cm⁻³)	0.949	
Boiling Point(°C)	153	
Vapor Pressure (kPa)	0.3	
Kinetic Diameter (Å)	5.2-5.5 [53]	

Table 3.2: Chemical structure and T_g values of polymers used in this work [51,52].

Polymer	Chemical Structure	T _g (°C)
Matrimid [®] 5218		308
6FDA-DAM		391

3.2 Titanium Silicalite-1 (TS-1) Synthesis

For TS-1 zeolites preparation, chemicals used are listed below with the purity and supplier :

- Tetraethoxysilane (TEOS), $(\text{C}_2\text{H}_5\text{O})_4\text{Si}$ - 99.9% - Alfa Aesar
- Titanium (IV) n-butoxide (TBOT), $\text{Ti}(\text{OCH}_2\text{CH}_2\text{CH}_2\text{CH}_3)_4$ - 99% - Acros Organics
- Tetrapropylammonium hydroxide (TPAOH), $(\text{CH}_3\text{CH}_2\text{CH}_2)_4\text{NOH}$, ~20% in water - Fluka
- Isopropanol, $(\text{CH}_3)_2\text{CHOH}$ - 99.8% - Merck

TS-1 zeolites were prepared by hydrothermal synthesis. The mother solution used to synthesize TS-1 particles was obtained by mixing two individually prepared solutions. Solution A, which is titanium source, was prepared by mixing desired amount of TEOS and TPAOH, while solution B, which is silica source, was prepared by mixing TBOT and 2-propanol. These two solutions were then mixed rapidly. After addition of water, it was stirring for 6-7 h at 65°C in order to complete the hydrolysis. After hydrolysis, different aging times such as 1, 2, 3 and 7 days and different aging temperatures such as room temperature, 40°C and 80°C were applied to the samples. Samples without applying any aging procedure were also prepared. The solution was then transferred into the autoclave for hydrothermal synthesis at different crystallization temperatures such as 140°C, 160°C and 180°C for 24 h. After hydrothermal synthesis, obtained crystals washed with distilled water and centrifuge was used to separate the powders from the solution. The TS-1 powders were dried at 120°C overnight. Template removal was carried out at 480°C for 24 h with the heating and cooling rate of 0.5°C/min. To synthesize powder with different ratio of Si/Ti such as 25, 50, 100 and 200, the amount of TBOT and 2-propanol varied while keeping the ratio of 2-propanol and TPAOH constant. The parameters that used in the experiments are summarized in the Table. 3.3.

3.3 Modification of TS-1 Fillers

The grafting procedure which was used in this study was previously reported by O.G, Nik et al. Firstly, 0.1 g / ml suspension of TS-1 in toluene was prepared and sonicated. Then it was transferred to round bottom flask and subjected to 1.5 h stirring. Nitrogen

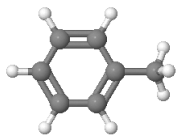
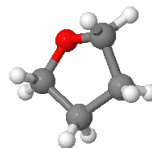
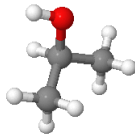
purge with condenser at ambient temperature was applied to the mixture, after 9 mmol APTES was added dropwise under stirring. After 24 h, the mixture was washed three times with anhydrous methanol, centrifuged 10 min at 20000 rpm and dried overnight at 80°C [38].

Table 3.3: The properties of synthesized TS-1 crystals.

Investigated Parameter	Si/Ti Ratio	Crystallization Temp. (°C)	Aging Temp. (°C)	Aging Duration (day)
Si/Ti Ratio	25	160	25	3
	50	160	25	3
	100	160	25	3
	200	160	25	3
Crystallization Temperature & Aging Duration	100	140	25	-
	100	140	25	1
	100	140	25	2
	100	140	25	3
	100	140	25	7
	100	160	25	-
	100	160	25	1
	100	160	25	2
	100	160	25	3
	100	160	25	7
	100	180	25	-
	100	180	25	1
	100	180	25	2
	100	180	25	3
100	180	25	7	
Aging Temperature & Aging Duration	100	140	40	1
	100	140	40	2
	100	140	40	3
	100	140	40	7
	100	140	80	1
	100	140	80	2
	100	140	80	3
	100	140	80	7

Toluene, tetrahydrofuran (THF) and isopropanol with dielectric constants 2.4, 7.6 and 19.9 were used in the modification of TS-1 powders as a solvent, respectively. As it is discussed in Chapter 2, the higher the polarity of the solvent, better performance of the modified zeolites was expected to be obtained [38]. Properties of the solvents are given in the Table 3.4.

Table 3.4: Properties of the solvents used in modification of TS-1 powders.

Solvents	Toluene [54]	THF [55]	Isopropanol [56]
Molecular Structure			
Molecular Formula	C ₇ H ₈	C ₄ H ₈ O	C ₃ H ₈ O
Molecular Weight (g/mol)	92.14	72.11	60.10
Density (g/ml)	0.87	0.89	0.79
Boiling Point (°C)	111	66	82.6
Dielectric Constant	2.4	7.6	19.9
Kinetic Diameter (Å)	6.1 [57]	4.63 [58]	4.5 [58]

3.4 Membrane Formation

General procedure for formation of a flat sheet dense membrane can be described as the following steps:

- Preparation of homogenous filler/polymer mixture (no zeolite in the case of neat membranes)
- Casting of solution on a smooth surface,
- Evaporation of solvent,
- Annealing at high temperatures.

It is difficult to create a standard protocol for formation of MMMs because every filler-polymer pairs with different solvents possess various behaviour. The detail of aforementioned general procedure can be modified based on the selection of the materials using in the formation of MMMs [45].

3.4.1 Formation of Pure Polymer Films

In this research, pure polymer films were prepared in order to determine the performance of the continuous phase of MMMs and to use as a reference for comparison with inorganic filler loaded MMMs. Matrimid[®] and 6FDA-DAM polymers were primarily dried in vacuum overnight at 110°C and 200°C, respectively. Desired amount of polymer and solvent (DMF) were used to acquire 15 wt.% polymer ratio. According to conventional solution-casting technique, the required amount of polymer was added into the particular amount of DMF solution in 5 equal portions with 2 h intervals to have an effective dissociation. The solution was then left to stir overnight on magnetic stirrer. Afterwards, the film solution was poured on a smooth mirror surface and cast into a film by the help of film casting blade and apparatus. Initial thickness of the blade was adjusted as 500 µm. The film swiftly placed into a oven at 80°C for a 3 hours until it was able to peel off from the mirror surface. It was subsequently placed in the oven again and dried at 80 °C overnight. The pure polymer film was then heated to 130°C with 0.5 °C/min heating rate and annealed at this temperature for 4 days under vacuum in order to remove the residual solvent completely. After cooling down to ambient temperature naturally, the pure polymers was kept in desiccator. It was obtained that the average thickness of the films were approximately 35 µm after annealing treatment.

3.4.2 Formation of Mixed Matrix Membranes (MMMs)

MMMs with containing TS-1 as an inorganic fillers were reported for the first time in this study. Therefore, the preparation method of the MMMs was decided based on the previous MMMs study of our research group due to lack of published literature [51-52, 61]. TS-1 fillers, Matrimid[®] and 6FDA-DAM polymers were primarily dried in vacuum overnight at 110°C and 200°C, respectively. All the MMMs were prepared containing 20 wt. % TS-1 as inorganic fillers. The desired amount of TS-1 fillers were dispersed in DMF by mechanical stirring. Well dispersed suspension was acquired by bath sonication for 30 min. The required amount of polymer to ensure 15/85 polymer/solvent ratio, was added in 5 portions with 2 h intervals into the dispersion. Subsequently, the same casting, heat and annealing treatment procedure as the preparation of pure polymer film was applied to the MMMs. In Figure 3.1, the membrane preparation procedure for MMMs containing TS-1 is depicted.

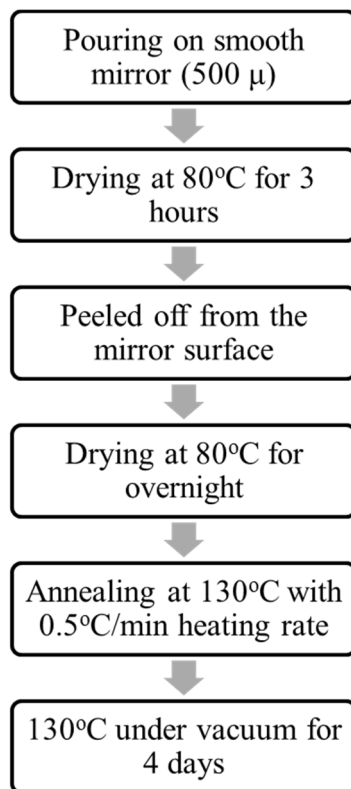


Figure 3.1: Preparation procedure of MMMs containing TS-1 fillers.

3.4 Characterization

In this section, characterization methods for both TS-1 zeolites and the membranes were presented. First of all, investigation of TS-1 synthesis and its potential as a inorganic filler in MMMs was examined in detailed. Secondly, typical characterization techniques were performed to membranes in order to determine their transport properties.

3.5 Characterization of TS-1 Fillers

Structural analysis of TS-1 crystals were performed by X-ray diffraction (XRD), fourier transform infrared spectroscopy (FTIR), scanning electron microscopy (SEM) and dynamic light scattering (DLS).

3.5.1 Powder X-Ray Diffraction

Powder diffraction is the most common characterization technique applied to solid state samples in order to identify and characterize materials. In this method, a crystal which possesses regular repeating units is irradiated by monochromated X-ray beam, a unique diffraction peak is then generated. Each material has different diffraction peak

which can be called as a fingerprint of the material. By this diffraction process, it is possible to identify crystalline components of a sample [60].

In this study, XRD analysis for TS-1 particles were performed in order to compare with the ones reported in the literature to decide the success of the synthesis. Panalytical X'Pert PRO diffractometer using $\text{CuK}\alpha$ ($\lambda=1.54\text{\AA}$) radiation in the 2θ range between 5° and 50° .

3.5.2 Fourier Transform Infrared Spectroscopy

In this method, a sample is exposed to infrared radiation, some of the infrared radiation is absorbed by the sample, while some of it transmitted. The wavelength of the absorbed beams which can be measured by a detector is specific for the material, thus it can be called a molecular fingerprint. This molecular fingerprint of the sample can be obtained via the resulting spectrum which depicts the molecular absorption and transmission of the material.

In this study, FT-IR spectrums of TS-1 samples were obtained for confirmation of Ti substitution into the zeolite structure of synthesized TS-1 crystals and verification of modification reaction of TS-1 samples. FT-IR analysis were performed with Perkin-Elmer Spectrum One was in the range of $400\text{-}4000\text{ cm}^{-1}$ wavelength by preparing potassium bromide (KBr) pellets which are transparent in the infrared region.

3.5.3 Scanning Electron Microscopy

The scanning electron microscope (SEM) is one of the most essential characterization technique with respect to its superior ability for visualization of the surface of a material that is almost identical to the reality. In general, the resolution of a SEM is approximately a few nms and magnification which can be easily adjusted vary between $10\text{x-}300000\text{x}$ [61].

In this study, Hitachi S4700 type SEM was used for the purpose of morphological characterization of synthesized TS-1 samples, while and JEOL JSM-6390LV type was used for membrane samples. Samples were attached on a sample holder with an adhesive carbon foil and coated with gold for TS-1 samples and platinum for membrane samples for 4 min at 15 mA with the help of Emitech K550x instrument, in

order to assure conductivity. Samples were then characterized under high vacuum and a potential difference of 10 kV, at magnifications x3000 and x20000.

3.5.4 Dynamic Light Scattering

Dynamic light scattering (DLS) is the process for measuring particle size of the particles, which have been dispersed or dissolved in a liquid with respect to their Brownian motions. When the laser beam applies to the sample, the laser beam scatters at different intensities due to Brownian motion of the particle. In this technique, Brownian motions are measured and relates with the particle size of the sample [62].

In this study, Malvern Zetasizer Nano-S was used in order to obtain particle size distribution of the TS-1 particles and all measurements were repeated 5 times. Suspensions of 1.0 g.L⁻¹ of the TS-1 samples dispersed in distilled water were sonicated for 30 min.

3.5.5 Volumetric and Gravimetric Sorption

Nitrogen adsorption-desorption isotherms at 77 K were obtained using Accelerated Surface Area and Porosimetry System (ASAP, 2050 V5.03). Bare TS-1 and modified TS-1 samples were previously degassed at 300°C and 150°C, respectively, for 24 h under the vacuum. The specific area, external area and micropore volume were calculated based on the Brunauer-Emmett-Teller (BET) model and t-plot model based on Harkins-Jura equation. The adsorption isotherms were also analyzed by linear form of the Langmuir equation:

$$\frac{p}{q} = \frac{1}{q_m} + \frac{1}{b * q_m} \quad (3.1)$$

Where p is the adsorbate pressure in kPa, q is the amount adsorbed in mmol per unit mass of the adsorbent. In the theoretical Langmuir description, q_m is the maximum adsorbed concentration corresponding to a complete monolayer coverage. When Langmuir equation is applied to a microporous solids, q_m is the maximum capacity of adsorption in the micropores. Parameter b is designated as the affinity constant or

Langmuir constant. It is a measure of how strong an adsorbate molecule is attracted onto a surface [38].

Intelligent gravimetric analyser (IGA) is another tool for determining the sorption properties of the materials. Its superior characteristic of accurately gravimetric measuring technique surpasses the volumetric sorption methods. Working principle of this technique can be explained briefly as follows: Pressurising the measurement chamber to the active setpoint and monitoring deviations in weight of the sample. When the deviations reaches minimum, the weight is recorded with respect to equilibrium assumption at that point. Thus, the sorption capacity of the sample for the specific gas at that temperature and pressure can be obtained. Analysis will continue with the next set point. By collecting the sorption capacities of the sample at constant temperature and various pressures, sorption isotherm of the material will be acquired.

In this study, IGA (Hiden Isochema, Model IGA-001) was used in order to characterize the sorption behaviour of the TS-1 fillers. The analysis were performed with the gases N₂, CH₄ and CO₂. Prior to the measurement sequence, all samples degassed which includes heating up to higher temperatures in vacuum to remove the sorbed gases from the samples. The degassing procedure follows this procedure: The sample was heated up to 150°C with the heating rate 1°C/min and then kept in this temperature for overnight. After degassing part was completed, the sample heated to analysis temperature 35°C. The weight of the degassed sample was tared and the measurement sequence performed in the range of adjusted pressures, in this case between 0-6 bars.

3.6 Membrane Characterization

Thermal properties of the membranes was primarily investigated with thermogravimetric analysis (TGA) and dynamic light scattering (DSC). Morphological characterization was performed with the help of SEM which is briefly explained in the previous section. Finally, transport properties of the samples were determined by using gas permeation system for both single gas and binary gas mixtures. Aforementioned membrane characterization techniques are described in detail in the following sections.

3.6.1 Thermal Characterization

Amount of residual solvent in the membrane samples were determined with TGA, whereas glass transition temperatures were identified by DSC.

3.6.1.1 Thermogravimetric Analysis

Thermogravimetric analysis (TGA) is a technique where the mass of a sample is measured as a function of time or temperature, while the sample is exposed to adjusted temperature programme in a controlled atmosphere. TGA is such an essential instrument that it gives information about the composition, extent of cure, and thermal stability. By the help of TGA, volatile components in a sample such as absorbed moisture, residual solvents, or low-molecular-mass additives or oligomers can be determined between ambient temperature and 300°C.

In this study, TGA measurements of MMMs were carried out with a Perkin-Elmer Diamond TG/DTA. A small amount of membrane was weighed and analysed between 30°C and 550°C with a heating rate 10°C/min under flowing nitrogen (N₂) of 100 ml/min. The resulted thermogram was used to determine the amount of residual solvent and moisture in the sample.

3.6.1.2 Differential Scanning Calorimetry Analysis

Differential Scanning Calorimetry is a very common thermal analysis technique mostly used for determination of glass transition (T_g) temperature and also for melting (T_m), crystallization (T_c) temperatures, and a heat of fusion for polymeric samples with respect to changes in specific heat capacity in the material. According to ASTM standard E473, DSC is a technique in which the heat flow difference into a substance and a reference material is measured as a function of temperature while the substance and reference material are subjected to a controlled-temperature program [63]. The glass transition temperature (T_g) is the temperature at which the behaviour of the polymer changes from glassy state, in which only vibrational motion of chain segments is active, to rubbery state, in which translational motion of polymer chain segments becomes active. This transition is accepted as second-order-transition because heat capacity jump is observed at the glass transition temperature [63].

DSC contains two heat sensitive plates in a furnace with thermocouples attached to the base of this holders. Sample and reference pans are sealed, and then placed into the holders. The analysis carried out by measuring temperature difference between the sample and reference pans as a function of temperature or time under controlled thermal conditions. The temperature difference is related with the change in heat flux. Phase transformations in the material causes the temperature difference between sample and reference. Thus, T_g of polymers can be measured easily with respect to differential increase in the heat capacity of the sample because of molecular motion in the polymer [64].

In this work, DSC measurements were performed with a Perkin Elmer Diamond Series DSC. The effect of introducing fillers into the polymer matrix on T_g was investigated in order to clarify the behaviour of the interface between zeolite and polymer matrix. Heating sequence were designed for each polymer with following these instructions [64]:

- Heating the sample to a temperature at least 15 to 30 °C above T_g .
- Annealing at this temperature for 5-10 min in order to delete the thermal history of the sample.
- Rapid cooling to a temperature at least 50°C below T_g .
- Re-heating the sample to a temperature above the predictable T_g with a constant rate.

Summarized heating sequences for each polymer can be found in Table 3.5. This procedure was carried out under inert N_2 atmosphere and T_g values was calculated by half C_p extrapolation method.

Table 3.5: Heating sequence for DSC measurements.

	Matrimid®	6FDA-DAM
Estimated T_g	308°C	390°C
Step 1: Heating	From 30 °C to 330°C, 20°C/min	From 30 °C to 410°C, 20°C/min
Step 2: Annealing	At 330 °C for 5 min	At 410 °C for 5 min
Step 3: Cooling	From 330 °C to 260 °C, 20 °C/min	From 410 °C to 230 °C, 20 °C/min
Step 4: Re-heating	From 260 °C to 400 °C, 10 °C/min	From 230 °C to 400 °C, 10 °C/min

3.6.2 Gas Permeation Measurement

The permeability measurements were carried out with in-house constant-volume-variable-pressure system which is depicted in Figure 3.2. The system is capable of measuring both single and mixed gas measurements for pure polymeric and mixed matrix membranes. The permeation system includes permeation cells, upstream and downstream transducers which measures the feed and permeation pressures, respectively, data acquisition system that collects the feed and permeate pressures per minute, and gas chromatograph which is used to identify the gas composition of mixed gas. The principle of measuring the permeability through constant-volume-variable-pressure system can be explained as following: The gas permeates through the membrane into a leak-tight container of calibrated-known volume. The rate of pressure increase can be converted to a molar flux by the help of Equation 3.2

$$P_i = \frac{(\alpha_m - \alpha_l) * V * l}{A * R * T * \Delta P} \quad (3.2)$$

where α_m is the rate of pressure increase in permeate during measurement, α_l is the rate of leak in the permeate side, V is the calibrated volume of the permeate side of the system, l is the thickness of the membrane, A is the permeation area of the membrane film, R is the ideal gas constant, T is the measurement temperature, and ΔP is the pressure difference between permeate and feed side of the system which can be referred as a driving force.

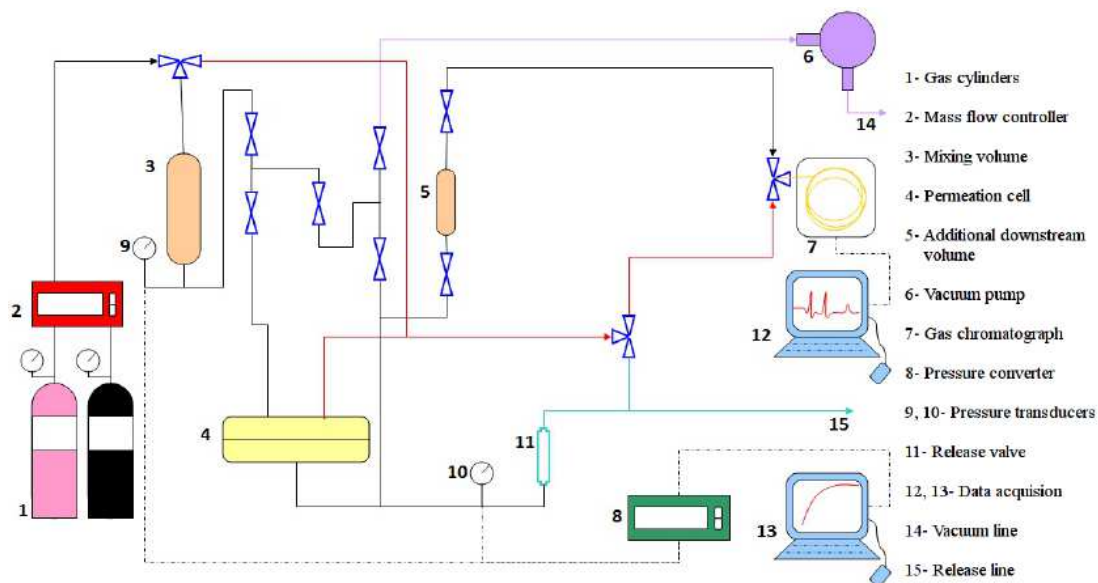


Figure 3.2: In-house constant-volume-variable-pressure system.

3.6.2.1 Leak Measurements

The leak measurement plays an important role for obtaining accurate permeability results. Although many precaution against the leakage were taken, the amount of gas leaking through the downstream side of the system must be taken into account. For application of a leak test, a sheet of impermeable aluminum sheet with one adhesive face was attached to the lower half of the cell, and then placing the upper half, the cell was sealed. The cell is connected to the system through Swagelok[®] VCR fittings using brand new stainless steel gaskets, which are leak tight equipment of the downstream side. Evacuation of permeate and feed side was applied to the system for overnight to remove the sorbed gases from the cell and the piping. In order to accelerate the period of measurements, CO₂ which is the fastest gas with respect to its kinetic diameter was used for the leak measurements. After the gas introduced to the system, the pressure increase in the permeate side of the system in spite of impermeable aluminum sheet was a result of a leak and it was recorded constantly. The leak rate was then subtracted from the rate of pressure increase, while calculating the permeability of the membrane.

3.6.2.2 Masking of Membranes

The membrane films were masked for permeation measurements, because the area of the membrane through where the gas permeate must be exactly known and controlled for accuracy of permeability calculations. A circle slightly smaller than the area of the membrane was cut out from impermeable aluminum sheet, and membrane film was placed on the adhesive face of the sheet. Another smaller piece of aluminum sheet in the shape of ring cut out was affixed to the other side of the membrane film in order to create impermeable area to control the active membrane film area. At last, boundary between membrane and aluminum sheet was sealed with epoxy to prevent leak from these connection parts. The masked membrane became ready after waiting for 24 hours, until epoxy was completely hardened.

3.6.2.3 Single Gas Measurement

The masked membrane was placed between two halves of permeation cell for single gas measurements. On both side of the permeation cell, there was O-rings in order to lessen leak. After the masked membrane attachment to lower half of the permeation

cell, the upper half of the cell was placed and then the cell was sealed. The cell attached to the system through Swagelok® VCR fittings using brand new stainless steel gaskets, which are leak tight equipment of the downstream side. Evacuation step which was applied using vacuum pump to both upstream and downstream took several hours in order to be ensure about removing residual solvent and sorbed gas. Afterwards, connection of upstream and downstream was cut and the gas fed to the upstream. Accelerating the time which was necessary for gas molecules to fill the free volume of the membrane was achieved by evacuation of the downstream side for several time prior to measurement. Observation of linear pressure increase in the downstream indicates that the membrane reaches steady-state. When the delta of three consecutive measurements was less than 1%, the rate of pressure increase in the downstream was accepted as it reached steady state and average of these measurements was used in Equation 3.1 for calculating permeability.

All single gas measurements were performed at 35°C and 4000 mbar upstream pressure. The film thickness was measured by using Byko-test 8500 coating thickness gauge. Ideal selectivity of membrane for gas pairs can be calculated by using ratio of single gas permeabilities, which can be expressed:

$$\alpha_{i/j} = P_i / P_j \quad (3.3)$$

3.6.2.4 Mixed Gas Measurement

The result of mixed gas measurements are very valuable in order to decide real performance of the membrane by converging the real application conditions. Mixed gas measurements can be different comparing with ideal properties of the membrane due to some possible reasons such as competitive sorption and diffusion, plasticization effect, and concentration polarization.

General principles of mixed gas measurement are identical to single gas measurements. However, adjusting and maintaining the feed composition, and analysing the permeation composition are the aspects from which the mixed gas measurements differ.

First of all, the gas mixture with desired gas pair prepared by feeding one of the gas to the tank up to corresponding pressure and adding the other gas to the tank up to final pressure. Prior to introducing the gas mixture to the membrane film, composition of the mixture was controlled by the help of gas chromatography (GC) tool which has been already connected to the permeation system. Feed composition of the mixture was measured both at the beginning and at the end of the measurements to ensure that the composition did not change excessively. Secondly, after ensuring the mixed gas compositions with at least three consistent measurements, the mixture was fed to the membrane cell. Steady-state approach was also applied in the mixed gas measurements. As it was aforementioned, after the rate of pressure increase in downstream side of the membrane cell was constant which means that the membrane reached steady state, the permeate sample was injected to GC at pressures of approximately 10 mbar in order to obtain composition of permeate and also real selectivity values of the membrane for desired gas pairs.

In this study, Agilent Technologies 7890 A GC system was used. Direct gas injections and fluid injections can be measured via GC. Prior to using GC, calibration with a standard mixture was required. As detectors, flame ionization detector (FID) which measure the combustion energy of compounds in hydrogen flame and thermal conductivity detector in which CO₂ is detectable were used. Helium was used as a carrier gas, whereas hydrogen and synthetic air were used as detector gases. Actual selectivity can be calculated with the following equation based on gas chromatography results:

$$\alpha^*_{i/j} = \frac{y_i/y_j}{x_i/x_j} \quad (3.4)$$

where y_i and y_j are the mole fractions of the component i and j in the downstream while x_i and x_j are the corresponding mole fractions in the feed stream [65].

4. RESULTS AND DISCUSSION

4.1 TS-1 Synthesis and Characterization

Titanium-silicalite-1 (TS-1) crystals are desired to use as an inorganic filler in the mixed matrix membrane application. Morphological properties of fillers have an important role in mixed membrane formation. Therefore, in this part of this thesis it is focused on obtaining fillers with small size and narrow particle size distribution. Effect of Si/Ti ratio, crystallization temperature, aging (aging temperature and duration) on these desired properties were investigated. Hydrothermally synthesized TS-1 crystals were characterized by XRD, SEM, FTIR and DLS. Volumetric and gravimetric sorption analyzer were also performed to determine sorption characteristic of the fillers.

XRD pattern of TS-1 crystals crystallized at 140°C with Si/Ti molar ratio 100 and aged at 40°C for 3 days is depicted in Figure 4.1 with comparison of literature [66]. The presence of MFI structure was detected by XRD patterns in which all the samples exhibit the characteristic peaks ($2\theta = 7.9^\circ, 8.8^\circ, 23.1^\circ, 23.9^\circ, 24.4^\circ$) which represent the TS-1 structure [13]. XRD results are also confirmed that all the samples are 100% titanium silicon oxide. No peaks at $2\theta = 25.3^\circ, 37.9^\circ, 48.4^\circ$; which are the fingerprint of the existence of anatase TiO_2 phase, were detected [13]. Therefore, XRD results demonstrate that TS-1 samples were synthesized without any impurities or other crystal phases. In Appendix A, all the XRD patterns of samples possess MFI structure can be found.

Figure 4.2–4.8 show the morphology of synthesized TS-1 samples and average particle sizes of the samples which were calculated from SEM images are given in Table 4.1. In general, a great majority of samples have good particle size distribution with the parallel epipeds with rounded edges which is typical for TS-1 [10]. On the other hand, the TS-1 particles which were synthesized with different Si/Ti molar ratios of 25, 50

and 200 have undesired size distribution and their particle size varies in the wide range of 500-2000 nm (Table 4.1). The SEM images of the zeolites with different Si/Ti molar ratios are given in the Figure 4.2. As it can be seen from the Figure 4.2 (a), TS-1 with the molar ratio Si/Ti=25 shows non-uniform particle size and shape. From the results, it can be inferred that the high content of Ti in the mother solution produce higher particle size distribution of particles. Despite the sample which was prepared with the Si/Ti molar ratio of 50 (Figure 4.2 (b)) presents uniform particle size distribution compares the others, the particle size was approximately 1200 nm which is relatively larger than the desired particle size for being used as a filler in MMMs formation. Uniform crystals are not achieved with low concentration of Ti which can be seen in Figure 4.2 (c). Therefore, Si/Ti ratio is selected as 100 in the synthesis of TS-1 zeolites for further investigation of parameters have influence on particle size (Figure 4.2 (d)).

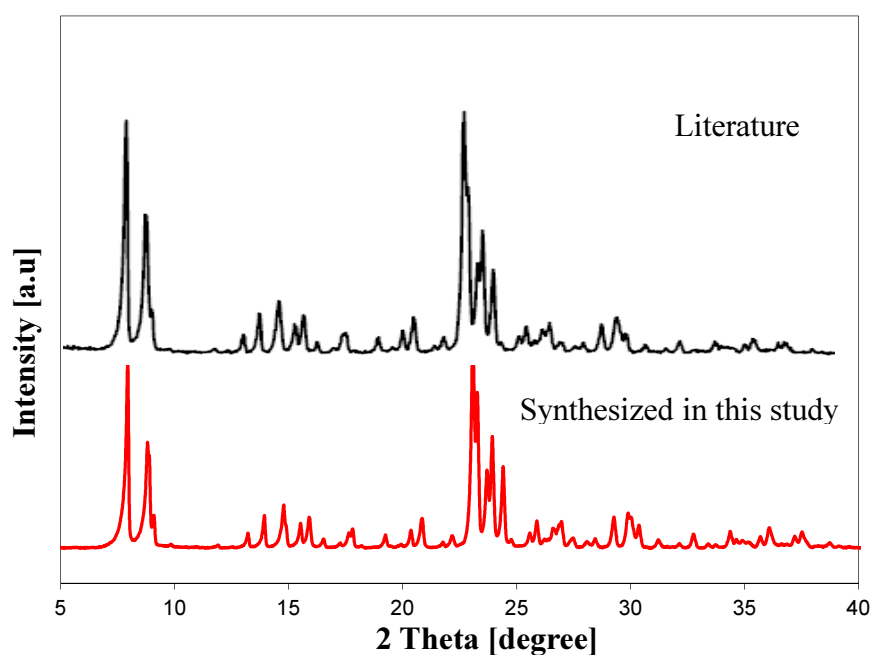


Figure 4.1 : XRD Patterns of TS-1 zeolites; literature [66] and synthesized in this study ($T_c=160^\circ\text{C}$, Si/Ti=100 and $T_{\text{aging}}=40^\circ\text{C}$, $t_{\text{aging}}=3$ days).

The effect of crystallization temperature was also investigated in this study. As it was derived from the Figure 4.3, crystallization temperature is not so influential on the particle size and morphology of the zeolites. The average particle size of the powders which is obtained from SEM images are in the range of 800-1500 nm, 650-1000 nm and 650-1000 nm for the crystallization temperature of 140°C , 160°C and 180°C , respectively (Table 4.1). Due to independence of particle size from crystallization temperature, 140°C can be suitable to obtain TS-1 samples with small particle size and narrow particle size distribution

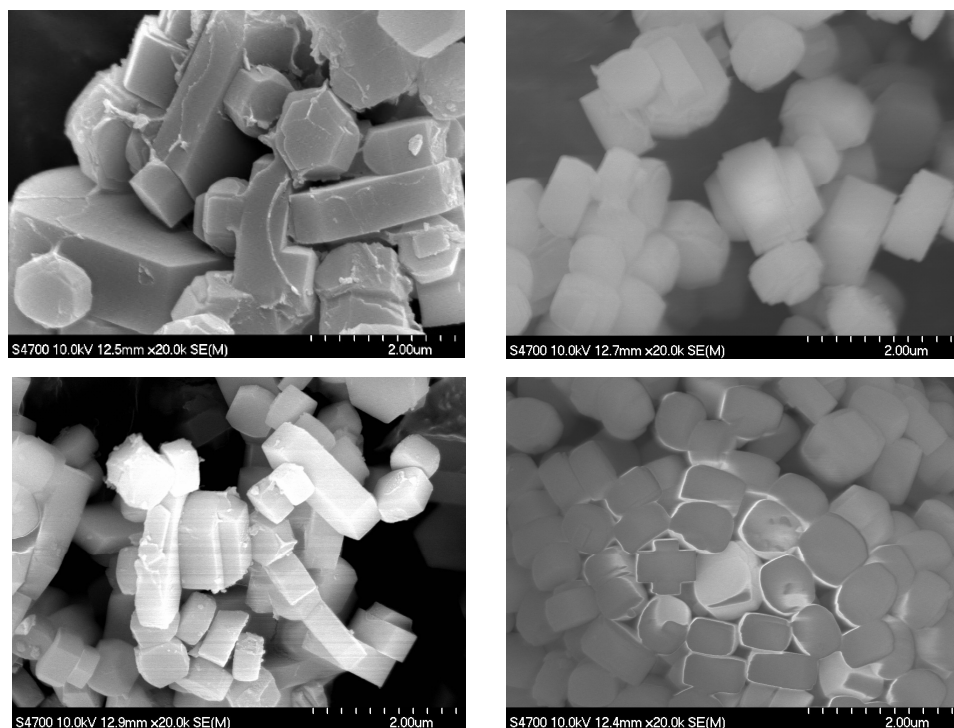


Figure 4.2 : SEM pictures of TS-1 samples prepared under different Si/Ti molar ratios (a) 25, (b) 50, (c) 200, (d) 100. The crystallization temperature 160°C, aging at room temperature for 3 days.

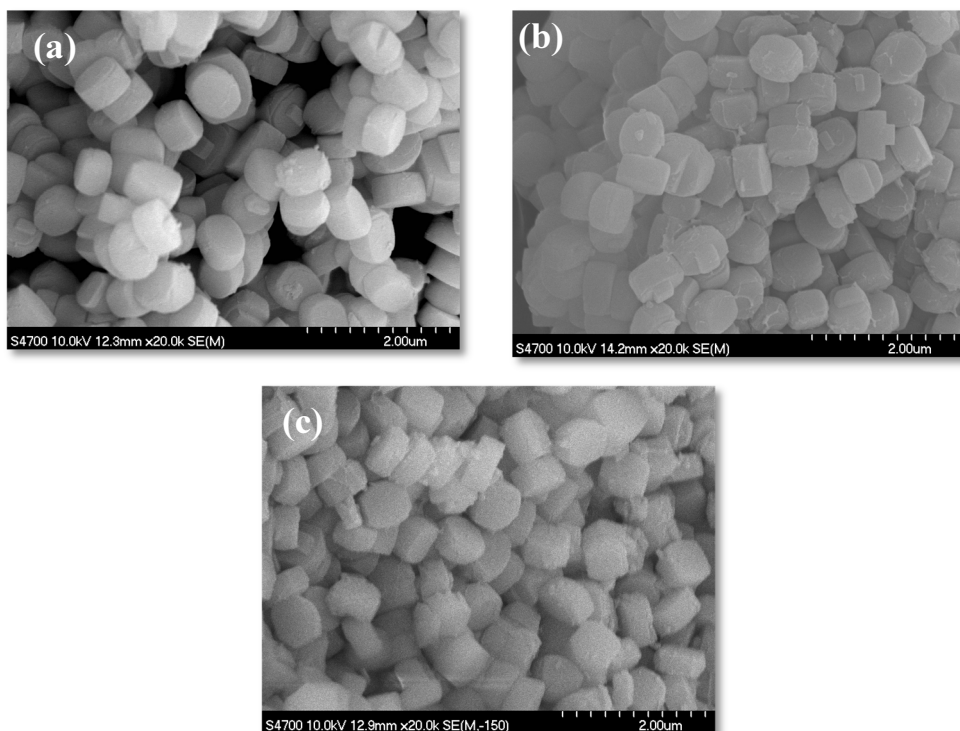


Figure 4.3 : SEM images of TS-1 samples prepared under different crystallization temperatures, (a) 140°C, (b) 160°C, (c) 180°C. Aging at room temperature for 7 days.

In this work, the effects of aging time and aging temperature were also examined. Aging is defined as the duration between homogenous mixing of the reactants and crystallization step and have effect on the nucleation and crystal growth kinetics which may result as reduction of crystal size [67]. The SEM images indicate that particle size is strongly affected by aging time. As it can be seen in Table 4.1, the smallest particle size is obtained when the aging duration was 7 days. The particle size of the TS-1 zeolites decreases when the aging time increases. Same phenomenon was also observed for different crystallization temperatures (Figure 4.4 - 4.6).

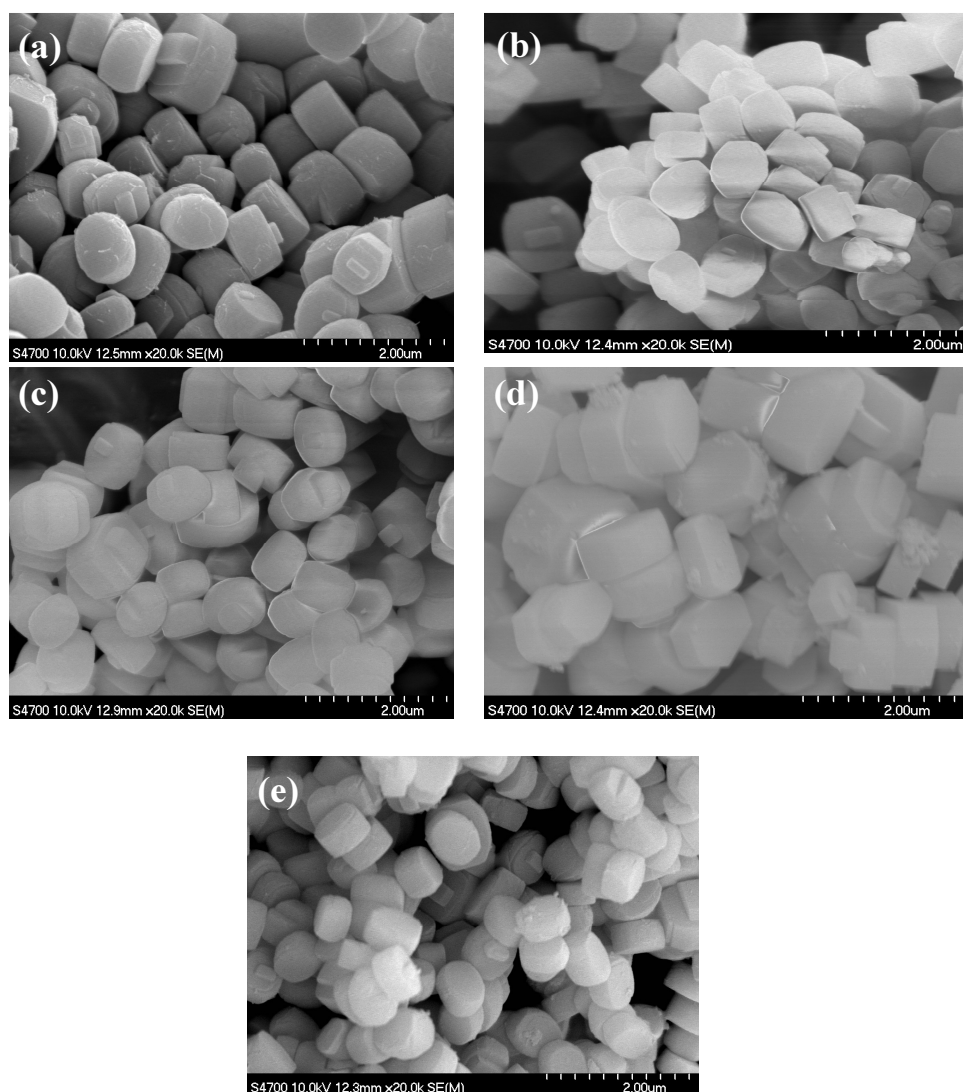


Figure 4.4 : SEM pictures of TS-1 samples prepared under different aging time, (a) no aging, (b) 1 day, (c) 2 days, (d) 3 days, (e) 7 days. The crystallization temperature 140°C and aging at room temperature.

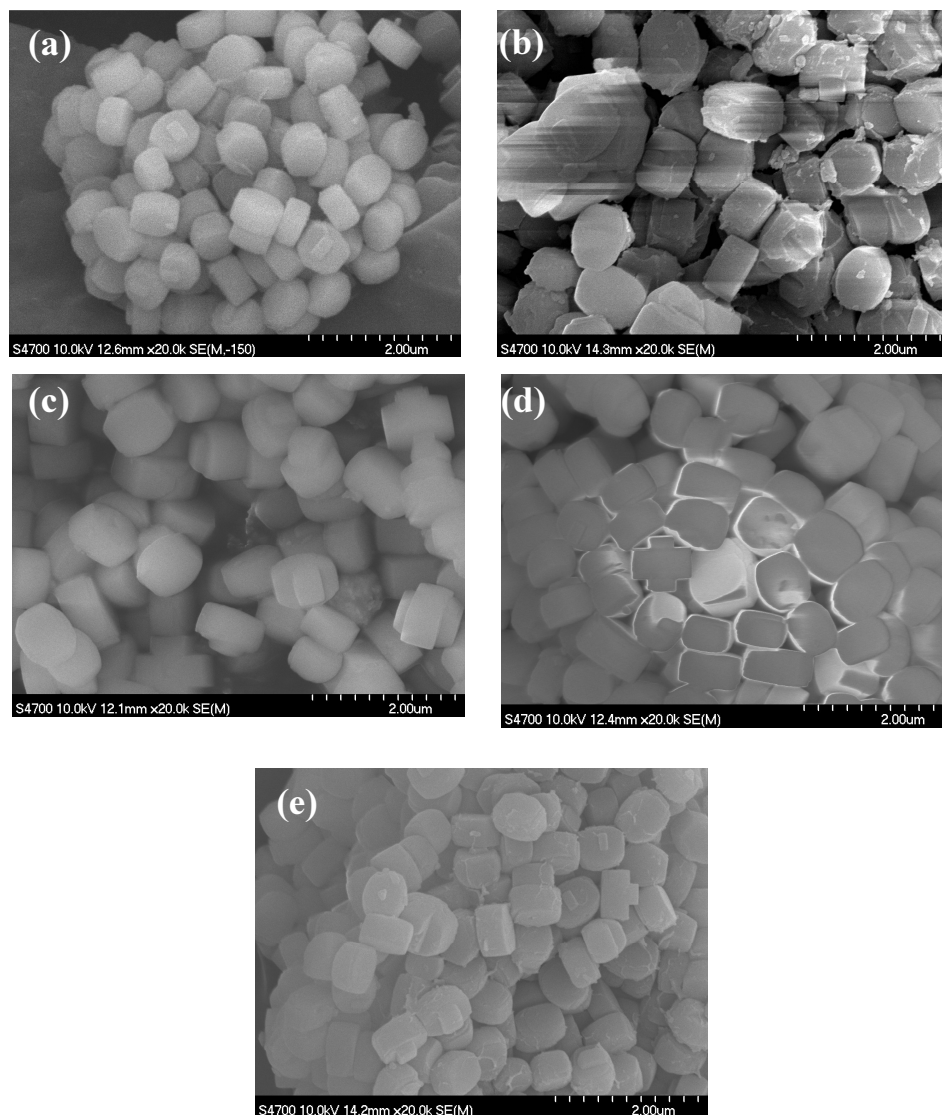


Figure 4.5 : SEM pictures of TS-1 samples prepared under different aging time (a) no aging, (b) 1 day, (c) 2 days, (d) 3 days, (e) 7 days. The crystallization temperature 160°C and aging at room temperature.

Considerable influence of aging temperature and duration on particle size can be clearly seen from Figure 4.7 and 4.8 for aging at 40°C and 80°C, respectively. The range of particle size of these samples are 330-650 nm with a good size distribution (Table 4.1). Particle size of TS-1 samples shows a decreasing trend with increasing the aging temperature and aging duration. As a result of increasing nucleation, smaller particle size can be obtained with higher aging temperatures.

To sum up, SEM images demonstrated that more uniform particles can be obtained, when Si/Ti ratio is selected as 100. Furthermore, crystallization temperature of hydrothermal synthesis has no impact on reducing particle size of the samples.

Aforementioned results shows that aging – both temperature and duration – has a noteworthy impact on morphology. Increasing aging temperature from room temperature to 40°C and 80°C resulted approximately 60% - 40% reduction in mean particle size of the TS-1 samples, respectively.

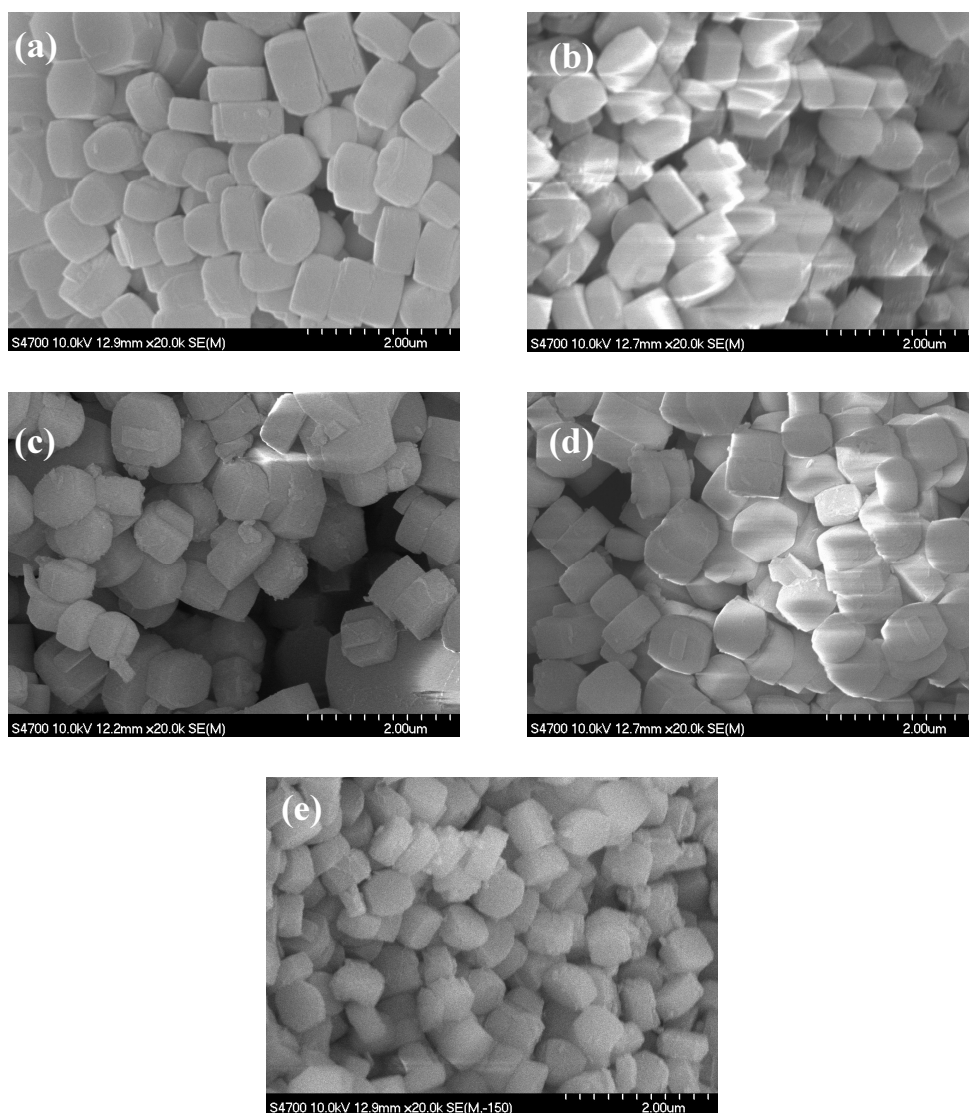


Figure 4.6 : SEM pictures of TS-1 samples prepared under different aging time, (a) no aging, (b) 1 day, (c) 2 days, (d) 3 days, (e) 7 days. The crystallization temperature 180°C and aging at room temperature.

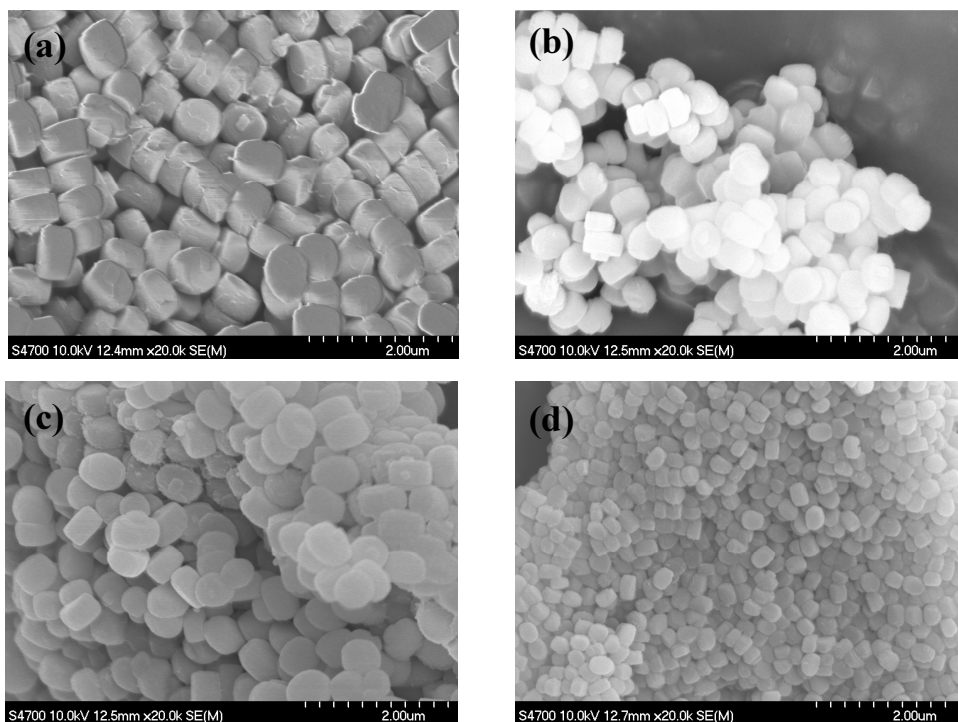


Figure 4.7 : SEM pictures of TS-1 samples prepared under different aging time (a) 1 day, (b) 2 days, (c) 3 days, (d) 7 days. The crystallization temperature 140°C and aging at 40°C.

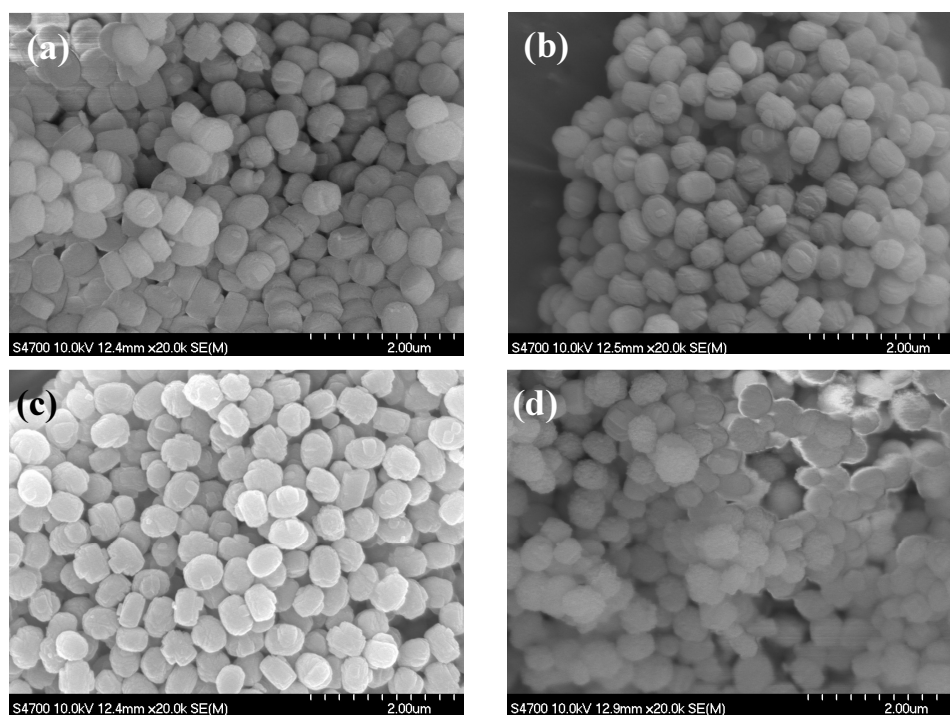


Figure 4.8 : SEM pictures of TS-1 samples prepared under different aging time: (a) 1 day, (b) 2 days, (c) 3 days, (d) 7 days. The crystallization temperature 140°C and aging at 80°C.

Table 4.1: Particle size of the TS-1 samples synthesized in different conditions.

Investigated Parameter	Si/Ti Ratio	Crystallization Temp. (°C)	Aging Temp. (°C)	Aging Duration (day)	Mean Particle Size (nm)
Si/Ti Ratio	25	160	25	3	1000 - >2000
	50	160	25	3	1200
	100	160	25	3	800
	200	160	25	3	500-2000
Crystallization Temperature & Aging Duration	100	140	25	-	950
	100	140	25	1	850
	100	140	25	2	850
	100	140	25	3	1500
	100	140	25	7	800
	100	160	25	-	700
	100	160	25	1	1000
	100	160	25	2	850
	100	160	25	3	750
	100	160	25	7	650
	100	180	25	-	900
	100	180	25	1	800
	100	180	25	2	1000
	100	180	25	3	800
	100	180	25	7	650
Aging Temperature & Aging Duration	100	140	40	1	650
	100	140	40	2	500
	100	140	40	3	500
	100	140	40	7	330
	100	140	80	1	550
	100	140	80	2	550
	100	140	80	3	600
	100	140	80	7	500

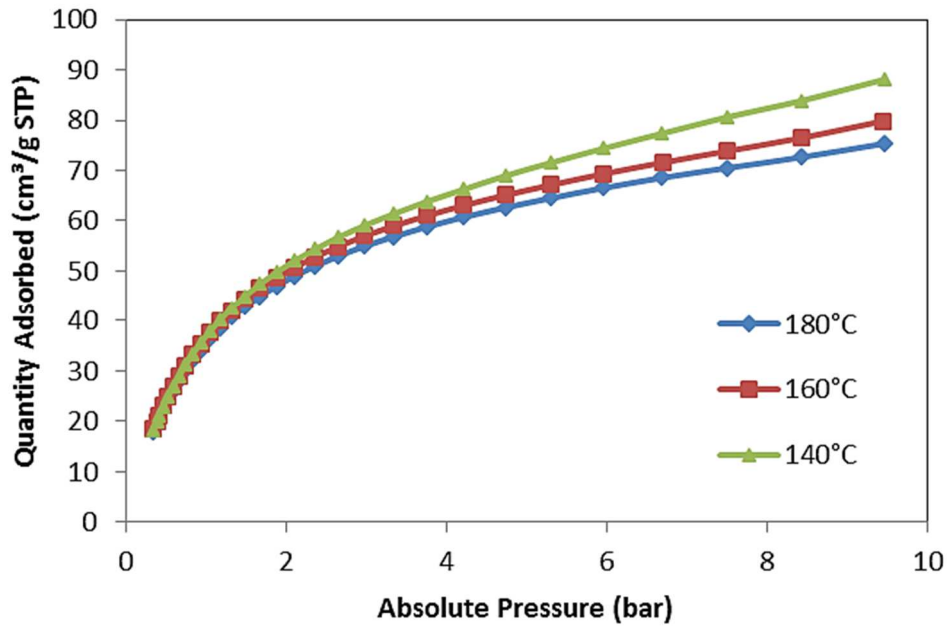


Figure 4.9 : Effect of crystallization temperature on CO₂ adsorption at 30°C, Si/Ti=100, aging time 3 days aging at room temperature.

In order to investigate the effect of the different molar ratios, aging times and aging temperatures, volumetric sorption analyses were examined for the related samples. The Figure 4.10-12 demonstrates that different molar ratio Si/Ti, aging time and aging temperature do not have significant influence on CO₂ adsorption. The isotherms show that the differences in adsorbed CO₂ amount are negligible, while molar ratio, aging duration and aging temperature vary.

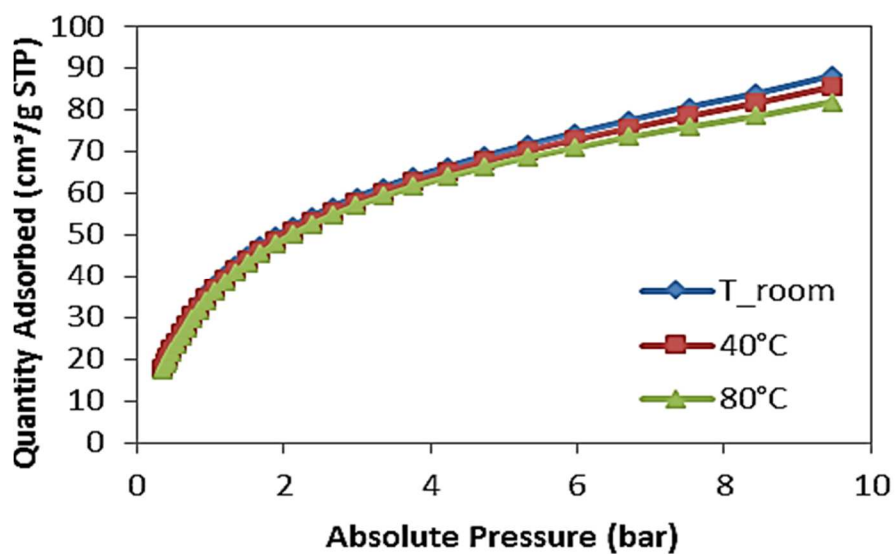


Figure 4.10 : Effect of aging temperature on CO₂ adsorption at 30°C, Si/Ti=100, crystallization temperature 140°C, 3 days aging time.

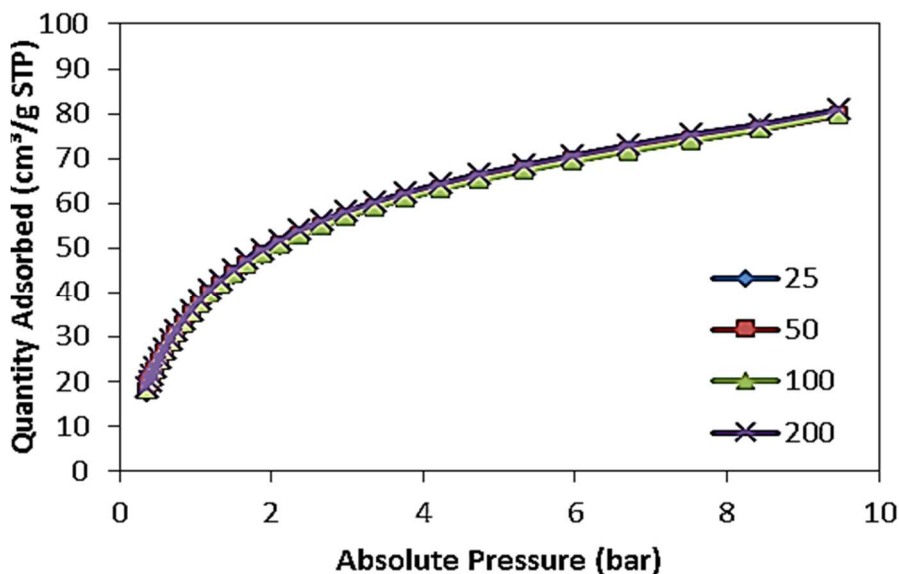


Figure 4.11 : Effect of molar ratios on CO₂ adsorption at 30°C, crystallization temperature 160°C, 3 days aging at room temperature.

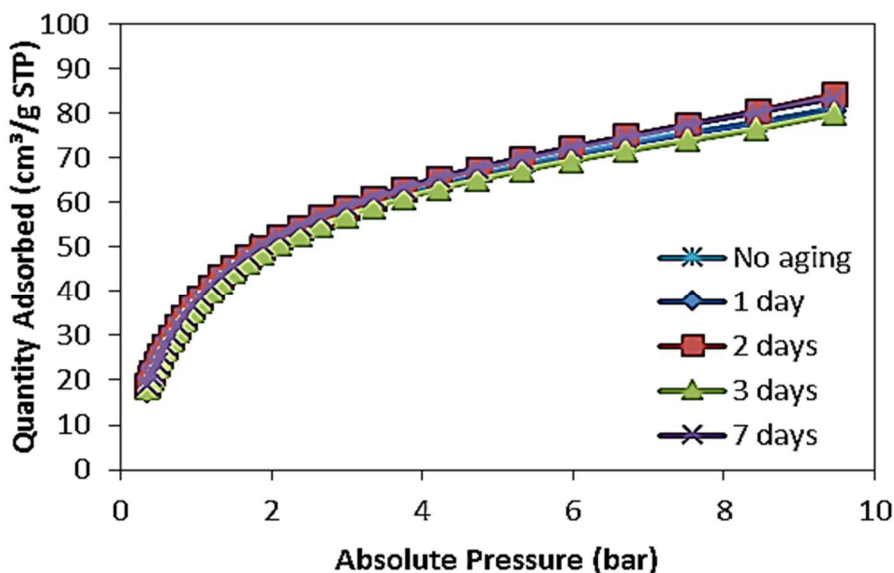


Figure 4.12 : Effect of aging time on CO₂ adsorption at 30°C, crystallization temperature 160°C aging at room temperature.

The maximum amount of adsorbed CO₂ at 30°C and 50°C for the TS-1 samples calculated on the base of Langmuir equation (Eq. 3.1) is summarized on the Table 4.2. The samples which were aged at 40 and 80°C have smallest particle size and uniform size distribution that were determined from SEM images have also good adsorption properties with the result of 4.186 mmol/g and 4.227 mmol/g at 30°C, respectively.

Table 4.2 : The maximum amount of adsorbed CO₂ at 30°C for the TS-1 samples calculated with Langmuir Equation.

Si/Ti Ratio	Crystallization Temp. (°C)	Aging Temp. (°C)	Aging Duration (day)	Max. CO ₂ uptake (mmol/g)
25	160	25	3	3.987
50	160	25	3	3.945
100	160	25	3	3.925
200	160	25	3	3.997
100	160	25	-	4.036
100	160	25	1	4.054
100	160	25	2	4.149
100	160	25	3	3.925
100	160	25	7	4.115
100	140	25	3	4.392
100	180	25	3	3.720
100	140	40	2	4.354
100	140	40	3	4.279
100	140	40	7	4.186
100	140	80	1	4.264
100	140	80	2	4.403
100	140	80	3	4.122
100	140	80	7	4.227

TS-1 samples which are synthesized in different crystallization temperatures such as 140°C, 160°C and 180°C and aged at room temperature for 3 days with Si/Ti ratio of 100 were characterized by N₂ isotherms to obtain surface area and micropore volume. The surface area is calculated based on Brunauer–Emmett–Teller and t-plot models. As it can be seen from Table 4.3, the BET surface areas vary between 439-475 m²/g, where as external surface area is in the range of 200-279 m²/g. Adsorbing more CO₂ may be related with the high external surface area of the crystals which were crystallized at low temperatures.

Table 4.3 : The effect of crystallization temperature on surface area characteristics of TS-1 samples.

Crystallization Temp. (°C)	BET Surface Area (m²/g)	External Surface Area (m²/g)	Micropore Volume (cm³/g)
140	439.34	279.22	0.07
160	474.62	209.10	0.11
180	457.85	200.41	0.10

4.1.1 TS-1 Samples As a Candidate Filler for MMM Formation

Synthesis of TS-1 samples was accomplished with the investigation of effect of many parameters such as crystallization temperature, aging and Si/Ti ratio. The goal of this work was obtaining suitable fillers with desired properties for MMM formation. These desired properties were small particle size with narrow particle size distribution and high CO₂ uptake. With respect to results obtaining from XRD, SEM and volumetric analysis, aging at 40°C for 7 days was determined as key parameter in order to obtain proper TS-1 samples with Si/Ti ratio as 100 and crystallization temperature as 140°C.

The FTIR spectrum between 400-1400 cm⁻¹ of TS-1 samples are depicted in Figure 4.13. As one of the common peaks of MFI peaks refers to Si-O-Si rocking, absorption bands at 450 and 550 cm⁻¹. The absorption band at around 800 cm⁻¹ refers to symmetric stretching/bending of Si-O-Si bridges, 1090 cm⁻¹ with a shoulder at 1226 cm⁻¹ belongs to Si-O-Si asymmetric stretching. These are all common MFI peaks. Ti substitution into zeolite framework in TS-1 samples is decided with the absorption bands at around 960 cm⁻¹ [13].

TS-1 samples dispersed in deionized water and was submitted to sonication for 1 h before performing the DLS analysis. The measurement was repeated three times. The result is depicted in Figure 4.14, it is very clear that TS-1 samples have narrow size distribution with number average particle size of 242 nm. SEM images of the samples are also compatible with DLS results. Based on SEM images, TS-1-1 have uniform particle size distribution with particle size as around 250 nm (Figure 4.15).

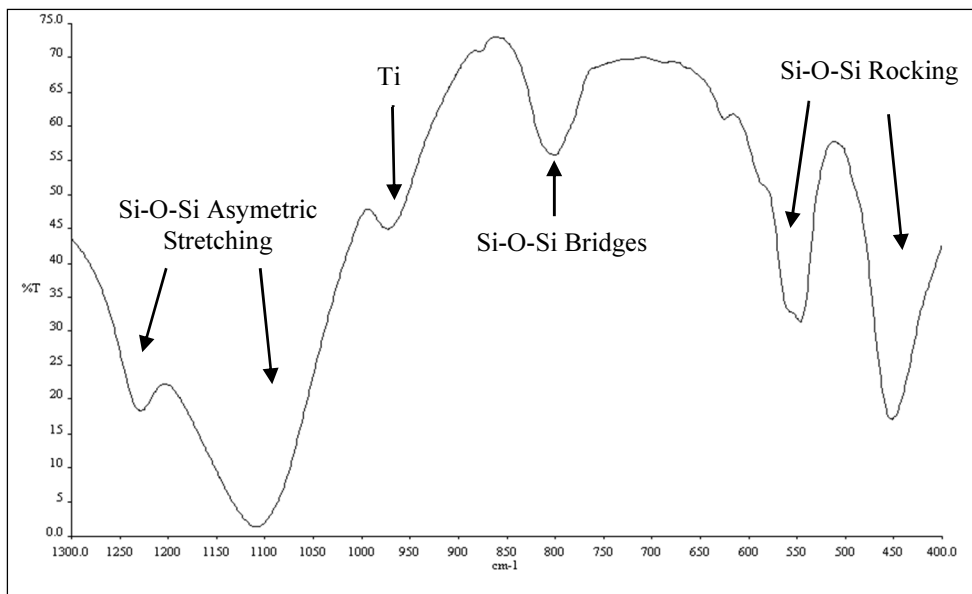


Figure 4.13 : FTIR spectrum of TS-1 sample.

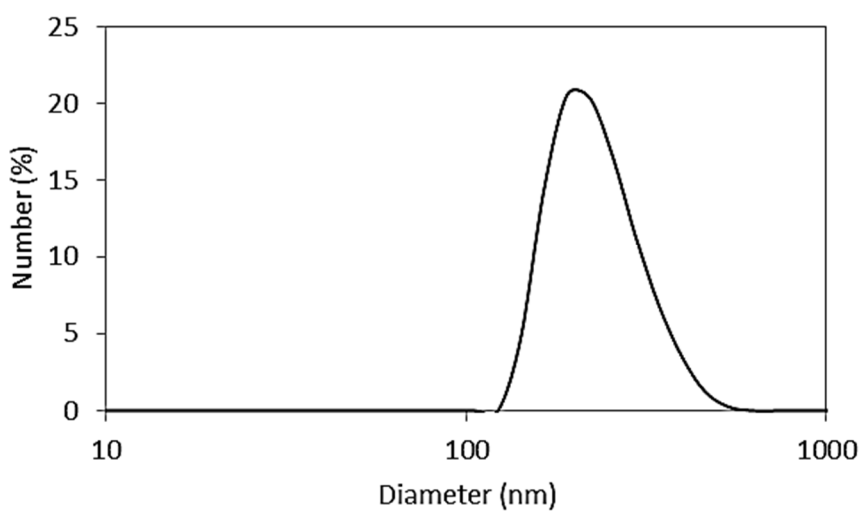


Figure 4.14: Size distribution of TS-1 samples by number.

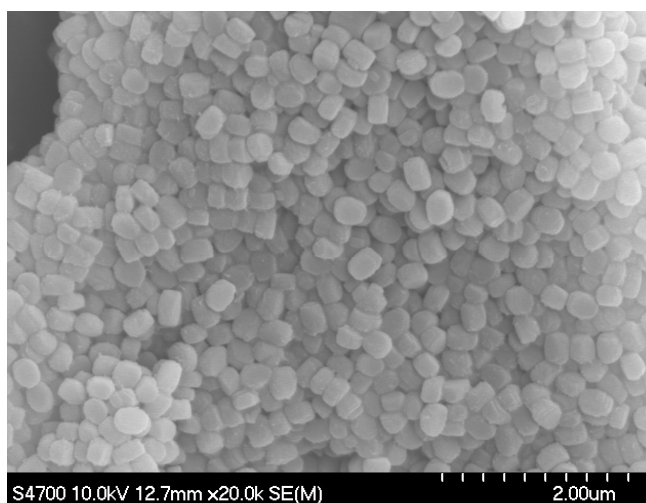


Figure 4.15 : SEM image of TS-1 sample.

4.2 Effect of Modification on TS-1 Properties

Modification is necessary implementation for TS-1 zeolites in order to enhance the interaction of filler with polymer. Modification was applied to TS-1 samples by using amino silane coupling agent; APTES and three different solvent with different dielectric constants and kinetic diameter; toluene (TOL), tetrahydrofuran (THF) and isopropyl alcohol (IPA). Transmission FTIR spectra was collected to observe effect of modification on TS-1 samples. Figure 4.16 and 4.17 depict the spectra of four samples between 1300-400 cm^{-1} and 3600-3000 cm^{-1} regions, respectively. All the spectra shows the characteristic peaks of TS-1. However, observation of the peak at around 960 cm^{-1} which is an indication of Ti incorporation to the framework becomes difficult by modification. This phenomena can be explained by overlapping with the peaks at around 1100 and 1230 cm^{-1} which are fingerprint of Si-O-Si asymmetric stretching. Investigation of the region between 3475 and 3200 cm^{-1} is expected to give more relevant results about success of modification. On the other hand, this region is including many overlapping bands such as -OH, Si-OH, N-H. The best explication can be made by the shift in the maximum intensity. This shifting to lower wave numbers represents the hydrogen bonding with introduction of amine groups. It was observed that TS1-APTES-THF does not showing the same trend in shifting to lower wave numbers. Therefore, modification of this sample may not as successful as the other samples. During the modification reaction, controlling of solvent, THF which has a low boiling point may fail and cause a problem in the reaction. IPA with high polarity and low kinetic diameter was promising solvent for modification. While high polarity of the IPA increases the mobility of the aminopropylsilanes molecules, IPA molecules can be easily removed from the zeolite structure without deteriorating the structure because its kinetic diameter is smaller than TS-1 samples.

The volumetric sorption isotherms of modified and non-modified samples are depicted in the Figure 4.19. As it can be seen from the isotherms, the amount of CO_2 adsorbed by TS-1 particles is almost in the same value with TS1-APTES-THF, but some small difference with the TS1-APTES-TOL was observed. The maximum adsorbed amounts of CO_2 of non-modified TS-1, TS1-APTES-TOL AND TS1-APTES-THF were calculated 3.9, 3.4 and 3.8 mmol/g by using Langmuir equation, respectively. The more significant differences between adsorption isotherms of non-modified and modified particles with APTES in toluene were observed. Although these differences

which were caused by blockage of the pores are negligible. It is assumed that this negligible difference does not affect the adsorption performance of the TS-1 particles significantly. In order to investigate the potential of TS-1 as filler in the gas separation applications, gravimetric sorption analysis were performed with the N_2 , CH_4 and CO_2 gases. Sorption capacities of TS-1, TS1-APTES-TOL and TS1-APTES-IPA are given in Figure 4.20. Same decreasing trend due to partial blockage of zeolite pores by aminosilane molecules with the modification is also observed in gravimetric sorption results. Reduction in CO_2 uptake of TS1-APTES-IPA is more negligible than TS1-APTES-TOL compared to parent zeolite. It can be said that TS1-APTES-IPA is more promising for MMM application. These results also showed that CO_2 adsorption on bare TS-1 was approximately four times more than that of N_2 and two times more than that of CH_4 .

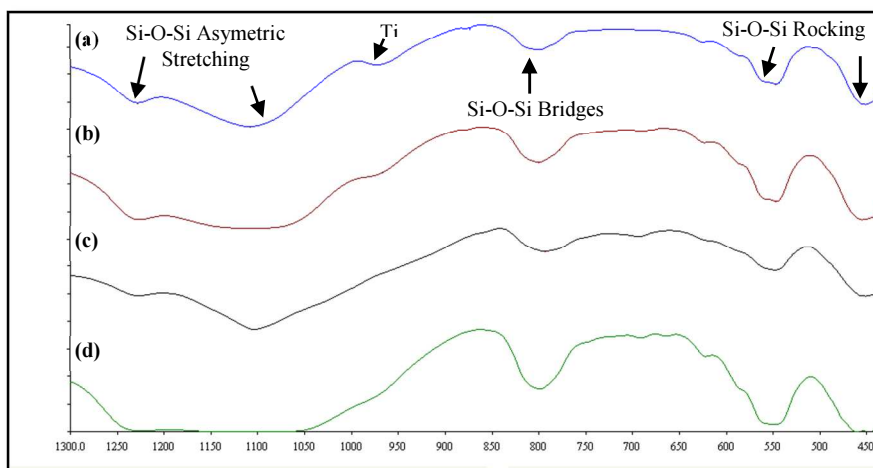


Figure 4.16 : FTIR spectrum of (a) TS-1, (b) TS1-APTES-TOL, (c) TS1-APTES-THF, (d) TS1-APTES-IPA samples between 400 and 1300 cm^{-1} .

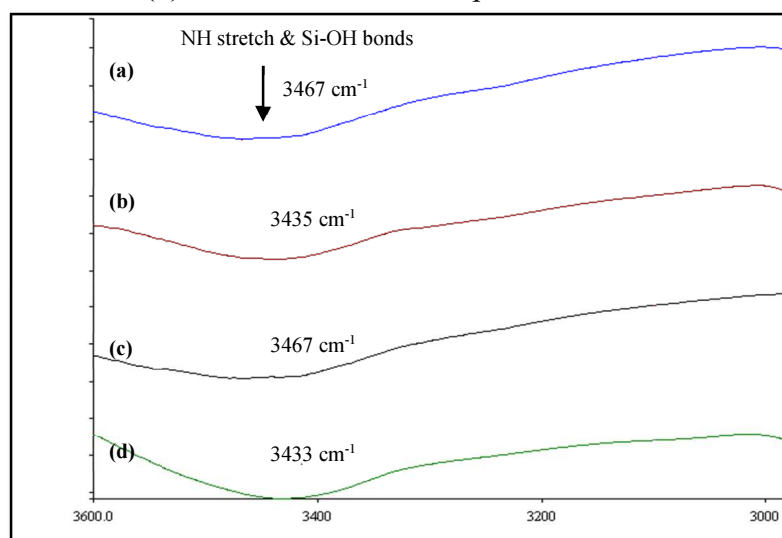


Figure 4.17 : FTIR spectrum of (a) TS-1, (b) TS1-APTES-TOL, (c) TS1-APTES-THF, (d) TS1-APTES-IPA samples between 3000 and 3600 cm^{-1} .

In the Figure 4.18, XRD patterns of modified samples are shown. They have all the characteristic peaks for MFI type of zeolite indicating that modification reaction did not alter the crystal structure.

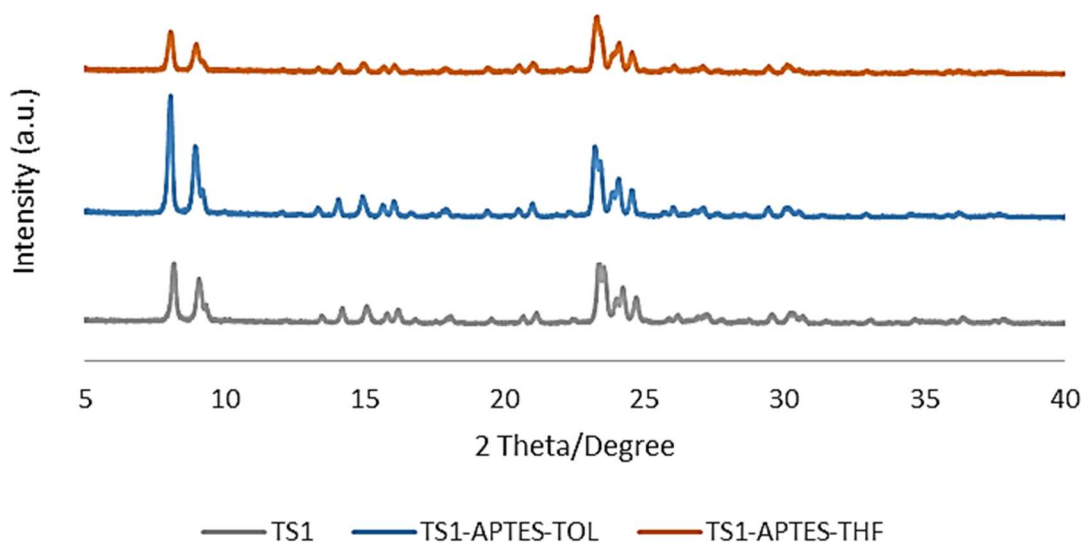


Figure 4.18 : XRD pattern of unmodified and modified TS-1 samples.

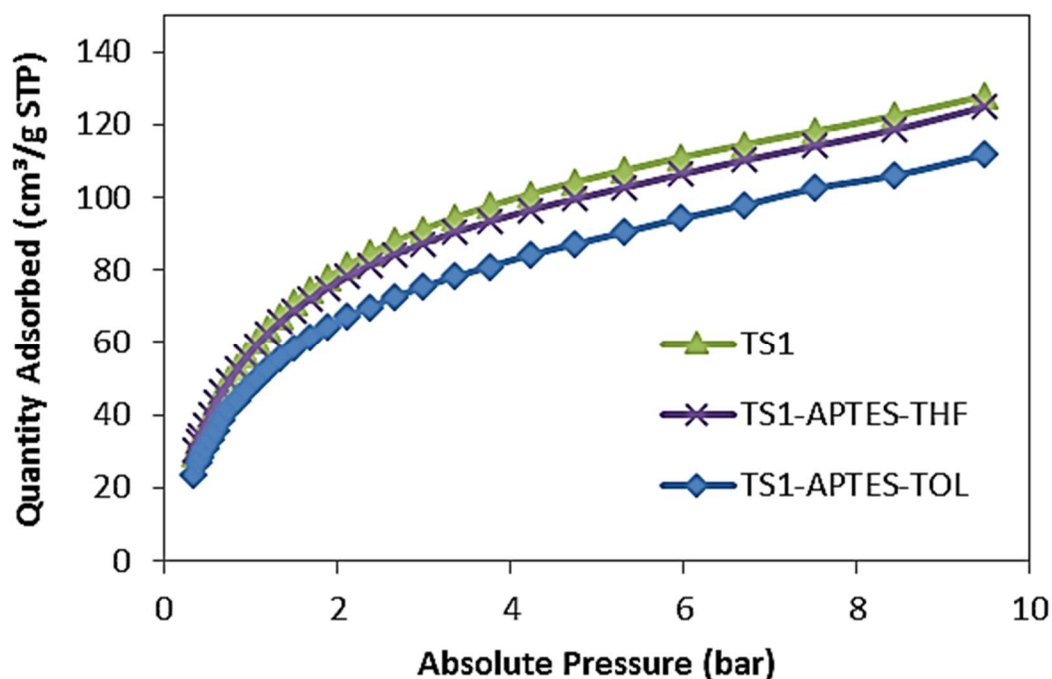


Figure 4.19 : Volumetric sorption isotherms of non-modified and modified TS-1 samples.

BET results showed that the surface areas and micropore surface areas of the materials modified with APTES varied between 343-390 m²/g and 201-240 m²/g, respectively

(Table 4.4). Both BET surfaces and micropore surface area were showing decreasing trend with the introducing of APTES to the TS-1 samples. However, amount of decrease was varying depending on the solvent using during modification application. As it can be seen from Table 4.4, BET surface of TS1-APTES-THF is less effected by modification step, while TS1-APTES-IPA has the lowest BET surface area. Lower BET results indicate that modification of the sample may not take place all over the zeolite surface but mostly at the pore mouth of the zeolites thus limiting N₂ access to the pores [38]. However, micropore surface area results show different trend. TS1-APTES-TOL has highest micropore surface area, following by TS1-APTES-THF and TS1-APTES-IPA. Surface characterization results indicate that TS1-APTES-TOL is a promising filler for dispersing into polymer matrix due its relatively high BET and micropore surface as well as micropore volume. Modification reactions are suffering from reproducibility due to many parameters effected the reaction. Therefore, investigating parameters for individual synthesis could be very challenging. The overall results of modified TS-1 samples point out that TS1-APTES-IPA has relatively higher CO₂ capacity, whereas TS1-APTES-TOL posseses higher BET and micropore surface area and micropore volume. These two properties are sufficient to make these samples candidate for the MMMs formation.

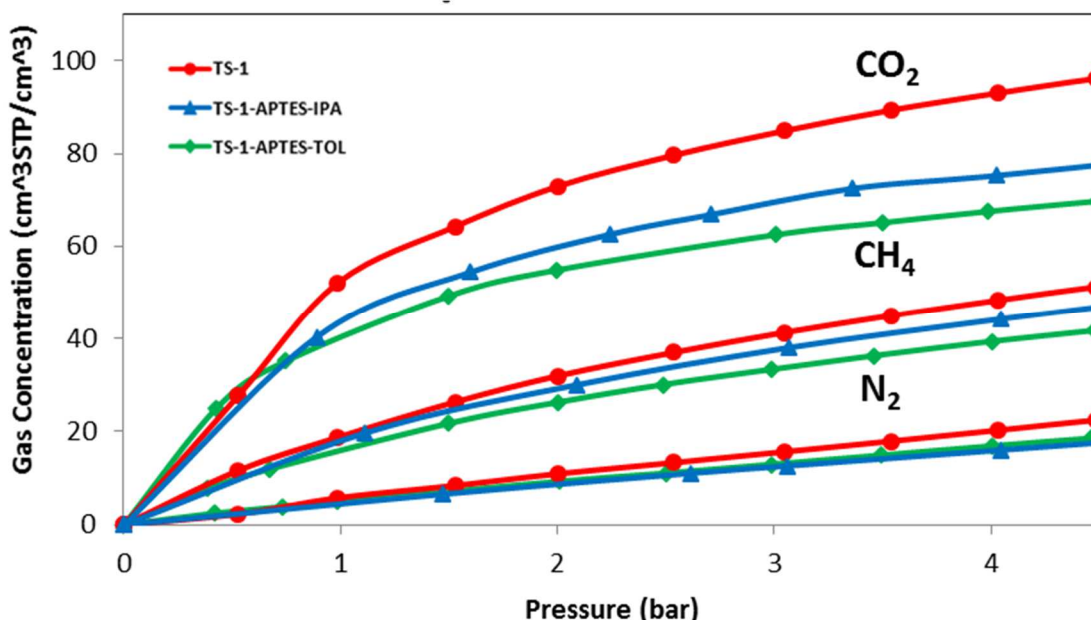


Figure 4.20 : Gravimetric sorption isotherms of bare TS-1, TS1-APTES-TOL and TS1-APTES-IPA.

Table 4.4: Surface characterization of bare and modified TS-1 samples.

Samples	BET Surface Area (m ² /g)	Micropore Surface Area (m ² /g)	Micropore Volume (cm ³ /g)
TS1	472.0	319.55	0.127
TS1-APTES-TOL	354.36	240.08	0.096
TS1-APTES-THF	389.79	217.44	0.089
TS1-APTES-IPA	343.31	200.60	0.083

4.3 Effect of Modification on Membrane Formation

Figure 4.21 and 4.22 show the morphology of MMMs prepared by incorporating TS-1 samples into Matrimid[®] and 6FDA-DAM, respectively. Although the MMMs prepared with using Matrimid and TS1-APTES-THF could not achieved to form membrane film during the casting step, SEM analysis were performed in order to investigate the reason of the failure.

As it was derived from the images, incorporation of untreated TS-1 into the MMMs cause undesired voids around the zeolites between polymer matrix (Figure 4.21-a and 4.22-a). In order to prevent those voids and enhance zeolite-polymer interphase, modified samples were dispersed into the continuous polymer phase. The TS-1 samples modified with different solvents show different behaviours in polymer matrix. Figure 4.21-b represents the good attachment of the TS1-APTES-TOL into Matrimid[®]. As it is obvious from the image, all the zeolite particles are surrounded by polymer phase and also distributed homogenously. On the other hand, distribution of TS-1 samples modified with APTES in THF was rather poor, which was verified by the two incompatible SEM images. As it is depicted in Figure 4.21-c, the distribution of fillers into the polymer matrix have failed by the agglomeration. On the contrary, when the different regions were investigated, the adhesion between the TS1-APTES-THF and Matrimid[®] improved (Figure 4.21-d). This phenomenon may happen due to either failure in modification reaction or during the formation of membranes. SEM analysis of 6FDA-DAM MMMs proved that MMMs prepared using TS1-APTES-IPA exhibits better polymer-zeolite interface than using TS1-APTES-TOL. However, TS1-APTES-IPA/6FDA-DAM possesses some clustered zeolite regions which can influence the gas separation performance of the membrane.

The membranes were also examined to TGA analysis in order to determine amount of moisture and residual solvent exist in the membrane. Figure 4.23 and 4.24 show the TGA thermograms of Matrimid[®] and 6FDA-DAM based membranes MMMs. TGA curve of pure polymers were also added for comparison. Table 4.5 also depicts the cumulative weight loss in these samples. The amount of moisture (until 100°C) was higher in some membranes such as TS-1/Matrimid[®], TS1-APTES-THF/Matrimid[®], pure 6FDA-DAM and TS1-APTES-IPA/6FDA-DAM which may be related with when the membranes were prepared. On the other hand, amount of residual solvent (100-153 °C) has been found in TS1-APTES-THF/Matrimid[®] higher than other Matrimid[®] based membranes. Moreover, 6FDA based membranes exhibits higher amount of residual solvent in MMMs compared to pure 6FDA-DAM membrane. This situation may be attributed to the polymer-filler interphase which is able to entrap more solvent. The amount of mass loss around 190-200°C may be related with the degradation of APTES for MMMs including modified TS-1 crystals. After 200°C the amount of mass loss is related to the thermal stability of the membranes which is higher for the MMMs with respect to inorganic particles.

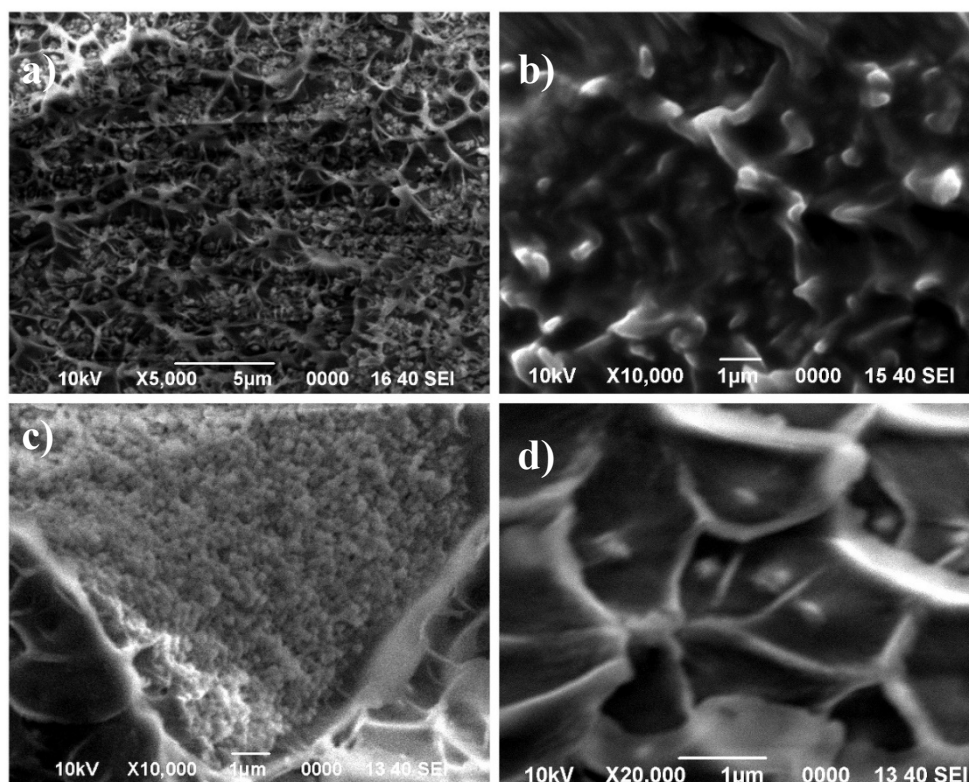


Figure 4.21: SEM images of Matrimid[®] MMMs prepared using a) TS-1 b) TS1-APTES-TOL c-d) TS1-APTES-THF.

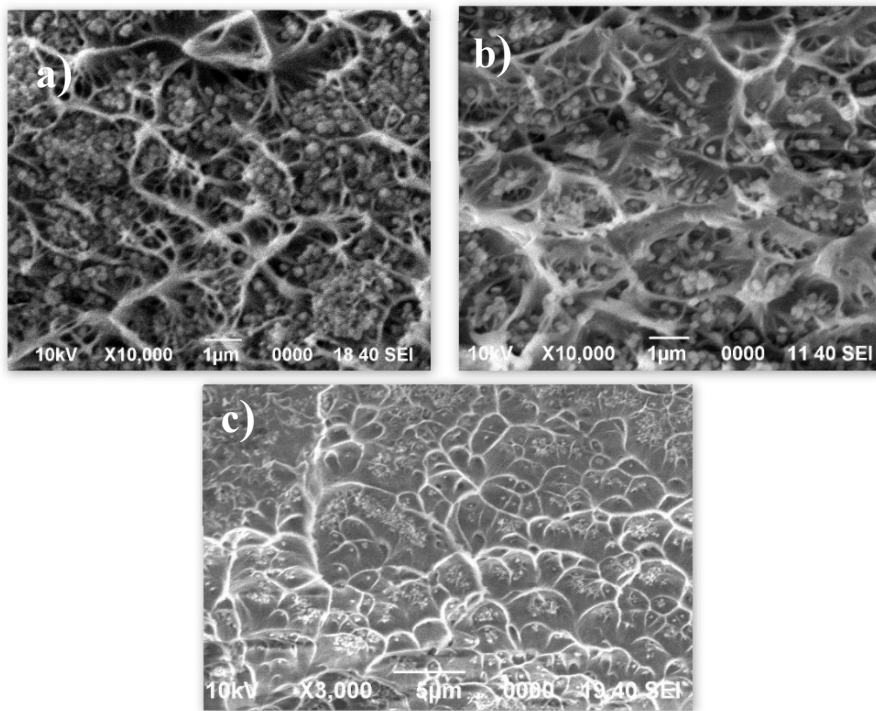


Figure 4.22 : SEM images of 6FDA-DAM MMMs prepared using a) TS-1 b) TS1-APTES-TOL c) TS1-APTES-IPA.

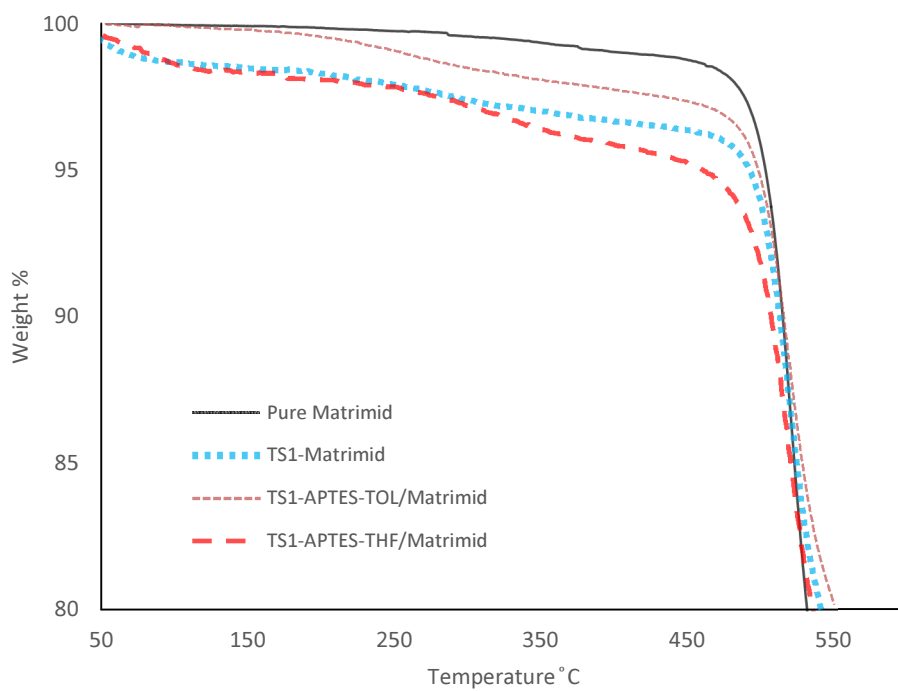


Figure 4.23 : TGA thermograms for Matrimid® based membranes.

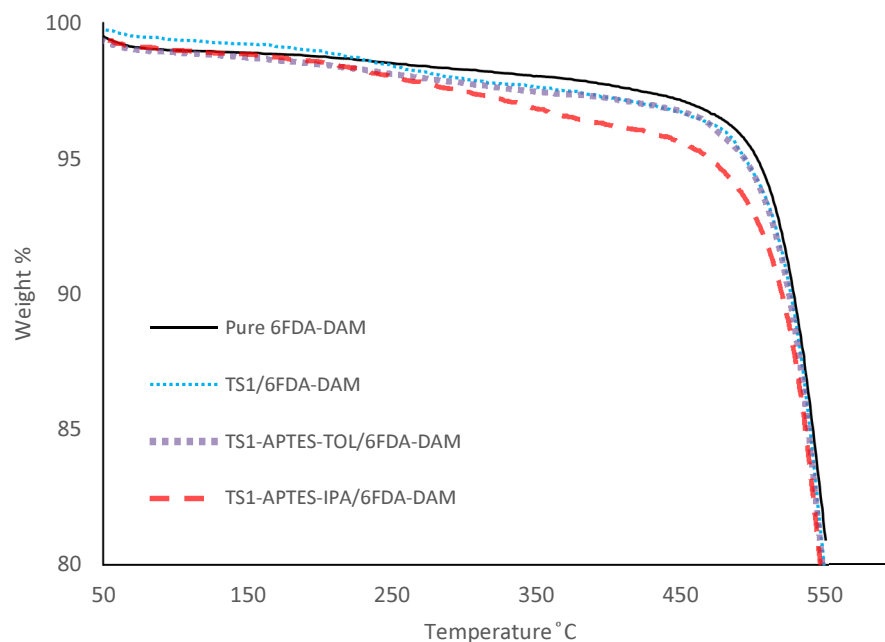


Figure 4.24 : TGA thermograms for 6FDA-DAM based membranes.

Table 4.5 : Cumulative weight loss (%) of the membranes obtained from TGA.

Membrane	Cumulative weight loss (%)					
	100°C	153 °C	200 °C	300 °C	400 °C	500 °C
Pure Matrimid®	0.133	0.235	0.382	1.276	2.080	5.734
TS1/Matrimid®	1.659	1.869	2.036	2.935	3.667	6.371
TS1-APTES-TOL/Matrimid®	0.075	0.221	0.45	1.507	2.256	5.32
TS1-APTES-THF/Matrimid®	1.361	1.662	1.909	2.794	4.132	8.210
Pure 6FDA-DAM	1.179	1.271	1.408	1.887	2.438	4.884
TS1-6FDA-DAM	0.646	0.805	1.048	2.088	2.779	5.531
TS1-APTES-TOL/6FDA-DAM	0.224	0.543	1.09	1.972	2.724	6.072
TS1-APTES-IPA/6FDA-DAM	1.352	1.507	1.772	2.874	4.095	7.323

DSC measurements were applied to MMMs in order to observe the presence of the interphase, which reveals itself as a change in the glass transition temperature (T_g) of the membrane compared to that of neat polymeric membrane. DSC results were presented in Table 4.6. It is observed that the T_g values of MMMs in majority was

increasing with the addition of TS-1 fillers into the polymer matrix. As the SEM images demonstrated the poor adhesion of the sample TS1-APTES-THF, T_g values of relating MMM may decrease due to agglomeration of zeolites. Moreover, the success of modified TS-1 fillers in attachment to the polymer matrix can be also evaluated from DSC analysis. Deviation in T_g values of MMMs prepared using modified TS-1 samples were found more dominant than bare TS-1 samples. The change in the T_g of a membrane is related with rigidify of polymer matrix. Surrounding of zeolites exhibits rigidified polymer which occupies small amount compared to all polymer matrix, so the effect of rigidified polymer phase around the zeolite particles results as small quantity of change in the overall T_g .

Table 4.6: T_g values of MMM measured by DSC.

Polymer	Filler	T_g (°C)
Matrimid [®]	-	318.36
Matrimid [®]	TS-1	318.35
Matrimid [®]	TS1-APTES-TOL	320.92
Matrimid [®]	TS1-APTES-THF	313.82
6FDA-DAM	-	391.93
6FDA-DAM	TS-1	393.91
6FDA-DAM	TS1-APTES-TOL	396.81
6FDA-DAM	TS1-APTES-IPA	392.11

4.4 Gas Separation Properties of MMMs

Table 4.7 shows the permeabilities and selectivities of MMMs with the neat polymer membrane in order to compare their performance. It was observed that the permeabilities of single gases increase and ideal selectivities decrease slightly with incorporation of TS-1 into the polymer matrix. Permeability increase was an expected result due to high molecular dimension of TS-1 zeolites (5.1-5.6 Å) than the gases investigated in this study (CO₂: 3.3 Å, N₂: 3.64 Å, CH₄: 3.80 Å). Gas separation properties of TS1-APTES-TOL / 6FDA-DAM show the evidence of the

poor attachment of TS-1 fillers to the polymer matrix, as it was also observed in SEM images. Gas separation results also indicates that difference in selectivities between neat 6FDA-DAM membrane and MMM prepared using TS1-APTES-IPA was negligible.

Table 4.7 : Gas separation properties of the MMMs.

Polymer	Zeolite	Permeability (Barrer)			Ideal Selectivity		Real Selectivity	
		CO ₂	CH ₄	N ₂	CO ₂ /CH ₄	CO ₂ /N ₂	CO ₂ /CH ₄	CO ₂ /N ₂
Matrimid	-	5.1	0.1	0.2	52.9	33.4	-	-
Matrimid	TS1-APTES-TOL	12.6	0.3	0.4	36.9	30.4	134.7	-
6FDA-DAM	-	638.3	32.0	40.0	19.9	16.0	-	-
6FDA-DAM	TS1-APTES-TOL	700.7	48.8	56.4	14.4	12.4	-	-
6FDA-DAM	TS1-APTES-IPA	776.7	39.7	46.9	19.6	16.6	50.4	27.8

Mixed gas permeation was measured using adjusting 50% CO₂ with a CH₄ and N₂ balance by the help of Gas Chromotography equipment. Comparasion of single gas and mixed gas permeations and selectivities are shown in Fig. 4.25 and 4.26 for TS1-APTES-TOL/Matrimid and TS1-APTES-IPA/6FDA-DAM, respectively. Mixed gas permeabilities of the MMMs were all less than single gas permeation measurements. However, the reducement in permeabilities were not in same ratios. Therefore, considerable enhancement in real selectivities compared to ideal selectivities were obtained from mixed gas analysis. This decreasement in permeabilities and increasement in selectivities may be due to to competitive adsorption between the gas pairs.

For a better understanding of the alteration of gas transport properties with loading of TS-1, Maxwell predictions of MMM, the single gas and mixed gas transport properties of MMMs and pure polymeric membranes were illustrated on Robeson plot in Figure 4.27 and 4.28 for CO₂/CH₄ and CO₂/N₂ performances, respectively. For both gas pairs, Maxwell predictions that was calculated using silicalite-1 and/or TS-1 permeability data indicates that the ideal case for the MMMs can be improvement in permeability and slight change in the selectivity. This phenomenon may be explained by the pore diameter of both silicalite-1 and TS-1 that are member of MFI family. The pore diameter of TS-1 and silicalite-1 is much larger than the gas penetrant, thus no molecular sieve effect is expected. When it is dispersed in a polymer matrix, gas molecules prefer to diffuse through the zeolite pores and enhancement in permeability

without any increase in selectivity. Single gas experimental results of MMMs consists of APTES-modified show that no significant improvements was accomplished compared to neat polymer membranes with respect to CO₂ permeability and selectivity. As Maxwell predictions indicates the possible ideal case, only permeability increase with slightly change in the selectivity observed for both Matrimid® and 6FDA-DAM based MMMs except for TS1-APTES-TOL/6FDA-DAM in which interfacial voids and poor compatibility with the polymer phase evaluated from SEM images. TS1-APTES-TOL / 6FDA-DAM may have interfacial voids in the order of gaseous penetrants, thus Case III type non-idealities will be demonstrated based on both gas transport properties and SEM images [31].

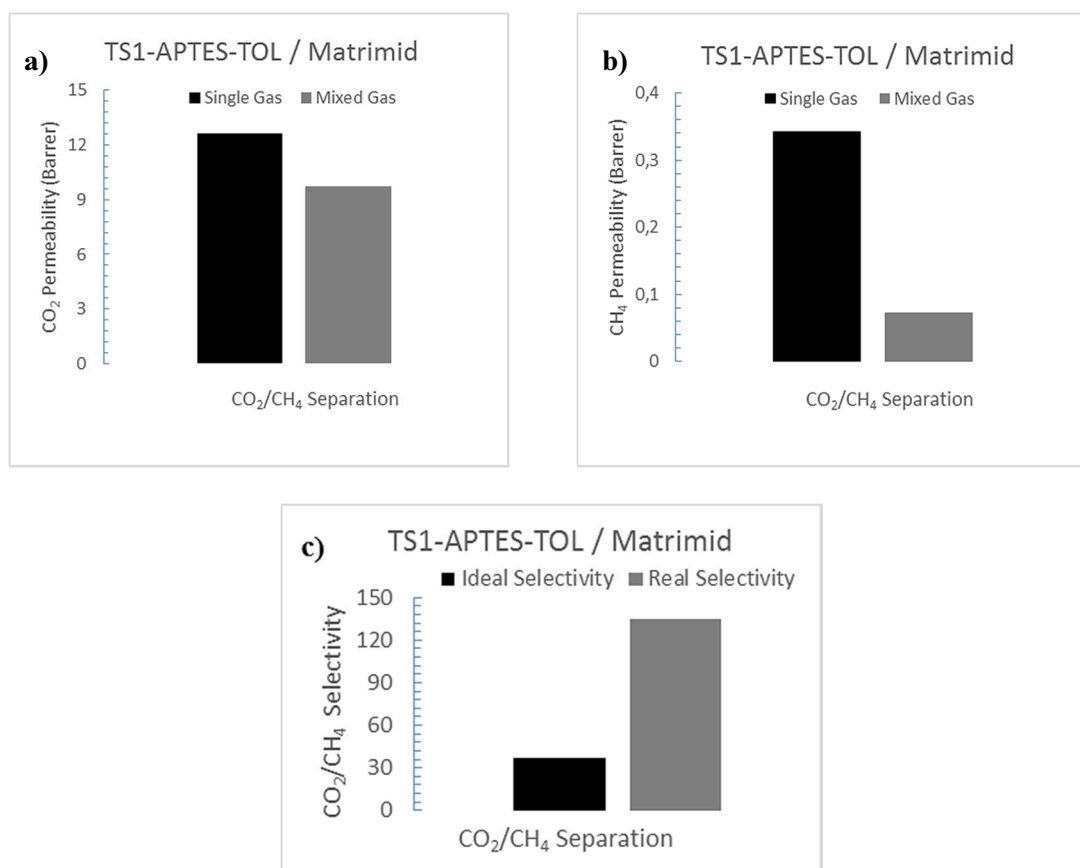


Figure 4.25 : Ideal and real gas separation properties of TS1-APTES-TOL / Matrimid® for CO₂/CH₄ separation: (a) CO₂ permeability (b) CH₄ permeability (c) CO₂/CH₄ selectivity.

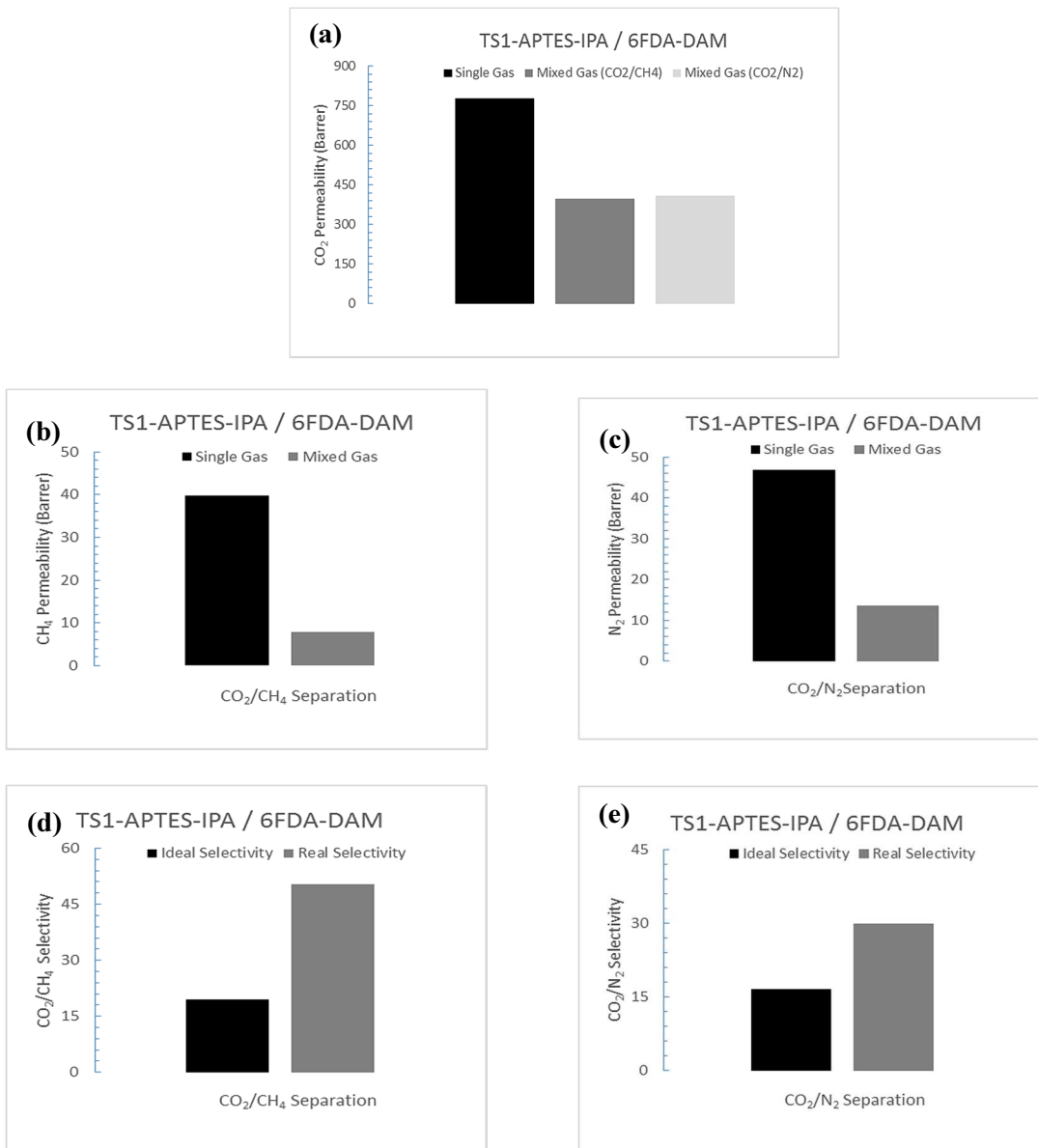


Figure 4.26 : Ideal and real gas separation properties of TS1-APTES-IPA / 6FDA-DAM for CO₂/CH₄ and CO₂/N₂ separation: (a) CO₂ permeabilities, (b) CH₄ permeability (c) N₂ permeability (d) CO₂/CH₄ selectivity, (e) CO₂/N₂ selectivity.

Mixed gas transport performances for CO₂/CH₄ took place beyond the upper bound of 1991 and 2008. This significant settlement in the Robeson diagram implies that gas behavior in the mixture could be more different from ideal situation. In the single gas experiments, while permeability increases due to large pore size of the zeolite, selectivity changes slightly. On the other hand, mixed gas experiments demonstrate that different CO₂, CH₄, N₂ adsorption capacities of TS-1 may lead competitive adsorption inside the zeolite pores in spite of the fact that they are large enough to host all gas molecules.

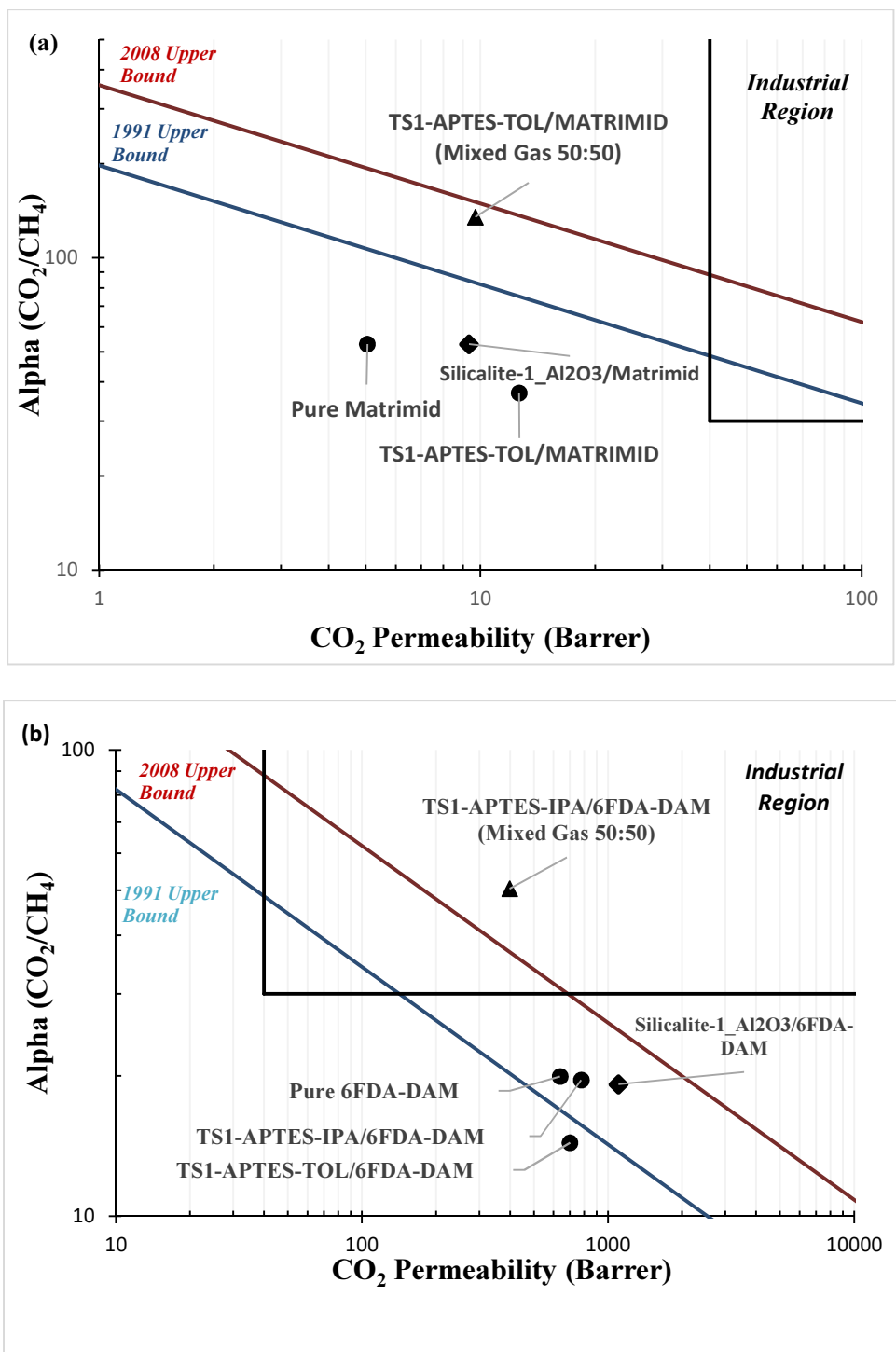


Figure 4.27: CO₂/CH₄ gas separation performances of MMMs on Robeson diagram with pure polymer and maxwell prediction results (a) Matrimid[®] (b) 6FDA-DAM as a continuous phase. Circles (●) for single gas measurements, diamonds (◆) for maxwell predictions and triangles (▲) for mixed gas measurements.

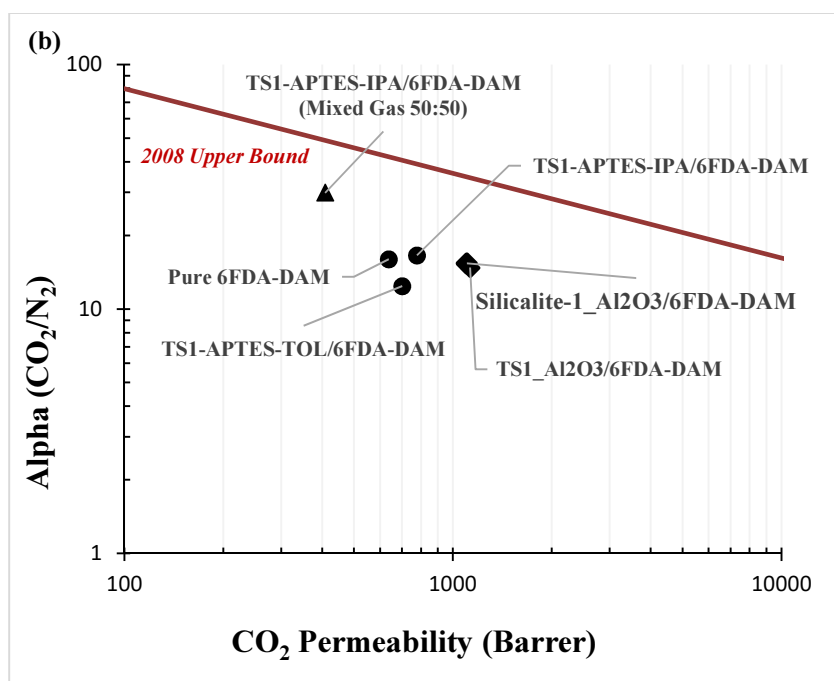
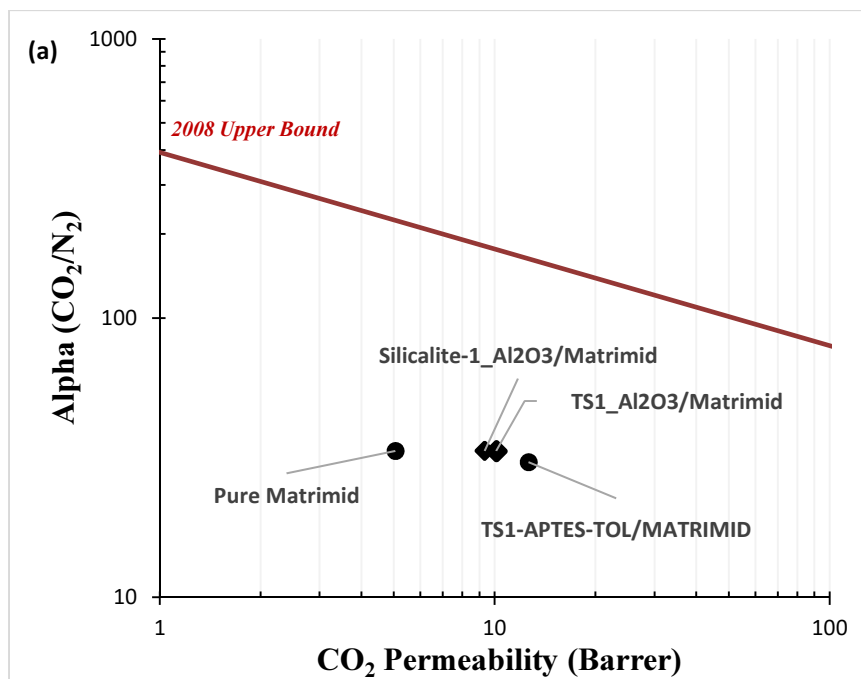


Figure 4.28: CO_2/N_2 gas separation performances of MMMs on Robeson diagram with pure polymer and maxwell prediction results (a) Matrimid[®] (b) 6FDA-DAM as a continuous phase. Circles (●) for single gas measurements, diamonds (◆) for maxwell predictions and triangles (▲) for mixed gas measurements.

5. CONCLUSIONS AND RECOMMENDATIONS

This study focused on utilization of titanium-silicalite-1 (TS-1) zeolites as a inorganic filler for mixed matrix membranes in the field of natural gas purification applications. TS-1 crystals were synthesized with hydrothermal method by investigating the effect of crystallization temperature, Si/Ti molar ratio, aging (duration and temperature) on particle size. FTIR and XRD analysis were also performed in order to confirm the success of the synthesis. TS-1 samples prepared at 140°C as a crystallization temperature, Si/Ti=100, aged at 40°C for 7 days were decided as a convenient filler candidate for MMMs application with respect to SEM images. The average particle size of the TS-1 was evaluated as 242 nm from DLS measurements.

Early investigation of TS-1 / Matrimid[®] samples showed that interfacial voids and poor attachment between TS-1 fillers and polymer phase was exist, although the high hydrophobicity of TS-1 zeolites contributed the compatibility with polymer phase. In order to enhance the filler/polymer intephase, 3-aminopropyltriethoxysilane (APTES) was used as a silane coupling agent which acts like a integral chain linker. Modification with APTES was performed in three different solvents; toluene (TOL), tetrahydrofluron (THF), isopropanol (IPA). Different polarities an kinetic diameters of the solvents in the modification reaction performances were also investigated. Modified TS-1 exhibited lower adsorption capacities compared to bare zeolite. The pore blockage by APTES or solvent may cause this reduction. The modification reaction occurred in IPA showed less depression due to its high polarity and small kinetic diameter. On the other hand, THF found as an inconvenient solvent for modification reaction. Although the properties such as polarity and kinetic diameter of THF was moderate among the other solvents, the low vapour pressue may cause the diffuculties of controlling the solvent during the reaction. Based on BET area, sorption measurements and FTIR results, no significant evidence was evaluated that modification was applied to the TS-1 zeolites. Preparation of MMMs was also resulted as supports the previous characterization that the even membrane film was not able to

form properly. Unreacted APTES with zeolites may contribute this phenomenon. TS1-APTES-TOL samples showed the most significant decrease in gas sorption measurements.

Mixed matrix membranes prepared by dispersion of bare and APTES-modified TS-1 nano-crystals into relatively low permeable Matrimid[®] and highly permeable in-house-synthesized-6FDA-DAM polymer matrixes. TS1-APTES-TOL exhibited good compatibility with Matrimid[®], while TS1-APTES-IPA was the one dispersed in 6FDA-DAM without any observable void in the SEM analysis. TGA analysis demonstrated that no significant solvent left in the MMM structure. Slight increment in the glass transition temperature of the polymer was observed in the DSC analysis.

Both maxwell predictions and single gas measurements demonstrated that incorporating TS-1 zeolites into the polymer matrix only concluded as increase in permeability and slight change in the selectivity due to lack of molecular sieving properties of the MFI zeolites for the gas pairs of CO₂/CH₄ and CO₂/N₂. Nevertheless, mixed gas experiments exhibited interesting results compared the single gas measurements. Deterioration of permeability and enhancement in the selectivity that transfer the position of related MMMs beyond the upper bounds for specifically CO₂/CH₄ separation. This change may be attributed to difference sorption capacity of the TS-1 zeolites for different gases, thus competitive adsorption inside the pore of the zeolites which is large enough to host each gas molecules.

For further investigation, elemental analysis of TS-1 zeolites should be performed. Explaining the effect of synthesis parameters oof TS-1 could be related with crystallinity. Enhancement in modification step by using different type of silane coupling agents and solvents is necessary for obtaining MMMs without non-ideal interphase problems. Reproducibility of the modification steps, membrane preparation and gas transport properties measurements must be done. The mixed gas measurements must be investigated and the mechanism causing this improvements in the selectivity should be explained by performing more measurements such as measuring sorption capacity of TS-1 zeolites in mixed gas conditions.

REFERENCES

- [1] **Shao, P., Dal-Cin, M. M. , Guiver, M. D. and Kumar, A.** (2013). Simulation of membrane-based CO₂ capture in a coal-fired power plant, *J. Memb. Sci.*, 427, 451–459.
- [2] **Adewole, J.K, Ahmad, L., Ismail, S. and Leo, C.P.** (2013). Current challenges in membrane separation of CO₂ from natural gas: A review, *Int. J. Greenh. Gas Control*, 17, 46–65.
- [3] **Othman, M.R, Tan, S.C and Bhatia, S.** (2009). Separability of carbon dioxide from methane using MFI zeolite–silica film deposited on gamma-alumina support, *Microporous Mesoporous Mater*, 121, 138–144.
- [4] **Kohl, A. and Nielsen, R.** (1997). *Gas Purification: Membrane Permeation Processes*, Houston, Texas: Gulf Publishing Company, 5th ed., 215–217.
- [5] **Stocker, T.F., Qin, D., Plattner, G.K. , Tignor, M. , Allen, S. K. , Boschung, J., Nauels, A., Xia, Y., Bex, V. and Midgley, P. M.** (2013). IPCC, 2013: Summary for Policymakers. In: *Climate Change 2013*, Cambridge, United Kingdom and New York, NY, USA.
- [6] **Baker, R.W** (2012). *Membrane Technology and Applications*, Chichester, UK: John Wiley & Sons, Ltd.
- [7] **Freemantle, M.** (2005). Advanced organic and inorganic materials being developed for separations offer cost benefits for environmental and energy-related processes, 83, 49–57.
- [8] **Bastani, D., Esmaeili, N. and Asadollahi, M.** (2013). Polymeric mixed matrix membranes containing zeolites as a filler for gas separation applications: A review, *J. Ind. Eng. Chem.*, 19, 375–393.
- [9] **Paul, D. R. and Kemp, D. R.** (1973). Diffusion Time Lag In Polymer Membranes Containing Adsorptive Fillers, *J. Polym. Sci. Polym. Symp.*, 41, 79–93.
- [10] **Taramasso, M., Milanese, S. D., Perego, G. and Notari, B.** (1982). Preparation Of Porous Crystalline Synthetic Material Comprised Of Silicon And Titanium Oxides, United States Patent.

- [11] **Polimeri Europa Spa** (2009). Titanium Silicalite (TS-1) zeolite based, Proprietary catalyst, Material Brochure.
- [12] **Wang, X., Yan, J. and Huang, W.** (2013). Synthesis of b-oriented TS-1 zeolite membranes with high performance in the oxyfunctionalization of n-hexane, *Thin Solid Films*, 534, 40–44.
- [13] **Qiu, F., Wang, X., Zhang, X., Liu, H., Liu, S. and Yeung, K.L.** (2009). Preparation and properties of TS-1 zeolite and film using Sil-1 nanoparticles as seeds, *Chem. Eng. J.*, 147, 316–322.
- [14] **Vasile, A. and Busuioc-Tomoiaga, A. M.** (2012). A new route for the synthesis of titanium silicalite-1, *Mater. Res. Bull.*, 47, 35–41.
- [15] **Parker, W. O. and Millini, R.** (2006). Ti coordination in titanium silicalite-1, *J. Am. Chem. Soc.*, 128, 1450–1451.
- [16] **Fujiyama, S., Seino, S., Kamiya, N., Nishi, K., Yoza, K. and Yokomori, Y.** (2014). Adsorption structures of non-aromatic hydrocarbons on silicalite-1 using the single-crystal X-ray diffraction method, *Phys. Chem. Chem. Phys.*, 16, 15839–15845.
- [17] **Zhang, G., Sterte, J. and Schoeman, B.** (1995). Discrete Colloidal Crystals of Titanium Silicalite-1, *J. Chem. Soc. Chem. Commun.*, 24, 2473–2670.
- [18] **Han, Y., Zeng, H. S. and Guan, N.** (2002). Thermal and hydrothermal stability of monolithic TS-1/cordierite catalyst, *Catal. Commun.*, 3, 221–225.
- [19] **Vernimmen, J., Meynen, V. and Cool, P.** (2011). Synthesis and catalytic applications of combined zeolitic/mesoporous materials., *Beilstein J. Nanotechnology*, 2, 785–801.
- [20] **Serrano, D. P., Calleja, G., Botas, J. and Gutierrez, F. J.** (2007). Characterization of adsorptive and hydrophobic properties of silicalite-1, ZSM-5, TS-1 and Beta zeolites by TPD techniques, *Sep. Purif. Technol.*, 54, 1–9.
- [21] **Sebastian, V., Motuzas, J., Dirrix, R. W. J., Terpstra, R., Mallada, R. and Julbe, A.** (2010). Synthesis of capillary titanosilicalite TS-1 ceramic membranes by MW-assisted hydrothermal heating for pervaporation application, *Sep. Purif. Technology*, 75, 249–256.
- [22] **Chen, X., Chen, P. and Kita, H.** (2008). Pervaporation through TS-1 membrane, *Microporous Mesoporous Materials*, 115, 164–169.
- [23] **Tak, L., Au, Y., Lik, J., Chau, H., Ariso, C. T. and Yeung, K. L.** (2001). Preparation of supported Sil-1, TS-1 and VS-1 membranes Effects of Ti and V metal ions on the membrane synthesis and permeation properties, *Journal of Membrane Science*, 183, 269–291.

- [24] **Motuzas, J., Mikutaviciute, R., Gerardin, E. and Julbe, A.** (2010). Controlled growth of thin and uniform TS-1 membranes by MW-assisted heating, *Microporous Mesoporous Materials*, 128, 136–143.
- [25] **Gascon, J., Kapteijn, F., Zornoza, B., Sebastián, V., Casado, C. and Coronas, J.** (2012). Practical Approach to Zeolitic Membranes and Coatings: State of the Art, Opportunities, Barriers, and Future Perspectives, *Chem. Mater.*, 24, 2829–2844.
- [26] **Robeson, L. M.** (2008). The upper bound revisited, *J. Membrane Sci.*, 320, 390–400.
- [27] **Robeson, L. M.** (1991). Correlation of separation factor versus permeability for polymeric membranes, *J. Memb. Sci.*, 62, 165–185.
- [28] **Zhang, Y., Sunarso, J., Liu, S. and Wang, R.** (2013). Current status and development of membranes for CO₂/CH₄ separation: A review, *Int. J. Greenh. Gas Control*, 12, 84–107.
- [29] **Goh, P. S., Ismail, A. F., Sanip, S. M., Ng, B. C. and Aziz, M.** (2011). Recent advances of inorganic fillers in mixed matrix membrane for gas separation, *Sep. Purif. Technol.*, 81, 243–264.
- [30] **Rezakazemi, M., Ebadi Amooghin, A., Montazer-Rahmati, M. M., Ismail, A. F. and Matsuura, T.** (2014). State-of-the-art membrane based CO₂ separation using mixed matrix membranes (MMMs): An overview on current status and future directions, *Prog. Polym. Sci.*, 39, 817–861.
- [31] **Moore, T. T. and Koros, W. J.** (2005). Non-ideal effects in organic–inorganic materials for gas separation membranes, *J. Mol. Struct.*, 739, 87–98.
- [32] **Aroon, M. Ismail, A.F., Matsuura, T. and Montazer-Rahmati, M. M.** (2010). Performance studies of mixed matrix membranes for gas separation: A review, *Sep. Purif. Technology*, 75, 229–242.
- [33] **Hillock, A. M. W., Miller, S. J. and Koros, W. J.** (2008). Crosslinked mixed matrix membranes for the purification of natural gas: Effects of sieve surface modification, *J. Memb. Sci.*, 314, 193–199.
- [34] **Junaidi, M. U. M., Khoo, C. P., Leo, C. P. and Ahmad, A. L.** (2014). The effects of solvents on the modification of SAPO-34 zeolite using 3-aminopropyl trimethoxy silane for the preparation of asymmetric polysulfone mixed matrix membrane in the application of CO₂ separation, *Microporous Mesoporous Mater.*, 192, 52–59.
- [35] **Burgraff, A. and Cot, L.** (1996). *Fundamentals of Inorganic Membrane Science and Technology*, Membrane Science and Technology, 1st edition, Elsevier B.V..

- [36] **Pechar, T. W., Tsapatsis, M., Marand, E. and Davis, R.** (2002). Preparation and characterization of a glassy fluorinated polyimide zeolite-mixed matrix membrane, *146*, 3–9.
- [37] **Pechar, T., Kim, S., Vaughan, B., Marand, E., Tsapatsis, M., Jeong, H. and Cornelius, C.** (2006). Fabrication and characterization of polyimide-zeolite L mixed matrix membranes for gas separations, *J. Memb. Sci.*, *277*, 195–202.
- [38] **Nik, O. G., Nohair, B., and Kaliaguine, S.** (2011). Aminosilanes grafting on FAU/EMT zeolite: Effect on CO₂ adsorptive properties, *Microporous Mesoporous Materials*, *143*, 221–229.
- [39] **Ismail, A.F., Kusworo, T. and Mustafa, A.** (2008). Enhanced gas permeation performance of polyethersulfone mixed matrix hollow fiber membranes using novel Dynasylan A-meo silane agent, *J. Memb. Sci.*, *319*, 306–312.
- [40] **Chen, X. Y., Nik, O. G., Rodrigue, D. and Kaliaguine, S.** (2012). Mixed matrix membranes of aminosilanes grafted FAU/EMT zeolite and cross-linked polyimide for CO₂/CH₄ separation, *Polymer*, *53*, 3269–3280.
- [41] **Mahajan, R. and Koros, W. J.** (2002). Mixed matrix membrane materials with glassy polymers. Part 2, *Polym. Eng. Sci.*, *42*, 1420–1431.
- [42] **Higuchi, W. I.** (1958). A new relationship for the dielectric properties of two-phase mixtures, *J. Phys. Chem. C*, *62*, 649–653.
- [43] **Bánhegyi, G.** (1986). Comparison of electrical mixture rules for composites, *Colloid Polym. Sci.*, *264*, 1030–1050.
- [44] **Maxwell, C.** (1973). *Treatise on Electricity and Magnetism*, London: Oxford University Press.
- [45] **Chung, T.-S., Jiang, L. Y., Li, Y. and Kulprathipanja, S.** (2007). Mixed matrix membranes (MMMs) comprising organic polymers with dispersed inorganic fillers for gas separation, *Prog. Polym. Sci.*, *32*, 483–507.
- [46] **Algieri, C., Bernardo, P., Golemme, G., Barbieri, G. and Drioli, E.** (2003). Permeation properties of a thin silicalite-1 (MFI) membrane, *J. Memb. Sci.*, *222*, 181–190.
- [47] **Çulfaz, P. Z.** (2005). *Synthesis of MFI Type Zeolite Membranes in a Continuous System*, MSc. Thesis, Middle East Technical University.
- [48] **Bernardo, P., Drioli, E. and Golemme, G.** (2009). Membrane Gas Separation: A Review/State of the Art, *Ind. Eng. Chem. Res.*, *48*, 4638–4663.
- [49] **Chaidou, C. I., Pantoleontos, G., Koutsonikolas, D. E., Kaldis, S. P. and Sakellaropoulos, G. P.** (2012). Gas Separation Properties of

Polyimide-Zeolite Mixed Matrix Membranes, *Sep. Sci. Technol.*, 47, 950–962.

- [50] **Kilic, A.** (2013). Sod-ZMOF/Matrimid Mixed Matrix Membranes for CO₂ Separation, MSc. Thesis, Istanbul Technical University, Institute of Science and Technology.
- [51] **Avcı, A. H.** (2013). Ternary Mixed Matrix Membranes for CO₂ Separation, MSc. Thesis, Istanbul Technical University, Institute of Science and Technology.
- [52] **Nasir, R., Mukhtar, H., Man, Z. and Mohshim, D. F.** (2013). Material Advancements in Fabrication of Mixed-Matrix Membranes, *Chem. Eng. Technol.*, 36, 717–727.
- [53] **Lively, R. P., Dose, M. E., Thompson, J. A., McCool, B. A., Chance, R. R. and Koros, W. J.** (2011). Ethanol and water adsorption in methanol-derived ZIF-71, *Chem. Commun.*, 47, 8667–8669.
- [54] **Url-1.** <<<http://en.wikipedia.org/wiki/Toluene>>> date retrieved 08.12.2014.
- [55] **Url-2.** <<<http://en.wikipedia.org/wiki/Tetrahydrofuran>>> date retrieved 08.12.2014.
- [56] **Url-3.** <<http://en.wikipedia.org/wiki/Isopropyl_alcohol>> date retrieved 08.12.2014.
- [57] **Ilyas, A., Ei, M., Zahediniaki, M. H. and Vasenkoy, S.** (2007). Towards Observation of Single-File Diffusion Using TZLC, *The Open-Access J. for the Basic Principles of Diff. Theory, Experiment and Application*, 6, 6–7.
- [58] **Shao, P. and Huang, R. Y. M.** (2007). Polymeric membrane pervaporation,” *J. Memb. Sci.*, 287, 162–179.
- [59] **Kertik, A.** (2010). Gas Purification Using Polymer/Zeolite Composite Membranes, MSc. Thesis, Istanbul Technical University, Institute of Science and Technology.
- [60] **Clearfield, J., Reibenspies A. and Bhuvanesh, N.** (2008). *Principles and Applications of Powder Diffraction*, 1st ed. Wiley.
- [61] **Evans, C., Brundle, R. and Wilson, S.** (1992). *Encyclopedia of Materials Characterization*, Butterworth–Heinemann.
- [62] **Url-4.** <<<http://www.malvern.com/en/products/technology/dynamic-light-scattering>>> date retrieved 25.11.2014.
- [63] **Menczel, J. D. and Prime, R. B.** (2009). *Thermal Analysis of Polymers: Fundamentals and Applications*, John Wiley & Sons, Ltd..

- [64] **Höhne, G. W. H., Hemminger, W. F. and Flammersheim, H.J.** (2003). Differential Scanning Calorimetry, Second Edition, Springer.
- [65] **Wind, J. D., Paul, D. R. and Koros, W. J.** (2004). Natural gas permeation in polyimide membranes, *J. Memb. Sci.*, 228, 227–236.
- [66] **Shan, Z. , Wang, H., Meng, X., Liu, S., Wang, L., Wang, C., Li, F. , Lewis, J. P. and Xiao, F.S.** (2011). Designed synthesis of TS-1 crystals with controllable b-oriented length., *Chem. Commun.*, 47, 1048–1050.
- [67] **Cejka, F. S. J., Van Bakkum, H., Corma, A.** (2007). Introduction to Zeolite Science and Practice, 3rd Revisi. Elsevier B.V..

APPENDICES

- APPENDIX A** : XRD patterns of TS-1 samples.
- APPENDIX B** : DSC thermogram of membranes.
- APPENDIX C** : Gas transport properties

APPENDIX A

Table A.1: Synthesis parameters employed for the preparation of TS-1 crystals.

Sample No	Sample Code	Aging Temp. (°C)	Crystallization Temp. (°C)	Aging Time (day)	Si/Ti ratio
1	A.140.0.SiTi100	-	140	-	100
2	A.140.1.SiTi100	Room temp.	140	1	100
3	A.140.2.SiTi100	Room temp.	140	2	100
4	A.140.3.SiTi100	Room temp.	140	3	100
5	A.140.7.SiTi100	Room temp.	140	7	100
6	A.160.0.SiTi100	-	160	-	100
7	A.160.1.SiTi100	Room temp.	160	1	100
8	A.160.2.SiTi100	Room temp.	160	2	100
9	A.160.3.SiTi100	Room temp.	160	3	100
10	A.160.7.SiTi100	Room temp.	160	7	100
11	A.180.0.SiTi100	-	180	-	100
12	A.180.1.SiTi100	Room temp.	180	1	100
13	A.180.2.SiTi100	Room temp.	180	2	100
14	A.180.3.SiTi100	Room temp.	180	3	100
15	A.180.7.SiTi100	Room temp.	180	7	100
16	A.160.3.SiTi25	Room temp.	160	3	25
17	A.160.3.SiTi50	Room temp.	160	3	50
18	A.160.3.SiTi200	Room temp.	160	3	200
19	B.140.1.SiTi100	40	140	1	100
20	B.140.2.SiTi100	40	140	2	100
21	B.140.3.SiTi100	40	140	3	100
22	B.140.7.SiTi100	40	140	7	100
23	C.140.1.SiTi100	80	140	1	100
24	C.140.2.SiTi100	80	140	2	100
25	C.140.3.SiTi100	80	140	3	100
26	C.140.7.SiTi100	80	140	7	100

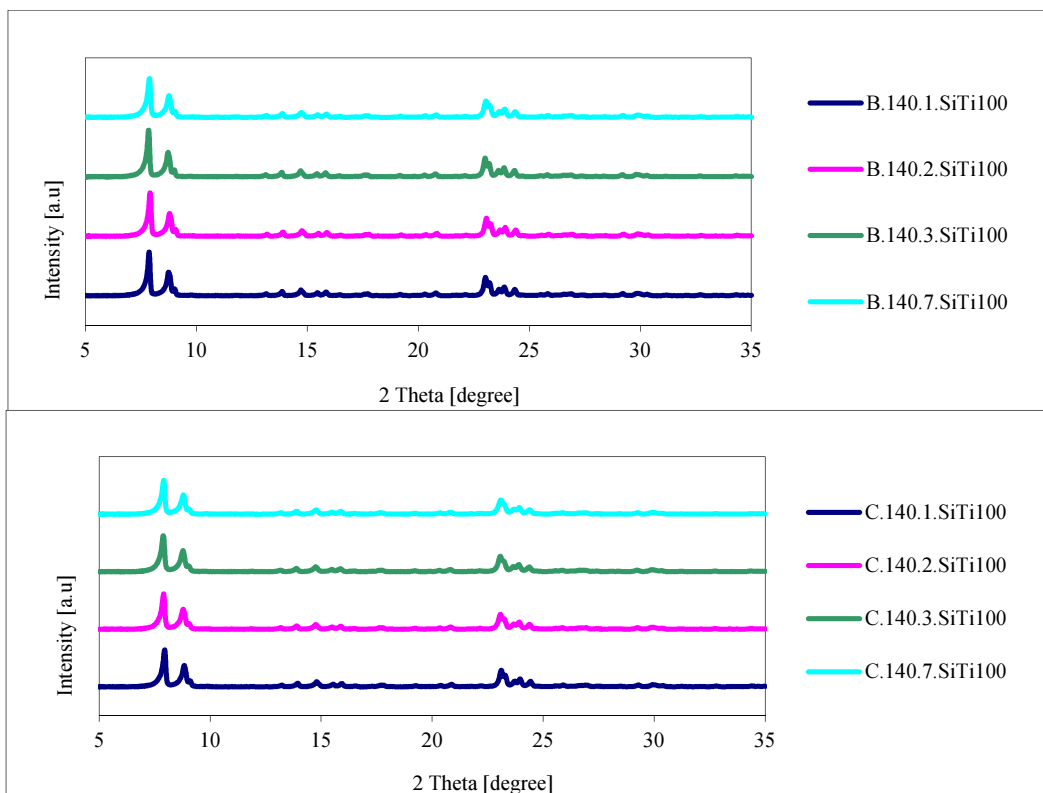


Figure A.1: XRD Patterns of TS-1 zeolites crystallized at 140°C with Si/Ti=100 and aged at 40°C (B) –above- and 80°C (C) –below- for different aging times.

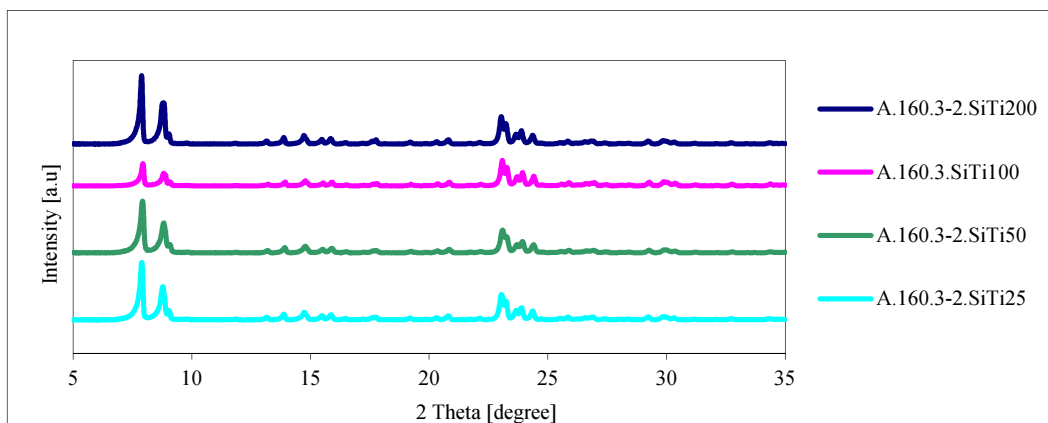


Figure A.2: XRD Patterns of TS-1 zeolites with different molar ratios Si/Ti=200, 100, 50, 25.

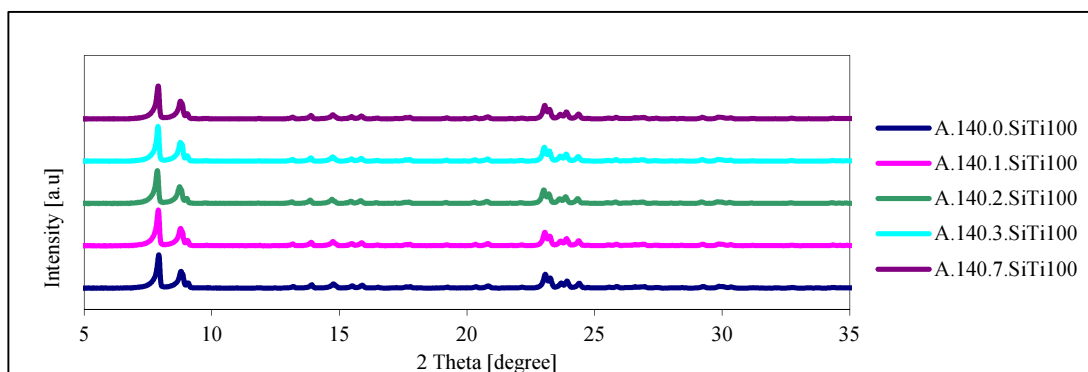
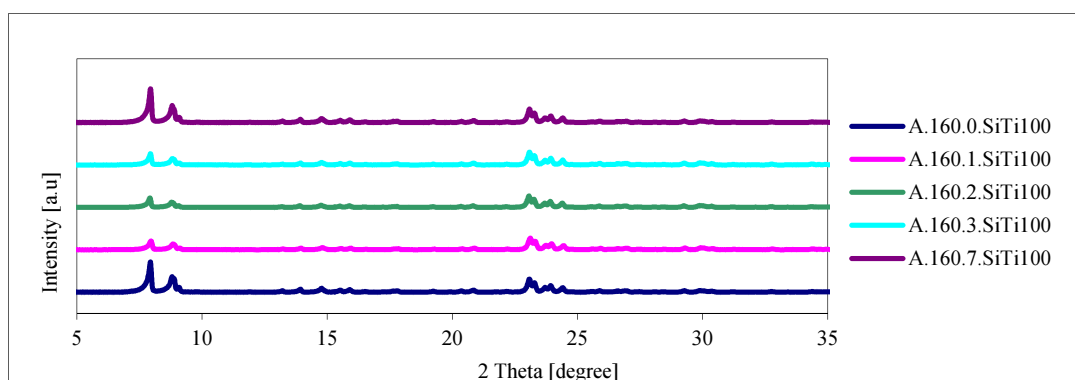
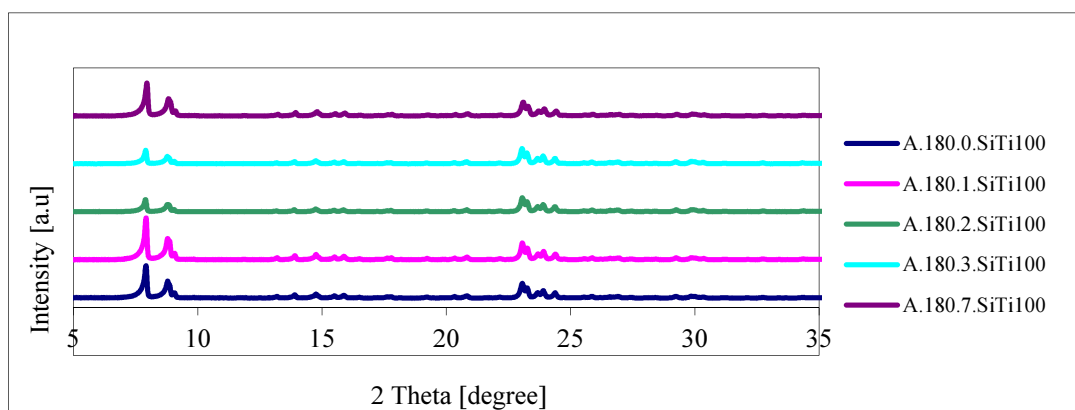


Figure A.3: XRD Patterns of TS-1 zeolites with Si/Ti=100 and crystallized at 180°C, 160°C and 140°C and aged at room temperature for different aging times.

APPENDIX B

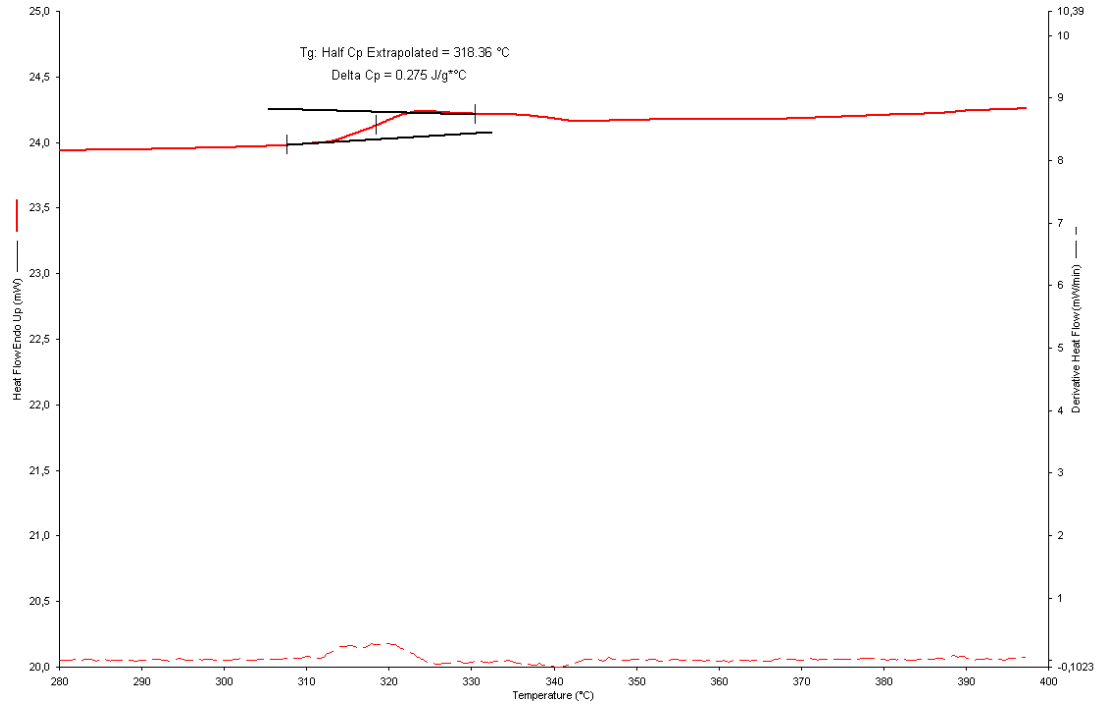


Figure B.1 : DSC thermogram of pure Matrimid[®] membrane.

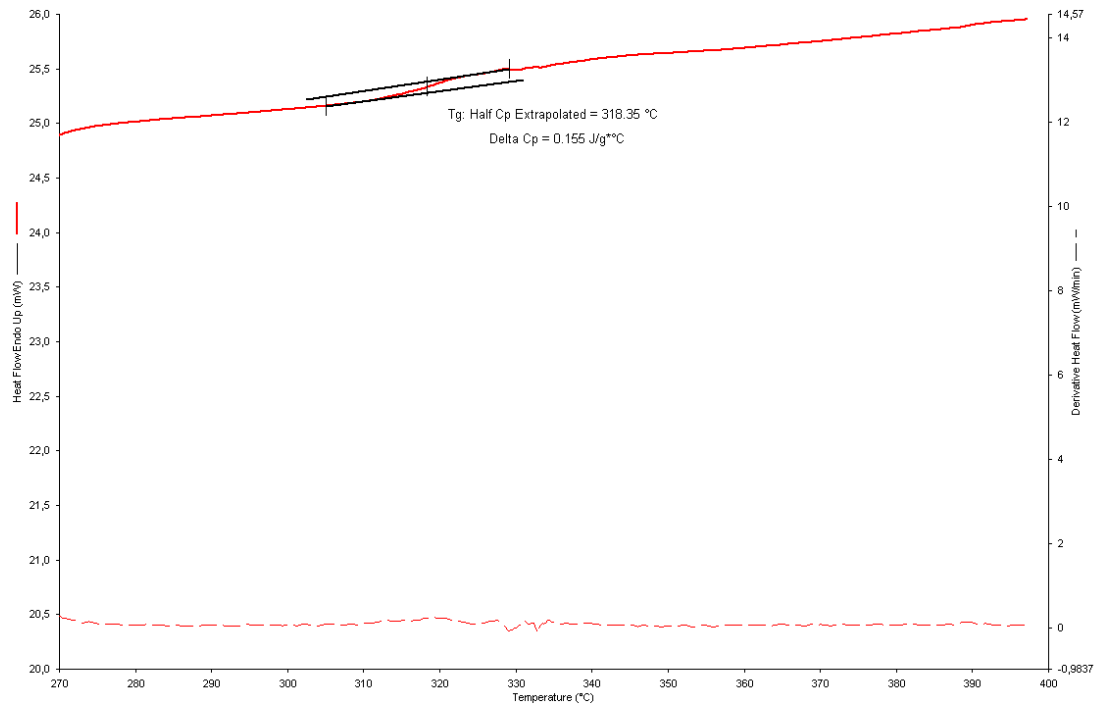


Figure B.0.2 : DSC thermogram of TS1 / Matrimid[®] MMM.

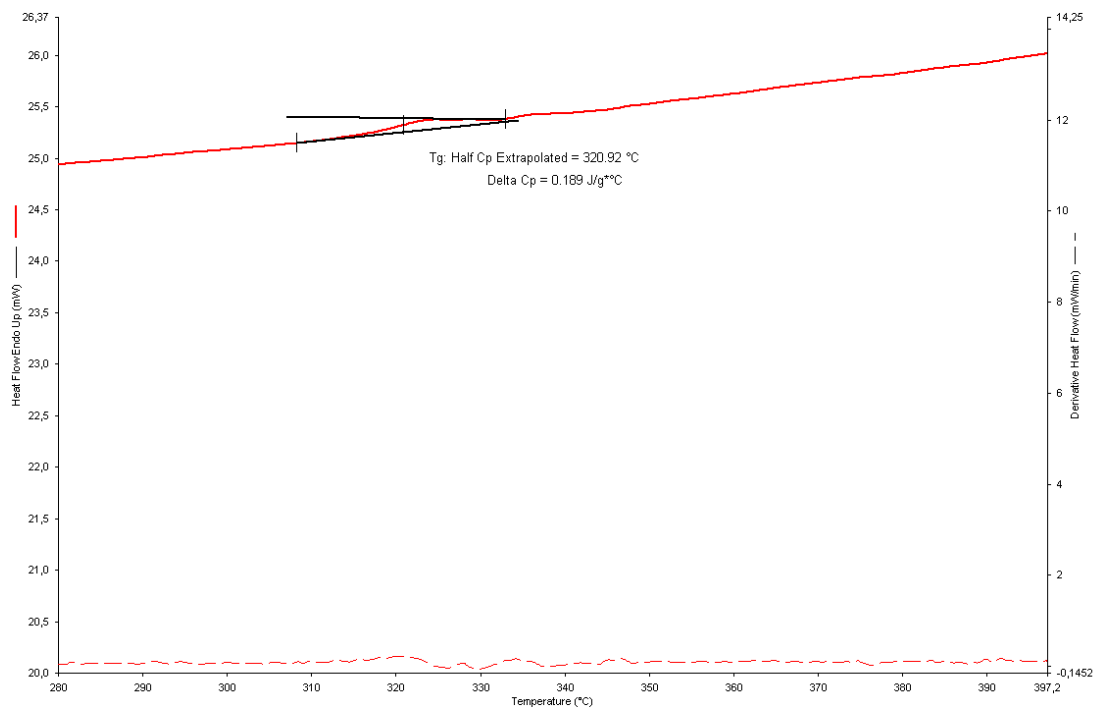


Figure B.3 : DSC thermogram of TS1-APTES-TOL / Matrimid[®] MMM.

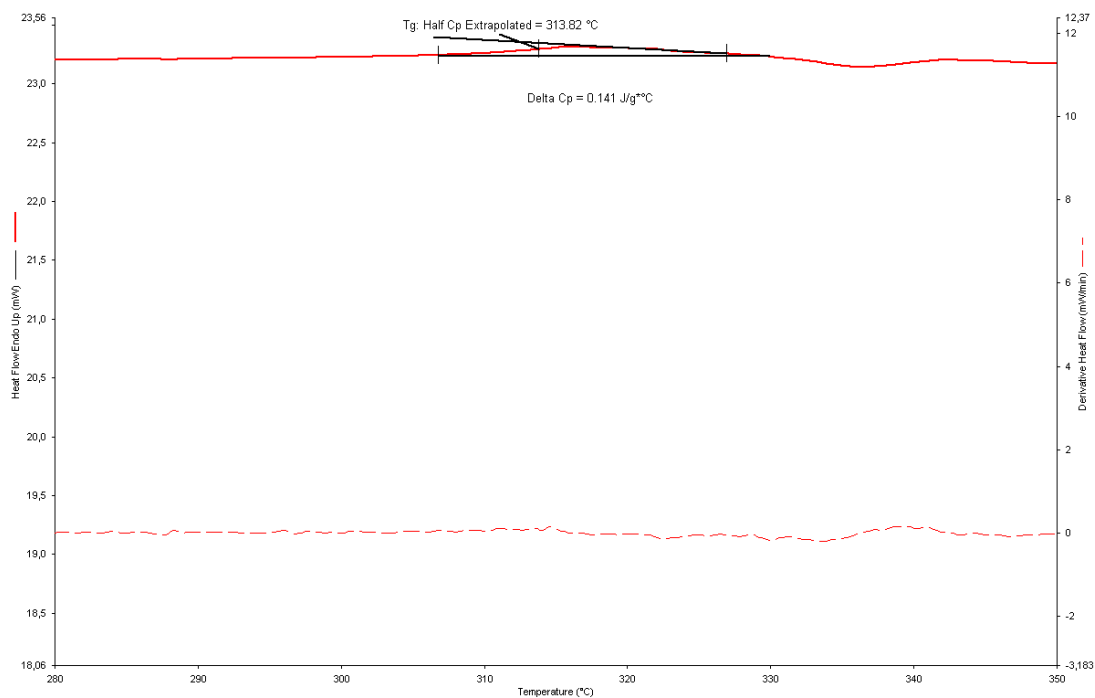


Figure B.4 : DSC thermogram of TS1-APTES-THF / Matrimid[®] MMM.

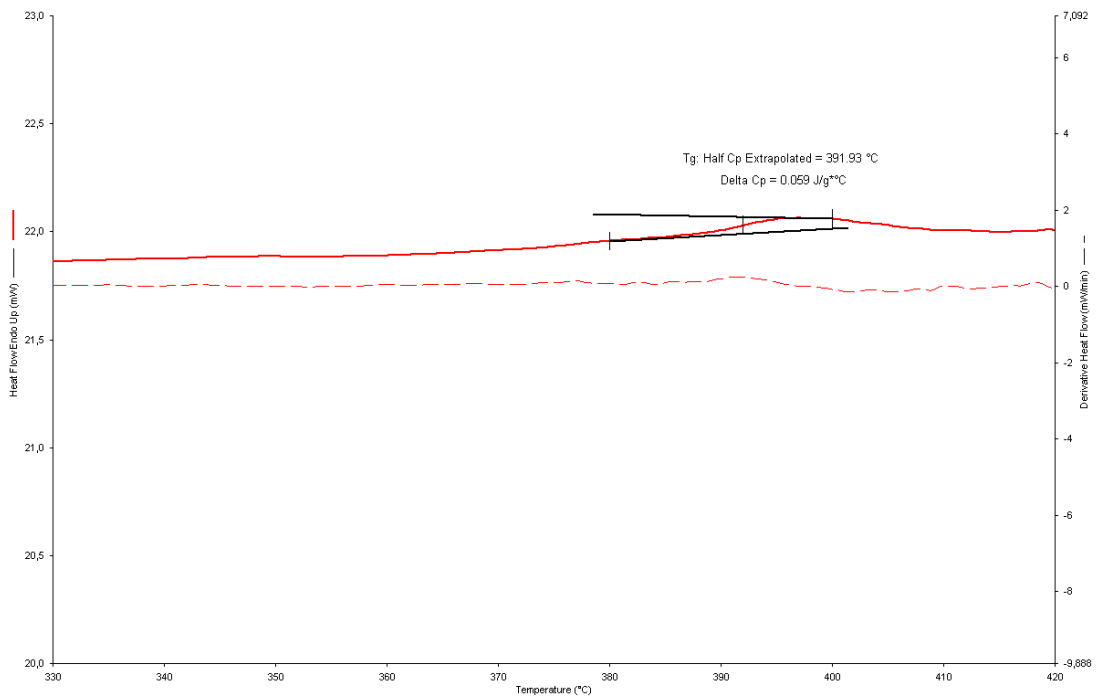


Figure B.5 : DSC thermogram of pure 6FDA-DAM membrane.

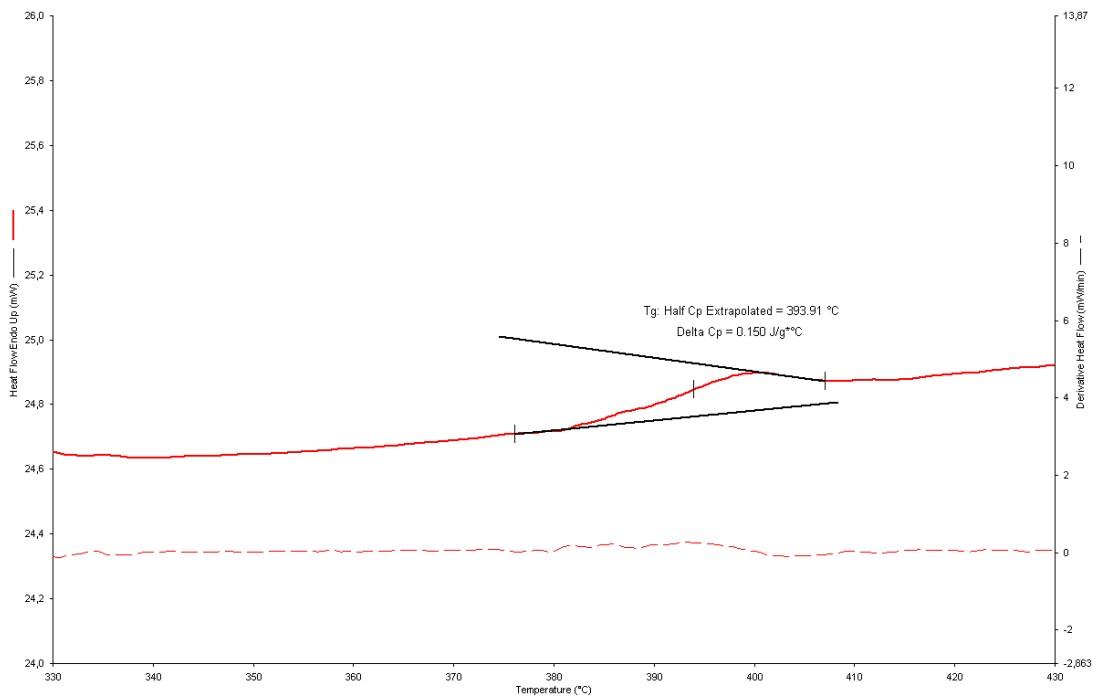


Figure B.6 DSC thermogram of TS1/6FDA-DAM membrane.

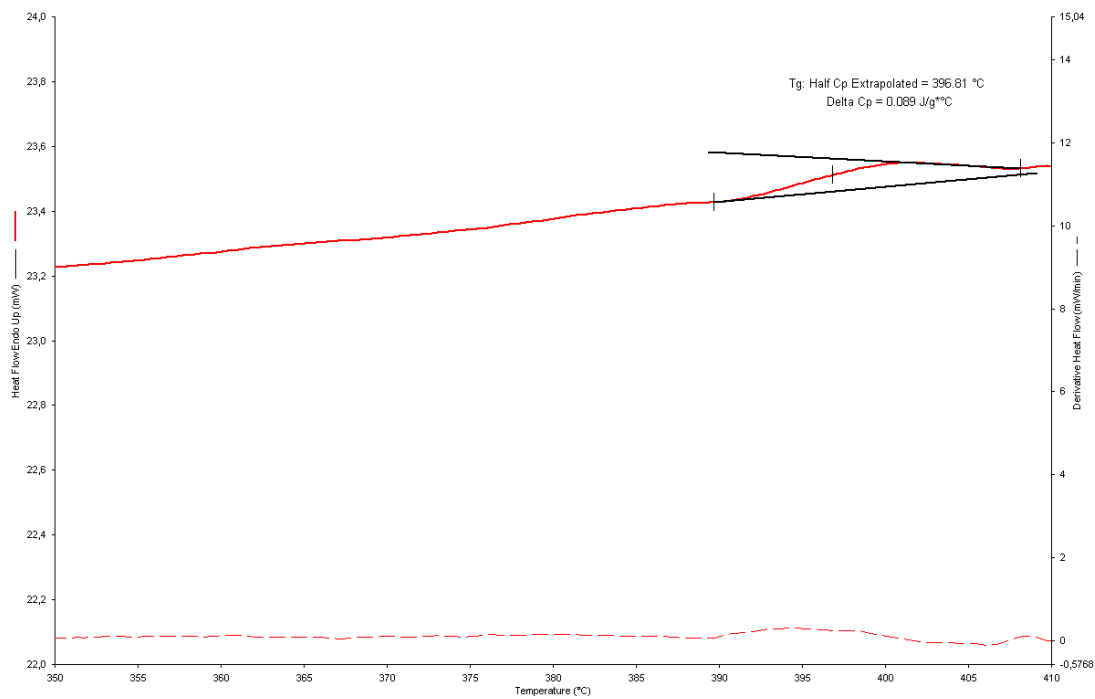


Figure B.7 : DSC thermogram of TS1-APTES-TOL/6FDA-DAM MMM.

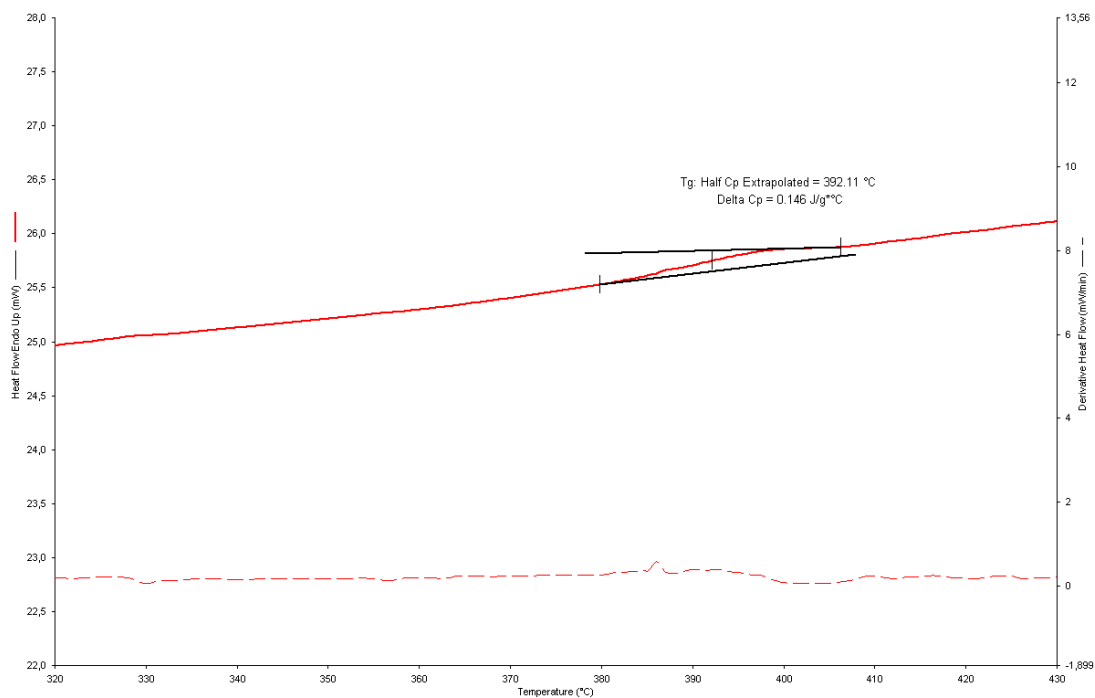


Figure B.8 : DSC thermogram of TS1-APTES-IPA/6FDA-DAM.

APPENDIX C

Table C.1 : Reproducibility measurements of MMMs prepared in this study.

Polymer	Zeolite	Permeability (Barrer)			Ideal Selectivity	
		CO ₂	CH ₄	N ₂	CO ₂ /CH ₄	CO ₂ /N ₂
Matrimid®	-	5.00	0.09	0.15		
		5.02	0.10	0.15		
		5.14	0.10	0.15		
		5.07				
		5.04			52.9	33.4
Matrimid®	TS1-APTES-TOL	12.61	0.34	0.42		
		12.61	0.34	0.41		
		12.65	0.34	0.40		
		12.64	0.34	0.41		
				0.42		
				0.42		
				0.42	36.9	30.4
6FDA-DAM	-	640.29	32.03	40.21		
		636.68	32.10	40.35		
		638.01	32.12	40.56	19.9	16.0
6FDA-DAM	TS1-APTES-TOL	693.10	48.49	57.81		
		699.84	48.78	56.23		
		700.54	48.98	56.06		
		702.67	48.88	55.99		
		700.15	48.85	55.96		
		703.89	48.80			
		702.35	48.78			
		703.31	48.73			
		48.65	14.4	12.4		
6FDA-DAM	TS1-APTES-IPA	774.14	39.66	46.07		
		776.21	39.64	46.80		
		777.88	39.67	46.89		
		778.69			19.6	16.6

CURRICULUM VITAE



Name Surname: Özlem Haval Demirel
Place and Date of Birth: Üsküdar – 12.06.1989
E-Mail: ohdemirel@itu.edu.tr
Adress: Istanbul Technical University, Faculty of Chemical and Metallurgical Engineering, B-513 34469 Maslak/ISTANBUL

Universities attended:

- Chemical Engineering B.Sc
Yildiz Technical University (2007-2011)
- Department of Inorganic Technologies, Erasmus Exchange Programme
Institute of Chemical Technology, Prague (2013)
- Chemical Engineering M.Sc
Istanbul Technical University (2012-2015)

PRESENTATIONS ON THE THESIS:

- Demirel, O. H., Fila. V., Martin. V., Tantekin-Ersolmaz, Ş.B., Utilization of Titanium-Silicalite-1 (TS-1) as Inorganic Filler in Mixed Matrix Membrane Formation for CO₂ Separation. ICOM 2014. Suzhou. China. July 20-25.2014. (Oral Presentation)
- Demirel, O. H., Fila. V., Martin. V., Tantekin-Ersolmaz, Ş.B., CO₂ Ayırımı İçin Karışık Matrisli Membranlarda (KMM) İnorganik Katkı Maddesi Olarak Titanyum-Silikalit-1 (TS-1) Kullanımı. 11. Ulusal Kimya Mühendisliği Kongresi. Eskişehir. 2-5 Eylül. 2014. (Oral Presentation)